Title
Placental Defenses Against Infection

Permalink
https://escholarship.org/uc/item/10k6d40v

Author
Zeldovich, Varvara

Publication Date
2011

Peer reviewed|Thesis/dissertation

Placental Defenses Against Infection

by

Varvara Zeldovich

DISSERTATION

Submitted in partial satisfaction of the requirements for the degree of

DOCTOR OF PHILOSOPHY

in

Biomedical Sciences

in the

GRADUATE DIVISION

of the

UNIVERSITY OF CALIFORNIA, SAN FRANCISCO

Acknowledgements

I would like to first thank Dr. Anna Bakardjiev for spending these past years mentoring me. From advising me on my Tissue & Organ proposal to taking me on as a rotation student and through the graduate school process, she has always made time and space for me. Her endless enthusiasm and curiosity have pushed me even when my own were waning. There were times when it was just the two of us in lab, and she has always had a good perspective, an encouraging word, an understanding ear. She has been an inspiration to me in many ways – from her scientific diligence and professional savvy to her kindness and strength of character. I am constantly amazed by her ability to balance every stress in work and life without sacrificing a detail or a smile. The past few years have been an exciting time in my life, with many challenges and changes, and I am truly grateful for having such an incredible woman as a role model.

The members of our lab have all contributed to this work. Cara Cooke and Sandi Wong took me in when I was a wee rotation student and taught me a thing or two about *Listeria*. Kasia Skrzypczynska was a good friend and my anchor for our rotation. Through qualifying exams and our first year together, she was often my example of determination and hard work. Jennifer Robbins regrettably only joins our lab in the summers; nevertheless, her influence on my work and life extends far past those months. We have done much of this work together, and she has been a wonderful teacher and an inspiring role model, invaluable in

that has funded me through graduate school. Greg Ku was an incredible teacher and laid the basics for my attitude and technique in graduate school. Finally, I'd like to thank Lisa Magargal and Monique Piazza for listening to me and getting me through everything from paperwork to exams to life hurdles; they are an amazing support team for a graduate student.

I also want to acknowledge a few friends who have been on my team these past years. Kathy Guis took me in when I first moved here and has been grounding me for years. Amber Gehrts has put me in my place when I needed it. Michele Hirsch & Emily Wolfe-Roubatis have been the best of friends, have listened to everything I have ever felt and told me it was legitimate. Angela Rojas and Jesse Green supported me through the first two years of the program. Noah Libby and Kiyoshi Foster have made me laugh harder than anyone ever has and continue to be two of the kindest people I know. Mark & Afton Moss have hugged me and fed me the most delicious mashed potatoes on many a rainy day.

Lastly, I want to thank my parents – Nadia Baranova and Boris Zeldovich for giving me the tools to succeed and supporting me from day one. Their brilliance and hard work have always been inspiration and motivation for my projects.

Chapters 2 and 3 are taken almost exactly from the published papers:

Robbins JR, Skrzypczynska KM*, Zeldovich VB*, Kapidzic M, Bakardjiev AI (2010) Placental syncytiotrophoblast constitutes a major barrier to vertical transmission of *Listeria monocytogenes*. PLoS Pathog 6: e1000732.
 *contributed equally

Zeldovich VB, Robbins JR, Kapidzic M, Lauer P, Bakardjiev AI (2011) Invasive extravillous trophoblasts restrict intracellular growth and spread of *Listeria monocytogenes*. PLoS Pathog 7: e1002005.

Abstract

Placental infections can lead to severe pregnancy complications as well as infection of the fetus with significant morbidity and mortality. Among pathogens that can cross the maternal-fetal barrier is the facultative intracellular bacterium, *Listeria monocytogenes*, which is highly amenable to experimental analysis. We used this model pathogen to study infection dynamics at the maternal-fetal interface.

Using human placental organ cultures, we found that the syncytiotrophoblast — which constitutes most of the placental surface and is bathed in maternal blood *in vivo* — is highly resistant to *L. monocytogenes* infection. We hypothesize this resistance to be a result of the unique biophysical characteristics of the syncytium. We present our preliminary data in support of this hypothesis and the development of the mouse trophoblast model system that will be used to study this further.

We next show that extravillous cytotrophoblasts (EVT) — which anchor the placenta in the decidua (uterine lining) — serve as the primary portal of entry for pathogens into the placenta. However, they restrict bacterial growth and represent another barrier to infection. Using primary human trophoblast cell culture, we characterized the intracellular fate of *L. monocytogenes* in EVT. We found that these cells entrap bacteria in vacuolar compartments where they are

degraded. Specifically, bacteria remain confined to acidified vacuoles and co-localize with LAMP1, consistent with bacterial degradation in lysozomes. Further studies show that autophagy is not responsible for this bacteriocidal phenotype of EVT, though reactive nitrogen species and cationic microbial peptides may play a role. Efforts to further discern the bacterial killing mechanism are underway. Specifically, we are in the process of defining the global EVT transcriptional response to infection. We hope to also use these data to study the role of EVT in the development of pregnancy complications.

Our studies show that the placenta has evolved multiple mechanisms to resist pathogen infection. The syncytium is a robust barrier to invasion by blood-borne pathogens, while EVT have innate cellular defense mechanisms to restrict pathogens. Our understanding of these novel placental barriers to infection may help develop new paradigms in the diagnosis and treatment of pregnancy complications.

Table of Contents

Preface

List of Figures

Chapter 1

Introduction

Infection & Pregnancy Complications

Maternal infection during pregnancy can lead to pregnancy complications such as pre-term labor or vertical transmission of the pathogen with fetal morbidity and mortality. While preterm birth can be caused by a myriad factors including fetal or maternal genetic abnormalities, maternal stress, hormonal imbalance, or exposure to environmental catalyst, infection is the most widely accepted and established cause [1]. In fact, the overwhelming majority of preterm births that occur before gestational week 28 can be correlated to infection and pathological inflammation [2, 3]. Pre-term labor is a significant problem worldwide, affecting 10% of all live births and resulting in 13 million premature infants each year [4]. In addition to neonatal mortality, prematurity can create various long-term health problems in the child. Other pregnancy complications, such as intrauterine growth restriction (IUGR) and pre-eclampsia, may also have an infectious background [5-8]. Pre-term labor and other pregnancy complications are often concurrent with placental abnormalities. The general explanation for this is that immune responses to a microorganism at the feto-maternal interface can lead to excessive inflammation and initiate the similarly inflammatory process of labor [9-11].

There has been a long-standing myth that pregnancy is a state of immune suppression and increased susceptibility to infectious disease. While this is no longer widely accepted as true, there are still many unanswered questions

2

regarding how the immune system functions during pregnancy. One of the biggest paradoxes is how the maternal immune system sustains an active state in order to protect the fetus from pathogen invasion, while also maintaining a tolerant environment for the semi-allogenic fetus to develop. There have been many studies describing various mechanisms employed by the feto-placental unit to prevent maternal immune response against paternal antigens (for recent reviews, see [12, 13]). One thing is clear - the implantation site is not simply immune-suppressed; it is a highly controlled, active, and functional immune environment [14]. It is reasonable to hypothesize that disruption of the highly controlled interactions between fetal and maternal cells by a placental response to infection would create a scenario for improper placentation and/or pregnancy complications.

The structure of the placenta

Understanding the structure of the placenta is key to exploring its defense mechanisms. The placenta is an incredible organ that serves a number of roles in the course of reproduction. First, it is the site of nutrient and waste exchange between mother and fetus; secondly, the placenta protects the fetus from rejection by the maternal immune system and from colonization by maternal pathogens. Placentas of different viviparous vertebrates exhibit great variability at the maternal-fetal interface, complicating cross-species comparisons [15]; we will focus on the human hemomonochorial villous placenta.

After fertilization of the egg in the fallopian tubes and rapid growth of the embryo in the first week, the embryo attaches to the uterine wall. The placenta develops over the course of gestation from the extraembryonic tissues of the blastocyst. The placenta is made of maternal and fetal tissues (see Figure 1) [16]. Maternal blood from spiral arteries in the decidua (uterine lining during pregnancy) flows into the intervillous space where it surrounds thousands of fetally derived floating villi. The entire villous surface is covered with a continuous layer of multinucleate syncytiotrophoblast (SYN) (Figure 1B), which is the major fetal surface in contact with maternal blood. The apical side of the syncytium consists of profuse, branched microvilli [17, 18] and provides abundant surface area for gas and nutrient exchange between mother and fetus. The syncytiotrophoblast is undergirded by cytotrophoblasts [19], which are separated from fetal capillaries in the villous stroma by a basement membrane. Some cytotrophoblasts leave the basement membrane and differentiate along the invasive pathway to form anchoring villi: columns of unpolarized cytotrophoblasts attach to and then penetrate the uterine wall where they give rise to extravillous cytotrophoblasts [20]. Extravillous cytotrophoblasts commingle with resident decidual, myometrial and immune cells. A subset of extravillous cytotrophoblasts breaches maternal spiral arteries in the decidua and differentiates into endovascular trophoblasts that replace the resident maternal endothelium to direct more blood into the intervillous space [20]. In thinking about the transmission of pathogens, human placental structure creates two points of direct

4

contact between maternal and fetal tissues: 1. the large surface area of the syncytium that is bathed in maternal blood and 2. the EVT that invade the decidua where they are juxtaposed to maternal immune cells. Both of these sites have been hypothesized to be a crossing avenue for vertically transmitted pathogens.

L. Monocytogenes

L. monocytogenes is a ubiquitous bacterial pathogen that causes food-borne disease in humans and many other mammals [21-23]. Among the intracellular microbes known to cross the maternal-fetal barrier, *L. monocytogenes* is particularly amenable to experimental analysis. *L. monocytogenes* has been used for decades as a model system to evaluate intracellular pathogenesis and the host's cell mediated and innate immune response to infection (for recent reviews see [24-26]). The intracellular life cycle of *L. monocytogenes* has been characterized in a variety of different cell lines as well as primary murine bone marrow-derived macrophages [27, 28]. *L. monocytogenes* is taken up either by phagocytosis or internalized via interaction of bacterial surface proteins, such as internalin A (InlA), with host cell receptors, such as E-cadherin [29, 30]. After internalization, the bacterium finds itself in an endocytic vacuole that develops into a late endosome and acidifies slightly [31]. Acidification activates the pore-forming toxin listeriolysin O (LLO) that is important for escape of the bacterium into the host cytosol, where *L. monocytogenes*

replicates rapidly [32, 33]. The listerial protein ActA nucleates actin and allows *L. monocytogenes* to spread from cell-to-cell without exposure to the extracellular milieu [34].

L. monocytogenes Infection During Pregnancy

Humans are exposed relatively frequently to *L. monocytogenes*: healthy adults in the United States are estimated to ingest 10^5 bacteria at least four times per year [35]. Ingestion of *L. monocytogenes* by an immunocompetent host is relatively innocuous, but in immunocompromised individuals and pregnant women listeriosis is a severe disease [22, 36]. In pregnant women *L. monocytogenes* can spread to the placenta and fetus, resulting in spontaneous abortion, stillbirth, or preterm labor, depending on the gestational age [36]. In the US there are ~530 recorded cases per year of listeriosis during pregnancy (FDA, 2009). The incidence of *L. monocytogenes*-induced spontaneous abortion during the first trimester is unknown; such early abortions are often due to chromosomal abnormalities [37] and therefore the aborted tissues are not routinely cultured. During the second trimester, *L. monocytogenes* has been found to cause ~3% of spontaneous abortions in humans and cattle [38-40]. Clinical infections of the mother at term are rare, but when they occur, they can result in neonatal disease with mortality of up to 50% [41]. The mechanisms by which *L. monocytogenes* infects the placenta and crosses the maternal-fetal barrier are controversial and still poorly understood.

The crossing of *L. monocytogenes* from mother to fetus has been studied in several systems: rodent systems including the mouse [42], gerbil [43], and guinea pig [44], human trophoblast cell lines and tissues [45] , as well as nonhuman primates [46]. It has been established in most systems that relatively high initial doses of bacteria are needed to actually seed the placenta. How bacteria traffic to the placenta has not been specifically defined, but both bacterial virulence factors InlA and ActA have been shown to be important for placental invasion in different models [47-49]. This suggests that both internalin-based cell invasion and cell-to-cell spread are important for placental infection. While some have suggested that direct InlA-based invasion of the placenta through the syncytiotrophoblast is key to infecting the placenta [50], we present evidence to the contrary, and hypothesize that InlA-based invasion is instead important for infection of trophoblasts at the implantation site. The overarching theory is that bacteria traffic to the placenta inside immune cells that are recruited to the developing decidua. Once infection in the placenta is established, it can serve as a reserve pool of bacteria that re-seeds host organs [51] and keeps the animal sick until the feto-placental unit is eliminated through spontaneous abortion or preterm labor.

We are broadly interested in understanding how pathogens interact with the host at the placenta to cause preterm labor and other pregnancy complications. Specifically, we wanted to study *L. monocytogenes* infection in the highly relevant system of human placenta. We were very fortunate to collaborate

with Dr. Susan Fisher, and through this collaboration have access to primary human first and second trimester placental tissues. We present our work in developing this system to study feto-placental listeriosis to address the questions of how placental infection develops, what defense mechanisms the placenta has against infection, and how this interplay results in pregnancy complications.

Figure 1.

A

MY
SA
DD
IVS
VT
CP
UC
AF

B

decidua
blood
EVT
sCTB
SYN
AV
STR
FV

C

D

◼ EVT   ◼ sCTB   ◼ SYN   ◻ STR   ▬ B.Mem
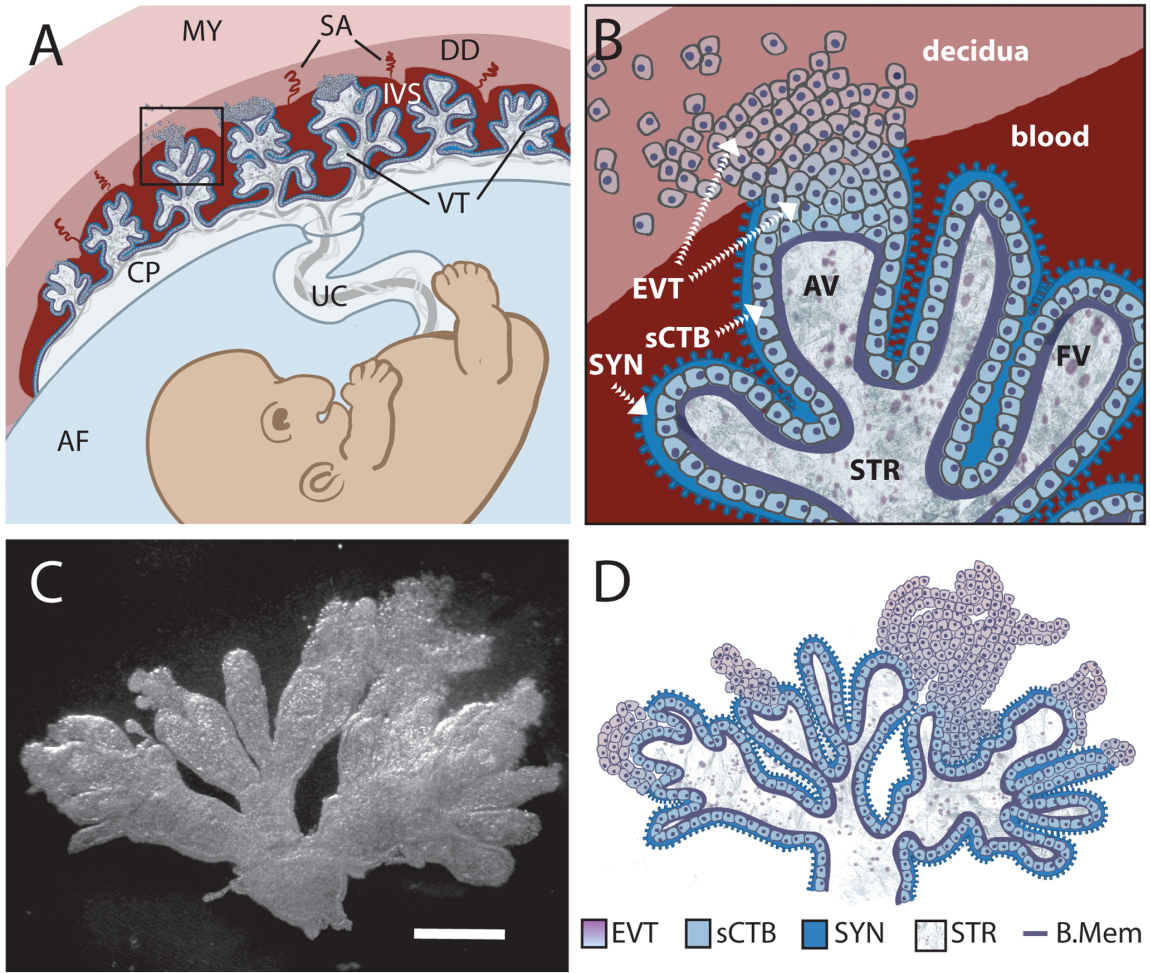
Figure 1. Human placental structure and placental explant model. (A) Structure and orientation of fetus and placenta in uterus at ~6 weeks of gestation. Fetal structures are represented in shades of blue and purple while maternal are in shades of red. Maternal structures: MY: myometrium, SA: spiral arteries, DD: decidua (uterine lining during pregnancy), IVS: intervillous space filled with maternal blood. Fetal structures: VT: villous tree, CP: chorionic plate, UC: umbilical cord, AF: amniotic fluid. **(B)** (Enlargement of boxed area in panel A) Maternal blood surrounds the villous tree composed of anchoring (AV) and floating villi (FV), which are covered by a syncytiotrophoblast (SYN) that is underlaid by subsyncytial cytotrophoblasts (sCTB) and a basement membrane. The subsyncytial CTB layer grows increasingly discontinuous in later trimesters. Gas and nutrient exchange with the maternal blood occurs across the syncytiotrophoblast to supply fetal capillaries in the stroma (STR). At the uterine wall, extravillous cytotrophoblasts (EVT) anchor the villous tree in the decidua. Some invade the decidua and move away from the tip to remodel maternal spiral arteries, with altered gene expression patterns as they move (not shown). Notably, E-cadherin expression decreases as VE-cadherin expression rises in distal (relative to fetus) extravillous cytotrophoblasts. **(C)** A six-week placental explant anchored in Matrigel. Bar = 1 mm. **(D)** Cartoon representation of the relevant structures seen in panel C.

Chapter 2

Placental Syncytium is a Barrier to Infection,

while EVTs are a portal of entry

Previously Published as:

Introduction

Infection is a major cause for pregnancy complications including premature labor and resultant maternal and fetal morbidity and mortality (WHO, 2005). Nevertheless, the underlying mechanisms of placental and fetal infection are poorly understood. The placenta and fetus are vulnerable to infection via two different routes: (a) pathogens in the lower genital tract may ascend through the cervix and (b) pathogens in the maternal blood or uterus can colonize the placenta and breach the maternal-fetal barrier. The later group includes many viruses, e.g. cytomegalovirus; protozoan parasites, e.g. *Toxoplasma gondii*; and bacterial pathogens, e.g. *Listeria monocytogenes*. It is striking that the majority of pathogens that are able to cross the placenta have either facultative or obligate intracellular life cycles. The reason for the predisposition of placental infection toward intracellular pathogens is unclear. It has been postulated that the unique immunological environment in the placenta—necessary to assure tolerance of the fetal allograft—contributes to this phenomenon [52-54], but other aspects of the placenta may also play a role.

L. monocytogenes is a ubiquitous bacterial pathogen that causes food-borne disease in humans and many other mammals [21-23]. In pregnant women *L. monocytogenes* can spread to the placenta and fetus, resulting in spontaneous abortion, stillbirth, or preterm labor, depending on the gestational age [36]. The incidence of *L. monocytogenes*-induced spontaneous abortion during the first trimester is unknown; such early abortions are often due to chromosomal

abnormalities [37] and therefore the aborted tissues are not routinely cultured. During the second trimester, *L. monocytogenes* has been found to cause ~3% of spontaneous abortions in humans and cattle [38-40]. Clinical infections of the mother at term are rare, but when they occur, they can result in neonatal disease with mortality of up to 50% [41].

Among the intracellular microbes known to cross the maternal-fetal barrier, *L. monocytogenes* is particularly amenable to experimental analysis. *L. monocytogenes* has been used for decades as a model system to evaluate intracellular pathogenesis and the host's cell mediated and innate immune response to infection. *L. monocytogenes* can infect professional phagocytic and non-phagocytic cells in many species. A family of bacterial cell wall surface proteins called internalins (Inl) promote bacterial adherence and internalization into non-phagocytic host cells [29]. Of these, internalin A (InlA) and internalin B (InlB) are the best characterized, binding to E-cadherin and c-Met-tyrosine kinase, respectively [30, 55]. After internalization, the bacterium escapes from the vacuole into the host cell cytoplasm where it multiplies rapidly [56, 57]. The listerial virulence determinant ActA facilitates spread from infected host cells to neighboring cells without bacterial exposure to the extracellular environment [34, 58-60]. Thus, *L. monocytogenes* is able to infect non-phagocytic cells by two different mechanisms: Inl-mediated direct invasion and cell-to-cell spread. In the work described herein, we determine the placental tissue barriers operative

against each mechanism and explore how *L. monocytogenes* might overcome them.

The anatomical site and mechanism by which *L. monocytogenes* breaches the maternal-fetal barrier are controversial. Of particular interest is whether InlA-mediated binding to E-cadherin is essential for transplacental transmission. Infection of isolated human cytotrophoblasts [44] or the BeWo choriocarcinoma cell line [50] with *L. monocytogenes* deficient in InlA leads to a 100-fold reduction in invasion. However, *in vivo*, cytotrophoblasts are covered with syncytiotrophoblast and may not be accessible to the bacteria. Lecuit et al. reported that E-cadherin is expressed at low levels on the apical surface of syncytiotrophoblast in explants from human term placentas [50], and postulated that *L. monocytogenes* breaches the maternal-fetal barrier by InlA-mediated invasion of the syncytiotrophoblast from the maternal bloodstream [50]. However, other groups have not observed E-cadherin expression on the surface of the syncytium [61-65]. Furthermore, InlA or InlB mutants do not affect feto-placental infection in guinea pigs [44] (unpublished observations), and show less than a 5-fold decrease in bacterial numbers in the gerbil placenta and fetus [43]. Wild type InlA does not interact with murine E-cadherin [66], but infection of wild type mice with *L. monocytogenes* expressing murinized InlA does not influence the course of feto-placental listeriosis [67], and in transgenic mice expressing human E-cadherin, InlA and/or InlB have a <5-fold effect on placental and fetal infection [43]. The minimal or absent *in vivo* phenotype observed with internalin mutants in

14

these four rodent models is surprising given the strong phenotype in isolated cytotrophoblasts and suggests that the syncytiotrophoblast may not be the initial site of infection.

InlA/E-cadherin is not the only mechanism for infection—*L. monocytogenes* can spread from cell-to-cell without exposure to the extracellular environment, and there is evidence that *L. monocytogenes* traffics to the placenta [51] or the brain [68] inside of cells. Furthermore, we and others have found cell-to-cell spread to be important for fetal infection [47, 48].

In this report, we probe the human maternal-fetal barrier using first trimester human placental organ cultures, which allow a detailed examination of the most likely sites of transplacental infection by direct incubation with extracellular *L. monocytogenes* as well as via co-incubation with infected human cells. We found intact syncytiotrophoblast to be resistant to infection by *L. monocytogenes*. The portal of entry for *L. monocytogenes* was instead a small subpopulation of E-cadherin-expressing extravillous cytotrophoblasts in anchoring villi that are not readily accessible from the maternal bloodstream *in vivo,* and infection of these cells occurred via both InlA-mediated invasion and cell-to-cell spread. Surprisingly, these cells were able to restrict the growth of *L. monocytogenes*. If infection progressed, the bacteria spread along subsyncytial cytotrophoblasts, mostly sparing the syncytiotrophoblast and villous stroma. Our results clarify the mechanisms of crossing the maternal-fetal barrier and provide

a unifying explanation for the conflicting *in vitro* and *in vivo* results mentioned above.

Results

Culture of first trimester human placental explants

In order to examine the role of direct invasion and cell-to-cell spread in breaching the human maternal-fetal barrier we turned to first trimester human placental organ cultures, a well-studied model system that allows examination of the trophoblast in a context that retains the cellular architecture of the tissue *in vivo* [69, 70]. Placental villous trees are dissected and explanted on substrates of extracellular matrix (Matrigel), where they form floating and anchoring villi (Figure 1C-D). All of the tissue is exposed to the media with the exception of the tips of anchoring villi that result from extravillous cytotrophoblast outgrowth and invasion into Matrigel [70, 71]. This mimics the conditions *in vivo* where extravillous cytotrophoblasts invade the decidua while the rest of the villous tree is bathed in maternal blood [20]. The syncytiotrophoblast covers the villi and remains largely intact for at least 24 hours (Susan Fisher, personal communication). First trimester placental explants therefore adequately represent the most probable placental sites that are potentially accessible to *L. monocytogenes* or infected phagocytes: intact syncytiotrophoblast, subsyncytial cytotrophoblasts underlying damaged syncytiotrophoblast, and extravillous cytotrophoblasts (Figure 1).

L. monocytogenes infection of human placental explants

We infected explants with 2 x 10^6 wild type *L. monocytogenes* (Figure 2). In order to measure intracellular growth we added gentamicin 1 hour post-inoculation to eliminate extracellular *L. monocytogenes*, and subsequently determined numbers of live bacteria per explant over 24 hours (Figure 2A). No significant differences in infection were observed between the wild type strains 10403S and EGDe (p = 0.38 by Student's T-test). The average bacterial growth from all placentas was less than 10-fold, which is slow compared to that found in cell lines [57] (Figure 2A), and infection rates were highly variable. Despite the relatively high inoculum, 11% of the explants were not infected and an additional 13% hosted <10 intracellular bacteria at 2 hours post-inoculation. The average percentage of intracellular bacteria at 2 hours post-inoculation was 0.6% ± 2% SD of the inoculum (n = 54 explants), similar to the bottleneck in the pregnant guinea pig model of listeriosis [51].

Explants vary in size, shape, age, donor and degree of Matrigel invasion, so variability is expected. However, we were able to distinguish two possible courses of infection by examining three explants from the same placenta at each time point. Roughly half of the placentas exhibited an increase in bacterial numbers from 2 to 24 hours (average = 77-fold, SD = 6.4) while the others showed a decrease (average = 0.25-fold, SD = 0.19).

It has been previously suggested that *L. monocytogenes* invades the syncytiotrophoblast [50]. If this is true for explants, then larger explants should be more highly infected, since >90% of each explant's bacterially accessible surface area is covered by syncytiotrophoblast. But we found no correlation between colony forming units (CFU) and explant size ($r^2 < 0.05$) in 30 explants from 11 placentas. Nor did explant age affect CFU ($r^2 < 0.02$). However, CFU at 2 hours post-inoculation did correlate with the number of anchoring villi ($r^2 = 0.49$, Figure 2B), suggesting that extravillous cytotrophoblasts are the preferred sites of *L. monocytogenes* infection. Examination by immunofluorescence histology revealed only a few foci of infection, usually in extravillous cytotrophoblasts of anchoring villi (Figure 2C).

Syncytiotrophoblast forms a barrier against infection

To better characterize which placental cell types are most vulnerable to *L. monocytogenes* infection, we increased both the inoculum and the time of incubation without gentamicin. These "permissive infections" increase the probability of infection at vulnerable sites. In addition to wild type bacteria, we also used bacteria deficient in ActA (ΔActA) that are incapable of intercellular spread, thus ensuring that the *L. monocytogenes*-containing cells we observe are those initially infected by the bacteria. After 8 hours, we examined explant sections by immunofluorescence (Figure 3).

Under these conditions, *L. monocytogenes* was detectable in three cell types (Figure 3A): subsyncytial cytotrophoblasts, extravillous cytotrophoblasts and syncytiotrophoblast. Infected syncytiotrophoblast could be subdivided into: 1) apparently intact syncytiotrophoblast where only the apical surface is exposed to bacteria; and 2) basolaterally accessible syncytiotrophoblast (bSYN), where the syncytiotrophoblast is naturally terminated by an invading CTB cell column (Figure 3A) or, in rare cases, torn away from the explant, presumably during dissection.

We enumerated the total number of infected cells in explant sections (Figure 3B). For syncytiotrophoblast, a "cell" was defined as a circular region similar in size to a CTB, roughly the area surrounding a single nucleus. Infection of subsyncytial cytotrophoblasts was infrequent, which is unsurprising since unlike syncytiotrophoblast and extravillous cytotrophoblasts they are largely inaccessible to bacteria in the media. However, syncytiotrophoblast infection was also low, even though it covers almost all of the explant surface. Roughly 75% of the infected cells were extravillous cytotrophoblasts, which comprise less than 5% of available surface. Furthermore, these cells were ~5 times more likely to contain multiple bacteria, possibly indicating multiple infections.

Transverse sections obscure a full view of the syncytiotrophoblast. To ensure that our observations were not a histological artifact, we fixed and mounted whole explants infected with *L. monocytogenes* expressing GFP. Confocal microscopy of these minimally manipulated explants confirmed that the

bacteria are highly localized within the extravillous cytotrophoblasts of anchoring villi (Figure 3C). Together, these results suggest that extravillous cytotrophoblasts may serve as the primary site of infection.

Although in cultured macrophage and epithelial cell lines cell-to-cell spread begins around 4-5 hours post-infection [34, 58], we found no significant difference between locations of ΔActA and wild type *L. monocytogenes* at 8 or even 24 hours (Figure 3B, p = 0.99 by chi-squared test), suggesting that the *L. monocytogenes* life cycle (intracellular growth and/or cell-to-cell spread) is delayed in primary trophoblast cells.

InlA mediates proximal extravillous cytotrophoblast invasion

E-cadherin is an important host cell receptor for *L. monocytogenes* binding and uptake. Lecuit et al. suggested that *L. monocytogenes* extracellular invasion of the placenta occurs via *L. monocytogenes* InlA interactions with host E-cadherin on the apical surface of syncytiotrophoblast [50]. However, other studies of the placenta have failed to find E-cadherin here [61-65]. Our results support this: we never observed E-cadherin staining on the apical surface of the syncytiotrophoblast, although it was expressed strongly on the basal surface (Figure 4A). Like others, we found E-cadherin was most abundant on subsyncytial cytotrophoblasts and proximal extravillous cytotrophoblasts, decreasing as cells migrate away from the villus tip.

Since proximal extravillous cytotrophoblasts were the very cells *L. monocytogenes* infected, we hypothesized that explant infection is InlA-dependent. Indeed, ΔInlA and ΔInlAB mutants were almost completely unable to invade explants (Figure 4B; $p < 10^{-20}$ by Student's T-test). We found no significant difference between invasion of wild type and ΔInlB *L. monocytogenes* in human explants (Figure 4B; $p = 0.68$ by Student's T-test) consistent with previous observations in isolated CTB and BeWo cells (human choriocarcinoma cell line) [44].

Damage of syncytiotrophoblast leads to infection of subsyncytial cytotrophoblasts

If the syncytiotrophoblast is relatively resistant to infection, as the preceding data suggest, then removing it should provide *L. monocytogenes* new sites of invasion. We enzymatically degraded the syncytiotrophoblast by soaking the explants briefly in a collagenase-containing solution before plating [72]. Although the extent of the syncytiotrophoblast removal varied, many subsyncytial cytotrophoblasts were exposed and extravillous cytotrophoblasts increased (Figure 5A). As expected, permissive infections of enzymatically-treated explants allowed for new sites of infection (Figure 5B). The total number of infected cells increased (from an average of 78 in two sections to 228 with enzymatic degradation), and nearly half of the infected cells were now subsyncytial cytotrophoblasts, which express E-cadherin (Figure 5C; $p < 0.05$ by Chi-square test).

Cell-to-cell spread leads to infection of proximal extravillous cytotrophoblasts

Infection of the placenta by extracellular pathogens in the maternal bloodstream must be mediated by the interaction of pathogen virulence determinants, e.g. InlA with host cell receptors like E-cadherin. However, *L. monocytogenes* also traffics *in vivo* to the placenta in a gentamicin-resistant manner [51], presumably traveling inside phagocytic leukocytes [68]. We wanted to test whether cell-to-cell spread can mediate placental infection, and, if so, what sites are vulnerable.

We introduced a fluorescent live cell dye to macrophage-like U937 cells (differentiated to adherent cells with PMA) and then infected them with 10403S-sGFP *L. monocytogenes*. The infected cells were added to explants in the presence of gentamicin to prevent infection of the explant by extracellular bacteria. After 24 hours transmission of *L. monocytogenes* from U937 cells to explants had occurred (Figure 6A-B). As with direct invasion, we found that *L. monocytogenes* infection by cell-to-cell spread from U937 cells to the placenta was largely confined to extravillous cytotrophoblasts at villous tips (Figure 6C). In fact, the cell populations infected were statistically indistinguishable from InlA-mediated infections after 24 hours (*p* = 0.99 by chi-squared test). Invasive CTB express chemokines that attract cells of the monocyte lineage [73-75], and indeed we observed clusters of U937 cells around the extravillous cytotrophoblasts as early as 4-8 hours post-inoculation (data not shown).

Placental infection was not observed upon co-cultivation with U937 cells carrying ΔActA mutants, which are defective in cell-to-cell spread (data not shown).

Bacterial dissemination occurs along subsyncytial cytotrophoblasts in anchoring villi

Regardless of how *L. monocytogenes* was introduced, the dominant site of initial infection was the extravillous cytotrophoblast at the tip of anchoring villi. Multiple explants from a single placenta showed strikingly similar progression over the course of infection. In three out of six placentas studied, *L. monocytogenes* advanced significantly beyond the tips of anchoring villi (Fig. 7). By 72 hours post-inoculation, subsyncytial cytotrophoblast infection was common in anchoring villi while syncytiotrophoblast remained largely uninfected, suggesting that the syncytium not only resists cell-to-cell spread from macrophage-like cells but also from neighboring cytotrophoblasts (Figure 7A). While infected anchoring villi were always colonized at the distal tips, infection of floating villi always began at proximal junctures shared by anchoring villi. At times floating villi exhibited infection of cytotrophoblasts on both sides of the villus without syncytiotrophoblast infection, indicating that *L. monocytogenes* trafficked through the subsyncytial cytotrophoblasts (Figure 7B). Spread into the stroma was rare and presumably restricted by the basement membrane underlying subsyncytial cytotrophoblasts. Some stromal cells were infected at later time

points (Figure 7C). In explants infected with ΔActA *L. monocytogenes*, bacteria remained in extravillous cytotrophoblasts (Figure 7D).

Overall, ~75 – 100% of anchoring villi were infected (Figure 7E) and infection of subsyncytial cytotrophoblasts and stroma increased over 72 hours (Figure 7F). In contrast, only 22% of explants exhibited any *L. monocytogenes* in floating villi (Figure 7E). Taken together, these results describe the cell-to-cell path *L. monocytogenes* follows in disseminating throughout placental explants over three days: from extravillous cytotrophoblasts of anchoring villi along lateral villous subsyncytial cytotrophoblasts and from there into floating villi and/or stroma, all while leaving the syncytiotrophoblast largely uninfected.

Discussion

Pathogens present in the maternal bloodstream may colonize the placenta, causing infection, inflammation, and ultimately spontaneous abortion, preterm labor, and neonatal morbidity and mortality [2]. Many pathogenic microbes are found transiently in maternal blood. For example, the simple daily act of brushing teeth is associated with bacteremia [76, 77], and *L. monocytogenes* is ingested frequently by healthy adults [35]. Yet neither result in significant maternal-fetal infection the majority of the time. This is surprising considering that twenty percent of maternal blood can be found circulating freely in the placenta's intervillous space, where it bathes fetal villi that are covered by a syncytiotrophoblast whose surface area ranges from 3000 cm^2 in the late first

trimester to 125,000 cm^2 at term [19]. Thus, it seems reasonable to hypothesize that the syncytium forms an extremely effective physical barrier against infection. In this study, we have conclusively shown that the syncytiotrophoblast is resistant to infection by *L. monocytogenes* and that extravillous cytotrophoblasts are the portal of entry.

For internalin-mediated infections the resistance of the syncytiotrophoblast can be reasonably explained by the tissue's lack of E-cadherin on the apical surface. When syncytiotrophoblast was infected, it was more likely to be basolaterally accessible syncytiotrophoblast, in which an E-cadherin expressing basolateral surface was exposed. Even for infections in uninterrupted syncytiotrophoblast, it remains possible that basolateral access was not apparent in the examined section but was available in an adjacent section. It is interesting to note that InlA and E-cadherin interactions mediating intestinal invasion are confined by anatomical and cellular barriers as well [78].

Even more surprising was the near absence of syncytiotrophoblast infection by cell-to-cell spread, either from U937 cells—which were observed near the syncytiotrophoblast—or from neighboring cytotrophoblasts at later time points. Three possible explanations exist: 1) the syncytiotrophoblast under-expresses unknown host molecule(s) required for cell-to-cell spread; 2) attachment of leukocytes to syncytiotrophoblast is insufficiently close in time or space for cell-to-cell spread to occur; or 3) the syncytiotrophoblast membrane is physically inhospitable to *L. monocytogenes'* actin-mediated protrusions. The

last two are especially plausible when considering the profuse covering of branched microvilli on the apical surface [79-84]. The basal surface may also be girded against protrusion by the especially dense cytoskeletal network that is presumably required to resist cytosolic surface tension in the laterally vast syncytium [79-82]. Interestingly, interaction of the bacterial virulence factor InlC with human actin regulatory proteins has recently been shown to promote cell-to-cell spread by decreasing cortical tension, thereby enhancing the ability of motile bacteria to deform the plasma membrane into protrusions [85].

The syncytiotrophoblast may act as a general barrier. We have observed that *T. gondii* is not able to efficiently colonize the syncytium either (unpublished observations), and other groups have reported similar results for herpes simplex virus [86] and cytomegalovirus [87, 88].

Instead, we present evidence that extravillous cytotrophoblasts, normally not easily accessible from the intervillous space, are the dominant sites of *L. monocytogenes* colonization from both extracellular and intracellular compartments. Our results are in accord with Lecuit et al. showing that invasion of placental explants by extracellular *L. monocytogenes* depends on InlA, but our findings differ on the initial site of invasion. An important difference is our experimental set-up: we used first trimester placental explants instead of term placentas. Term placental organ cultures do not form anchoring villi after removal from the mother and are maintained in floating culture. Damage of the term explant syncytiotrophoblast has been reported as early as 4 h under selected

culture conditions [89] and term explants cannot be used to evaluate extravillous cytotrophoblasts [90]. Thus, first trimester explants better represent the architecture of the maternal-fetal barrier *in vivo*.

However, placental organ cultures from all gestational ages omit the decidua and the maternal vessels. The later are remodeled by extravillous cytotrophoblasts, which differentiate into endovascular trophoblasts that replace the endothelium of the maternal spiral arteries and therefore are in direct contact with maternal blood. Endovascular trophoblasts do not express E-cadherin [61] but it may be possible that they are targets of cell-to-cell spread *in vivo*.

It has recently been postulated that the conjugated action of InlA and InlB leads to breaching of the maternal-fetal barrier [43]. This is particularly intriguing since InlA and InlB are in the same operon and expression of these invasion proteins is most likely co-regulated [29]. Disson et al. show a 10-fold reduction in invasion of the human intestinal cell line Caco-2 with *L. monocytogenes* strain EGDe, deficient in InlA or InlB, and an almost 100-fold reduction with the InlAB double deletion mutant [43]. Other groups using *L. monocytogenes* strains derived from 10403S have observed a 2-3-fold effect of InlB on intestinal invasion (Amieva, personal communication). We do not observe a difference between WT and ΔInlB in infection of early gestation placental organ cultures. It may be that the variability of the human placental explants is too high to resolve a potentially small effect of InlB on invasion of placental explants.

We did examine the role of cell-to-cell spread from infected U937 cells to the placenta, which seems highly relevant considering the importance of *Listeria*'s intracellular life cycle for virulence [91] and the published evidence that *L. monocytogenes* traffics between organs inside of cells [51, 68]. It is striking that extravillous cytotrophoblasts remain the primary portal of entry, leading us to hypothesize that access to extravillous cytotrophoblasts represents the first bottleneck for *L. monocytogenes* infection of the placenta. How can *L. monocytogenes* overcome this hurdle? Extravillous cytotrophoblasts are present in the decidua and are known to actively recruit macrophages, monocytes and natural killer cells [73-75]. Therefore, we postulate that *L. monocytogenes* reaches the placenta in maternal phagocytes that are recruited to the decidua where they infect extravillous cytotrophoblasts by cell-to-cell spread or internalin-mediated invasion.

Another striking finding was that extraordinarily high doses of *L. monocytogenes* were required to infect placental explants, and that *L. monocytogenes* growth rates were relatively slow, on average increasing only ~10-fold over 24 h. However, we could distinguish two placental populations: in about half of the placentas *L. monocytogenes* did not grow, while in the other half bacterial numbers increased by ~77-fold. Lecuit et al. used slightly higher doses and reported an increase of ~100-fold over 24 h. But they also report having removed gentamicin from the culture medium at 2 hours post-inoculation. Therefore, their 24 h CFU and histological assays may have included

extracellular bacteria that escaped dying cells. In addition, we found little to no cell-to-cell spread at 24 hours, while in most cell lines cell-to-cell spread begins as early as 4 hours post-inoculation [34, 58]. In some placentas we observed that infection remained confined to the extravillous cytotrophoblasts for at least 72 hours. It is intriguing that the sites of infection correlated with the host cell's proliferative capacity [92, 93], which may provide interesting avenues for future studies. The slow rate of intracellular bacterial growth and cell-to-cell spread suggest the possibility that extravillous cytotrophoblasts restrict the intracellular life cycle of *L. monocytogenes*, thus representing the second bottleneck in the placenta.

Once the placenta is infected, *L. monocytogenes* can spread to the fetus. One probable route of spread to the fetus is via the fetal capillaries in the villous stroma. Indeed, we observed low numbers of bacteria that had penetrated the basement membrane and infected the stroma suggesting that this is the third bottleneck *L. monocytogenes* encounters. It is interesting to note that although some bacteria were observed in syncytiotrophoblast at early time points, only anchoring villi acted as an origin of colonization.

Our model is consistent with previous findings *in vivo* that the guinea pig placenta is colonized by 10^4 times fewer bacteria than maternal liver and spleen, and subsequently only 1 out of 10^4 bacteria are able to spread from placenta to fetus [51]. It is also in agreement with the epidemiology of human listeriosis, which is a rare disease during pregnancy despite its ubiquity in the environment,

as well as the observation that pregnant animals have to be inoculated with high doses of *L. monocytogenes* to observe consistent placental and fetal infection [43, 51, 67]. In addition, our results provide an explanation for the absent or minor phenotype the internalin mutants exhibit in multiple different pregnant animal models [43, 51, 67].

Although it may be attractive to describe the route taken by a pathogen as a single mechanism, we do not believe that this accurately reflects what occurs *in vivo.* There is mounting evidence that pathogens have evolved to exploit multiple strategies to breach the intestinal and blood-brain barriers [94, 95], and it is reasonable to expect the same of the maternal-fetal barrier. The mechanisms by which the placenta excludes most pathogens to generate the maternal-fetal barrier are poorly understood, but our results suggest that the syncytiotrophoblast plays a significant role. Given its extensive contact with the maternal blood, this important tissue may have evolved to exclude pathogens, and our model system offers a powerful way to probe the mechanisms by which this occurs. Pathogens that can breach the syncytiotrophoblast or exploit sites of syncytial damage may colonize the placenta via subsyncytial cytotrophoblasts. Our study of *L. monocytogenes*, a model pathogen that colonizes the placenta, strongly suggests that the placenta's most vulnerable site is the extravillous cytotrophoblast, where cells anchor the placenta in the maternal decidua but have little to no contact with maternal blood. This finding suggests a reason for the observation that almost all pathogens capable of crossing the maternal-fetal

barrier are either facultative or obligate intracellular: dissemination in the blood is not enough.

Methods

Ethics statement

This study was conducted according to the principles expressed in the Declaration of Helsinki. The study was approved by the Institutional Review Board at the University of California, San Francisco, where all experiments were performed (H497-00836-28). All patients provided written informed consent for the collection of samples and subsequent analysis.

Human tissue collection and culture

Placentas from elective terminations of pregnancy (gestational age 4 to 8 weeks) were collected and prepared as previously described [90]. Briefly, fragments from the surface of the placenta were dissected into 1-3 mm tree-like villi, placed on Matrigel (BD Biosciences, San Jose, CA) coated Transwell filters (Millipore, Bedirica, MA, 30-mm diameter, 0.4 μm pore size) and cultured in Dulbecco's modified Eagle's medium-F12 medium (DMEM-F12; 1:1, vol/vol) supplemented with 20% fetal bovine serum (FBS, Fisher Scientific), 1% L-glutamine and 1% penicillin/streptomycin (Invitrogen, Carlsbad, CA). For surface area and perimeter measurements, cultured explants were photographed pre-infection on a Leica MZ16F stereomicroscope (Leica Microsystems, Wetzlar, Germany) using an Axiocam MR monochrome camera (Carl Zeiss, Munich,

Germany). Measurements were made using ImageJ software (NIH, Bethesda, MD).

Removal of syncytiotrophoblast

Syncytiotrophoblast was removed from villous trees as previously described [72]. Briefly, placental explants were soaked for 5-15 minutes in a solution containing Type IA collagenase (100,000 U), hyaluronidase (150,000 U), DNAse (120,000 U) and 0.1% BSA in PBS without divalent cations (UCSF Cell Culture Facility, San Francisco, CA). Explants were observed continuously via a dissecting microscope and when syncytiotrophoblast degradation was apparent they were transferred to Matrigel.

Pathogen strains and growth conditions

The wild type strain of *L. monocytogenes* used in this study is 10403S [96].   Mutant strains included ΔInlA (DPL4405), ΔInlB (DPL4406), ΔInlAB (DPL4455) [44], ΔActA (DPL3078) [97], and sGFP-expressing 10403S *L. monocytogenes* (DH-L1039) [98]. EGDe *L. monocytogenes* (M. Loessner) was used for some experiments. Bacteria were cultured using brain heart infusion (BHI) broth or agar (Becton Dickenson Company, Sparks, MD).

L. monocytogenes infections of placental explants

Intracellular growth assays of *L. monocytogenes* were performed as previously described [99] with following modifications: placental explants were incubated in antibiotic free media for 1 hour prior to infection, 1 x 10^6 bacteria/mL were added for 30 minutes and gentamicin (50 μg/mL) was added at 60 minutes post-inoculation. Gentamicin was subsequently maintained in the media, which was refreshed every 24 hours. At specified times after infection, explants were removed from Matrigel and homogenized in 1mL dH$_2$O using a T25 digital Ultra-Turrax (IKA, Staufen, Germany). Aliquots were plated on BHI agar and grown at 37° C. For permissive infections explants were incubated with 2 x 10^7 bacteria/mL for 5 hours before adding gentamicin.

Infection of explants by cell-to-cell spread

Human macrophage-like U937 cells (ATCC 1593.2 [100]) were grown in RPMI-1640 (UCSF Cell Culture Facility) containing 4500 mg/L glucose, 10% FBS and 1% penicillin/streptomycin (Invitrogen). 48 hours prior to infection, cells were differentiated by addition of phorbol 12-myristate 13-acetate (PMA; concentration 18 nM; Sigma) to the medium. On the day of infection, cells were labeled with CellTracker Green CMFDA (Invitrogen) and infected with *L. monocytogenes* for 1 h at an MOI of 1:1. Cells were washed once with PBS and lifted from culture plates by incubation in ice cold PBS without divalent cations for 5 minutes. U937 cells were re-suspended in explant medium containing 50 μg/mL gentamicin, and

1×10^6 cells per transwell were added to the explants. Every 24 hours, fresh media containing gentamicin was added.

Immunofluorescence and Histology

Explants were removed at the times indicated and placed into vinyl cryomolds (Ted Pella, Redding, CA), then covered with optimal cutting temperature (OCT) media (Ted Pella) and flash-frozen. Histological slicing was performed using a Hacker-Slee cryostat. Glass slides with sections were incubated ~5 minutes in acetone at 4° C. All antibody staining was conducted at room temperature. When dry, slides were soaked 60 minutes in blocking solution (1% bovine serum albumin (BSA, Sigma) in PBS), then rinsed and exposed to primary antibodies in 0.5% BSA/PBS. Slides were rinsed three times for 5 minutes each in 0.5% BSA/PBS, then secondary antibodies were added at the indicated concentrations and incubated for 60 minutes. After three rinses, coverslips were affixed over Vectashield mounting medium with DAPI (Vector Laboratories, Burlingame, CA). Uninfected explants did not stain with anti-*Listeria* antibodies. Primary antibodies: polyclonal rabbit *Listeria* O antiserum (1:1000 Becton, Dickenson), monoclonal mouse anti-human cytokeratin 7 (1X, Clone OV-TL, Dako, Carpinteria, CA), monoclonal mouse anti-human E-cadherin (1:200, Clone NCH-38, Dako), monoclonal mouse anti-human bHCG (1:500, clone SPM105, Neomarkers, Fremont, CA) and monoclonal mouse anti-human EGFR (1:250, Clone cocktail R19/48, Biosource, Camarillo, CA). Secondary antibodies:

Alexa Fluor 594 goat anti-mouse IgG (1:500) and Alexa Fluor 488 goat anti-rabbit IgG (1:1000, both Invitrogen). All immunofluorescence conditions were compared to no-primary controls to ensure that non-specific binding did not occur.

Slides were viewed using an inverted TE2000-E microscope (Nikon, Tokyo, Japan) equipped with a 12-bit cooled CCD camera (Q Imaging, Surrey, Canada). Images were collected using Simple PCI software (Hamamatsu, Sewickley, PA). Counts of *L. monocytogenes* localization were made by tallying every infected cell in each section at 100X magnification.

Confocal microscopy

Whole mount explants were prepared by rinsing explants with PBS and then soaking in 3% paraformaldehyde in PBS (Ted Pella) for 12 hours at 4° C. Explants were then rinsed three times with PBS and suspended in 1:100 Alexa Fluor 594 phalloidin and 1:100 DAPI (both Invitrogen) for 24 hours at 4°C. Explants were mounted onto glass slides in Vectashield and sealed under coverslips. Imaging was performed at the Nikon Imaging Center at UCSF using an upright Nikon C1 spectral confocal microscope equipped with 405, 488 and 561 nm lasers.

Image processing for figures

Images were prepared using Photoshop and Illustrator (Adobe, San Jose, CA). RGB color hues were linearly adjusted for better CMYK printing but no non-linear alterations were performed.
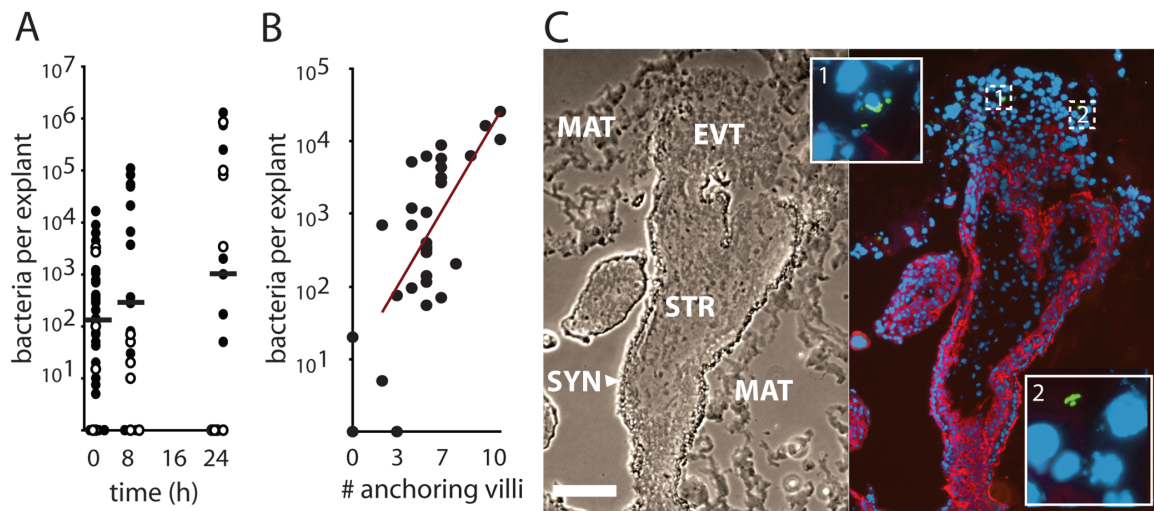
Figure 2.

Figure 2. *L. monocytogenes* **grows variably in placental explants. (A)** Intracellular survival of *L. monocytogenes* in 86 explants from 18 placentas infected with ~2 x 10^6 10403S (filled circles) or EGDe (open circles) wild type strains for 30 min. Gentamicin was added at 60 min to kill extracellular bacteria and maintained in media thereafter. Infection is highly variable and growth is slower than in most cell lines. Bars = median values. **(B)** Number of internalized bacteria at 2 hours post-inoculation (p.i.) correlates with the number of anchoring villi in the explant (n = 30 explants, r^2 = 0.49). **(C)** Histological section of explant frozen and sliced at 8 h p.i., then stained for *L. monocytogenes* (green), DNA (blue), and EGFR (red), which stains trophoblast membranes. Bacteria are found in extravillous cytotrophoblasts (EVT) but not syncytiotrophoblast (SYN). Matrigel (MAT) and stroma (STR) are also indicated. Bar = 100 µm.
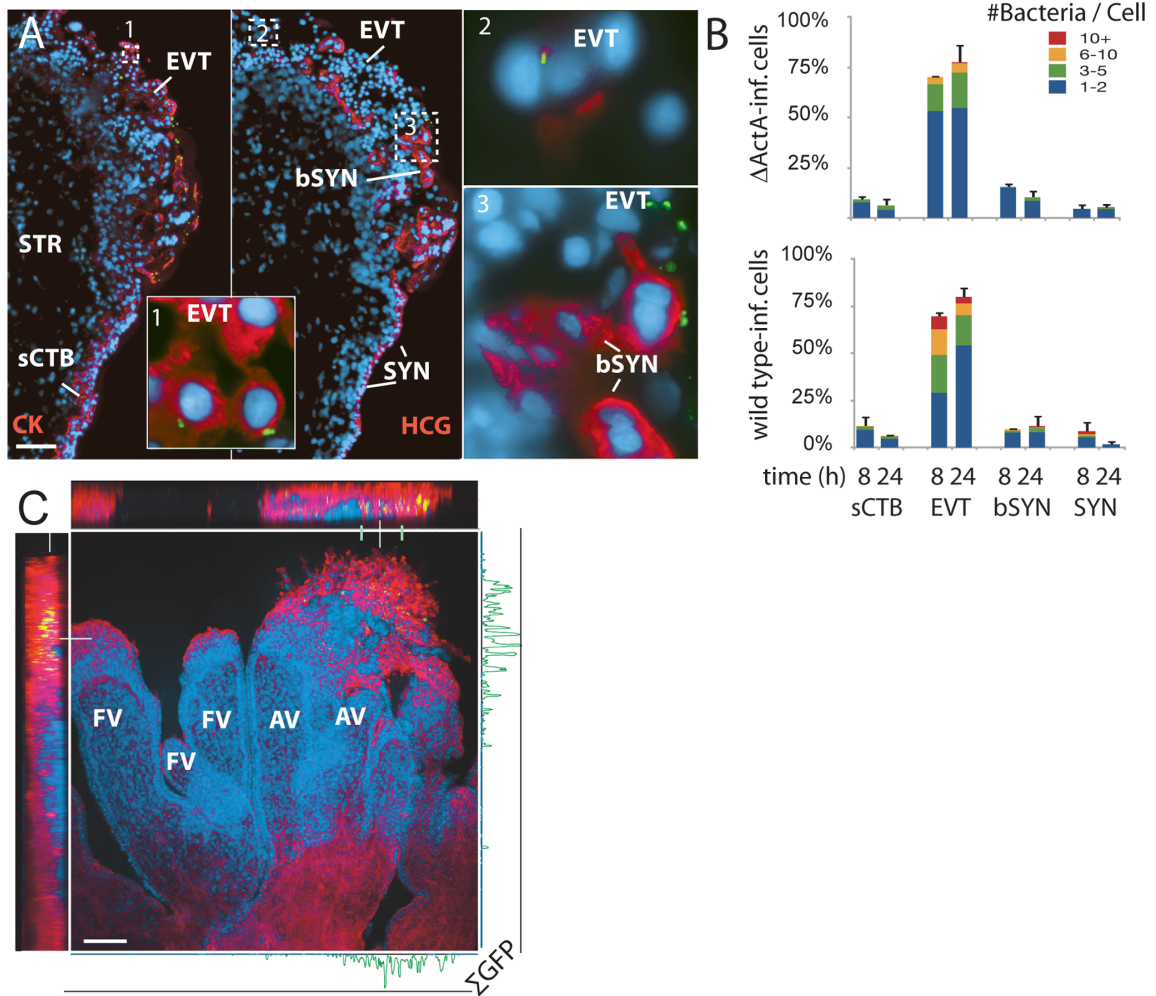
Figure 3.

Figure 3. *L. monocytogenes* **enters the placenta primarily at invasive villus tips. (A)** Consecutive histological sections of a permissively infected explant at 8 hours post-inoculation, frozen and stained for *L. monocytogenes* (green) and DNA (blue). Left panel and inset 1: red = cytokeratin (CK), expressed by cytotrophoblasts (CTB). In middle panel with insets 2 and 3: red = ßHCG (HCG), which primarily stains syncytiotrophoblast (SYN). Subsyncytial cytotrophoblasts (sCTB) underlie the syncytiotrophoblast. Where cytotrophoblasts invade from the

villus into the decidua, syncytiotrophoblast breaks, exposing basal surfaces (bSYN). Scattered, isolated bacteria are found mainly in proximal extravillous cytotrophoblasts (EVT). Bar = 100 µm. **(B)** Distribution of infected cell types in explants infected with ΔActA (top) or 10403S wild type *L. monocytogenes* (bottom). Each graph represents two sections in each of three explants (average of infected cells counted per explant = 135). For SYN and bSYN, a "cell" was considered to be the area around a single nucleus, roughly the size of a cytotrophoblast. Bars are SEM. **(C)** Projection of a 3D confocal image showing a whole explant permissively infected with GFP-expressing *L. monocytogenes* and fixed at 8 h. Anchoring villi (AV), which include invading extravillous cytotrophoblasts, and floating villi (FV), which remain covered with syncytiotrophoblast, are indicated. Red = F-actin. Green = *L. monocytogenes*. Blue = DNA. Left and top: reconstructed Z series. Because of high F-actin levels in extravillous cytotrophoblasts, bacteria appear yellow. Right and bottom: sum of total GFP intensity over 70 µm Z stack for each X/Y position after background subtraction shows the majority of bacteria are in anchoring villi, in extravillous cytotrophoblasts. Bar = 100 µm.
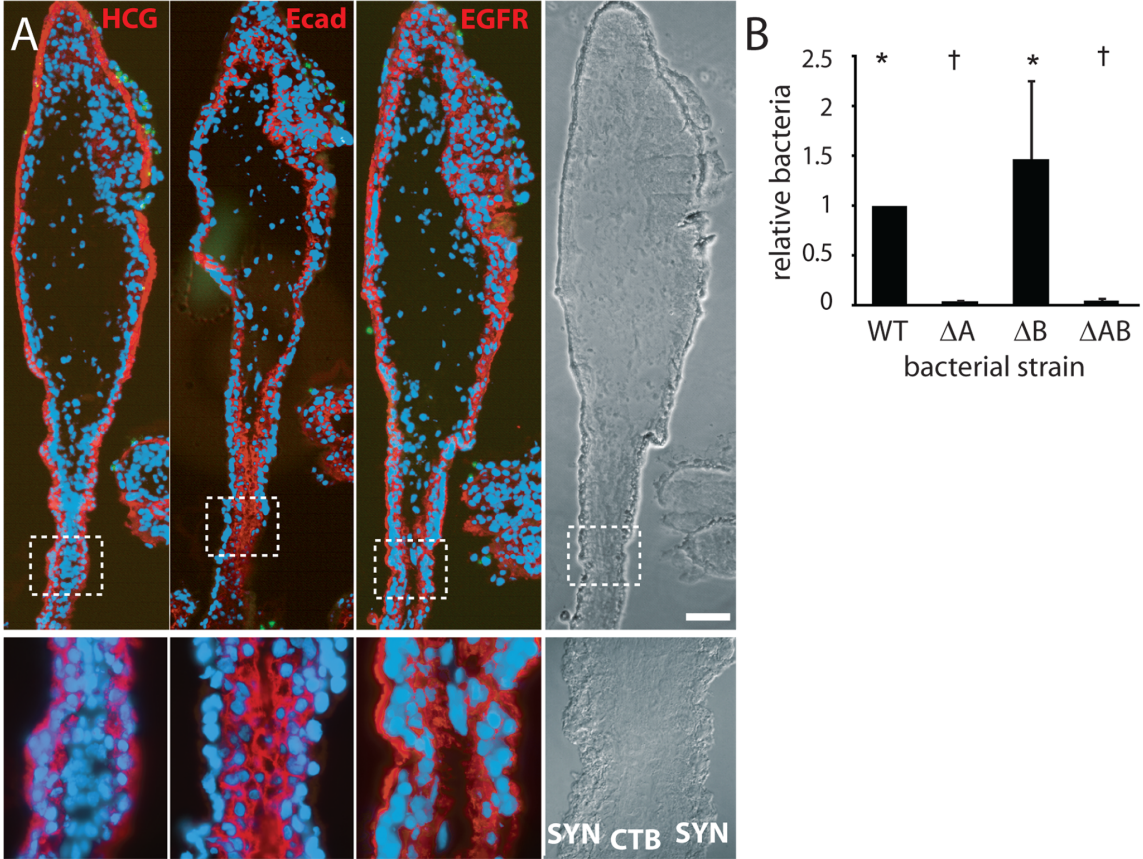
Figure 4.

Figure 4. Bacteria invade primarily via InlA binding to E-cadherin on cytotrophoblasts not covered by syncytiotrophoblast. (A) Immunofluorescence of consecutive histological sections. From left to right: red stains ßHCG (HCG, a syncytiotrophoblast marker), E-cadherin (Ecad) and EGFR (stains cytotrophoblasts (CTB) and syncytiotrophoblast (SYN) membrane). E-cadherin does not appear on the apical surface of syncytiotrophoblast but is abundant in cytotrophoblasts. Green = *L. monocytogenes.* Blue = DNA. Bar = 100 μm. **(B)** Intracellular invasion of *L. monocytogenes* strains deficient in InlA (DA), InlB (DB), or InlA/InlB (DAB) at 2 hours post-inoculation. Each condition represents at least 4 placentas and 3 explants per placenta. Asterisks and crosses denote statistically similar populations.

Figure 5.
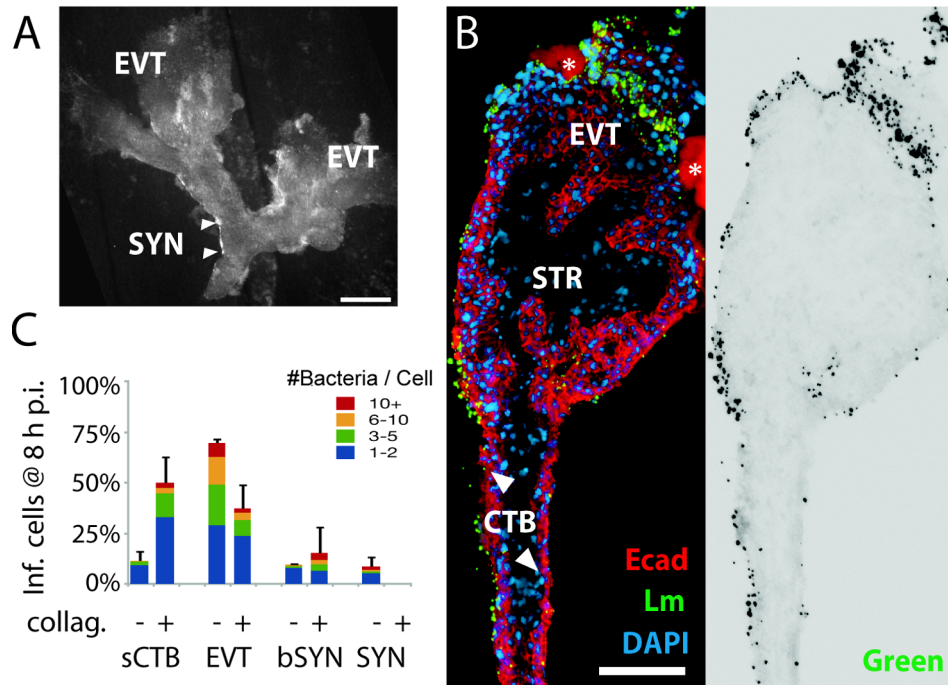
Figure 5. *L. monocytogenes* **infects villous cytotrophoblasts when syncytiotrophoblast is removed. (A)** Placental explant treated with collagenase-containing solution to degrade the syncytiotrophoblast (SYN). Treatment varies; some areas of syncytiotrophoblast remain (e.g. between arrowheads). All villi anchor to form extravillous cytotrophoblasts (EVT). Bar = 1 mm. **(B)** Left: histological section of enzymatically-treated villus arm, 8 hours post-inoculation (p.i.). No syncytiotrophoblast remains, permitting infection of both villous cytotrophoblasts (CTB) and extravillous cytotrophoblasts (EVT). Red = E-cadherin (Ecad). Green = *L. monocytogenes*. Blue = DAPI. Asterisk = Matrigel. Right: Green channel only, color inverted to show *L. monocytogenes* (solid black) with background fluorescence (faint grey) to show explant outline. Bar = 100 μm. **(C)** Distribution of infected cell types in enzymatically-treated explants compared to that in untreated explants at 8 h p.i. Here, sCTB refers to villous trophoblasts, which are subsyncytial in untreated explants but exposed after syncytiotrophoblast removal in enzymatically-treated explants. Each condition represents two sections from each of three explants. For syncytiotrophoblast (SYN) and basally accessible syncytiotrophoblast (bSYN), a "cell" was considered to be the area around a single nucleus, roughly the size of a cytotrophoblast. Bars = SEM.

Figure 6.
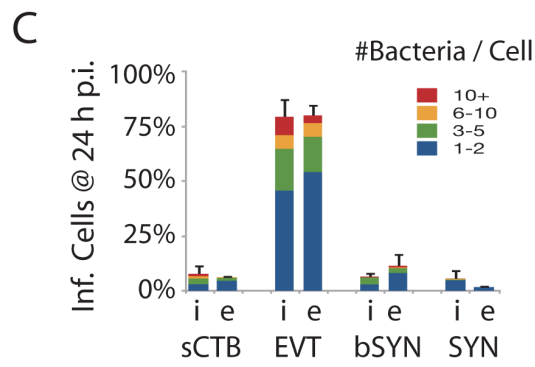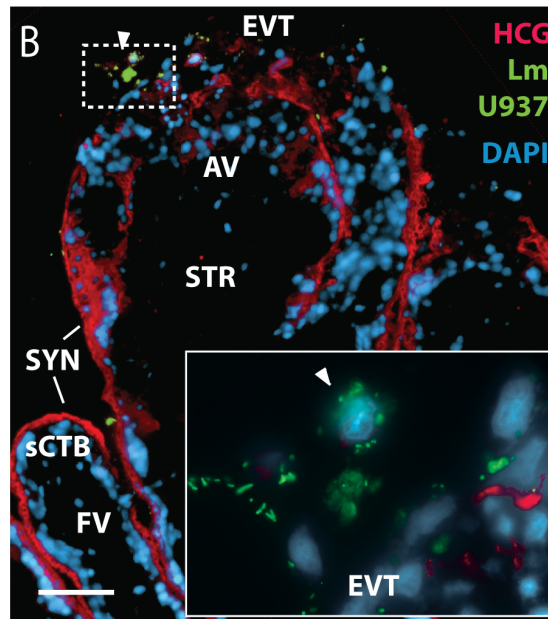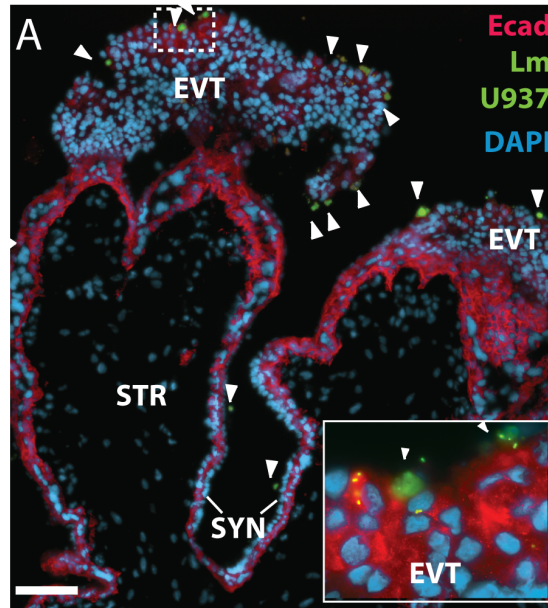
Figure 6. *L. monocytogenes* **infects anchoring villi by cell-to-cell spread.**

(A) Histological sections of explant infected by *L. monocytogenes*-containing U937 macrophage-like cells loaded with green dye (arrowheads). *L. monocytogenes* are also stained green. Photos are 24 h post-inoculation (p.i.). Both bacteria and U937 cells localize primarily to the E-cadherin-expressing extravillous cytotrophoblasts (EVT). Red: = Ecad. Blue = DNA. Bar = 100 μm. **(B)** Bacteria are excluded from syncytiotrophoblast (SYN) and subsyncytial cytotrophoblasts (sCTB). ßHCG (red) is primarily expressed by syncytiotrophoblast. Only anchoring villi (AV) are infected, while floating villi (FV) covered in syncytiotrophoblast remain uninfected. Bar = 100 μm. **(C)** Localization of *L. monocytogenes* in explants when introduced in extracellular media (e) or by cell-to-cell spread from the intracellular compartment (i) of U937 cells (in the presence of gentamicin) at 24 h p.i. Each condition represents two sections in each of three explants. Bars = SEM.

Figure 7
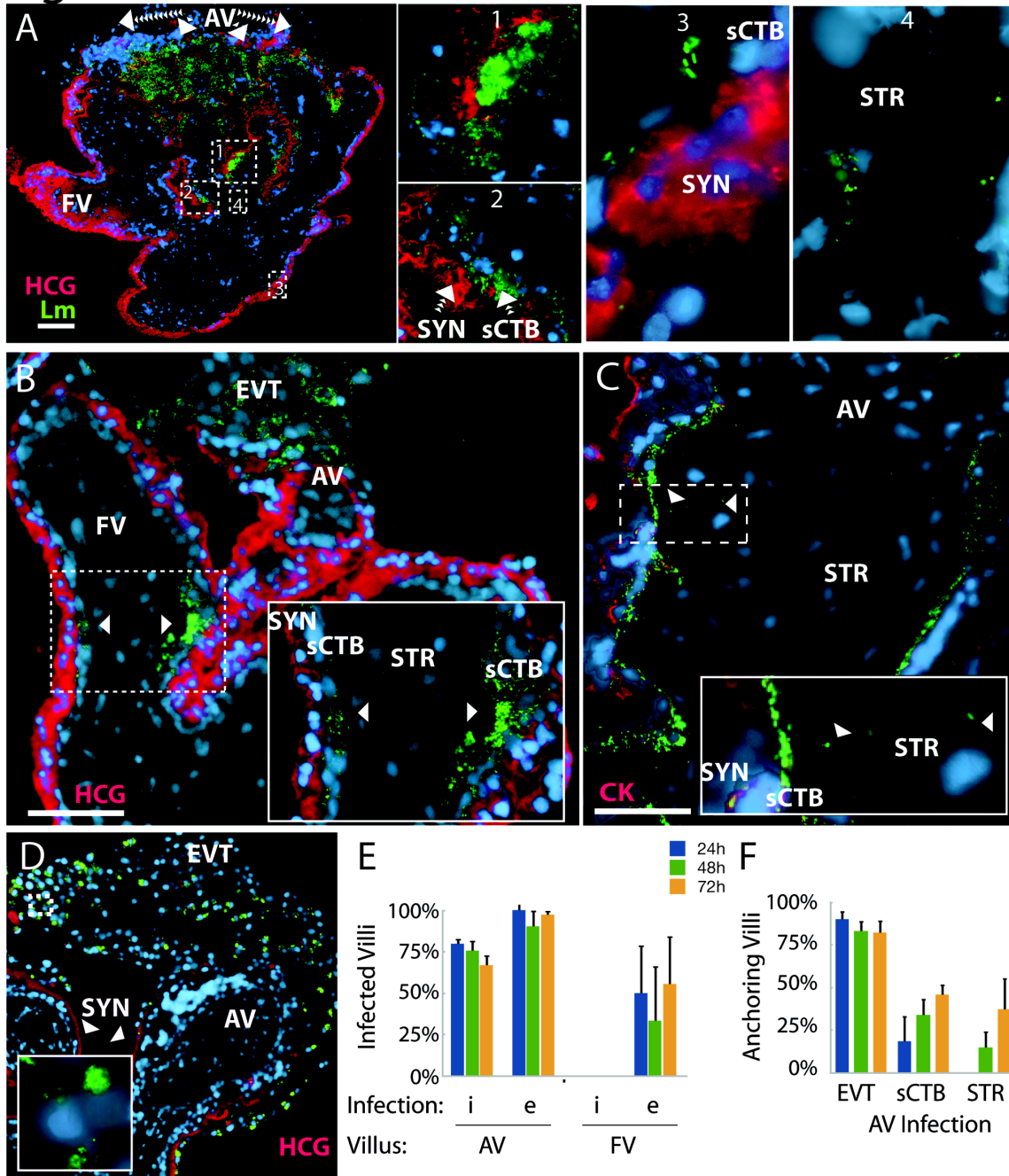
Figure 7. Infection progresses from extravillous cytotrophoblasts to stroma over 72 hours. (A) Histological section of explant permissively infected by *L. monocytogenes* at 72 hours post-inoculation (p.i.)**.** Inset numbers correspond with right panels. Anchoring villi (AV) are major loci of infection, while floating villi

(FV), which lack extravillous cytotrophoblasts (EVT), remain relatively uncolonized. Syncytiotrophoblast (SYN), indicated by ßHCG (HCG, red) is still largely uninfected, with spread moving down the subsyncytial cytotrophoblasts (sCTB, insets 1 - 3) and occasionally crossing into stroma (STR, inset 4). **(B)** AV infection progresses from EVT toward fetus, while FV infection begins at the villus base. Here, a permissive infection shows dissemination from an anchoring villus (top center) to an FV, where bacteria circumnavigate the sCTB (arrowheads) while leaving SYN uninfected. **(C)** Infection from U-937 cells at 72 hours p.i. shows bacteria concentrated in sCTB and bounded by the basement membrane that underlies them. A few bacteria have spread into STR (arrowheads, inset) where fetal capillaries are found. Red = cytokeratin (CK, stains cytotrophoblasts). **(D)** Explant permissively infected with ΔActA *L. monocytogenes*, which cannot spread from cell to cell. EVT are filled with bacteria (inset). Red = ßHCG. **(A-D)** Green = *L. monocytogenes*, Blue = DAPI. Bar = 100 µm. **(E)** Percentage of AV and FV infected by *L. monocytogenes* introduced by cell-to-cell spread (i) or from extracellular media (e). FV infection was sporadic. **(F)** Dissemination of bacteria introduced by both means in AV. All infected AV contained bacteria in EVT. At later time points, infection of subsyncytial cytotrophoblasts and stroma rose. Stromal infection was not observed without sCTB infection. **(E-F)** Each condition represents two sections separated by at least 30 µm on the Z-axis in each of three placentas infected by each means. Bars = SEM.

Chapter 3

Invasive EVT Restrict Intracellular Growth and

Spread of *Listeria monocytogenes*

Previously published as:

Zeldovich VB, Robbins JR, Kapidzic M, Lauer P, Bakardjiev AI (2011) Invasive

extravillous trophoblasts restrict intracellular growth and spread of *Listeria*

monocytogenes. PLoS Pathog 7: e1002005.

Introduction

L. *monocytogenes* is a ubiquitous, facultative intracellular, Gram-positive bacterium that causes food-borne disease in humans and other mammals [22, 23]. Humans are exposed relatively frequently to L. *monocytogenes*: healthy adults in the United States are estimated to ingest 10^5 bacteria at least four times per year [35]. Ingestion of L. *monocytogenes* by an immunocompetent host is relatively innocuous, but in immunocompromised individuals and pregnant women listeriosis is a severe disease [22, 36]. In the US there are ~530 cases per year of listeriosis during pregnancy (FDA, 2009). The clinical manifestations depend on the gestational age. During the second trimester L. *monocytogenes* is the cause of ~3% of spontaneous abortions [39, 40]. Infection around term results in neonatal disease with mortality of up to 50% [41]. The mechanisms by which L. *monocytogenes* infects the placenta and crosses the maternal-fetal barrier are controversial and still poorly understood.

The intracellular life cycle of L. *monocytogenes* has been characterized in a variety of different cell lines as well as primary murine bone marrow-derived macrophages [27, 28]. L. *monocytogenes* is taken up either by phagocytosis or internalized via interaction of bacterial surface proteins, such as internalin A (InlA), with host cell receptors, such as E-cadherin [29, 30]. After internalization, the bacterium finds itself in an endocytic vacuole that develops into a late endosome and acidifies slightly [31]. Acidification activates the pore-forming toxin listeriolysin O (LLO) that is important for escape of the bacterium into the host

cytosol, where *L. monocytogenes* replicates rapidly [32, 33]. The listerial protein ActA nucleates actin and allows *L. monocytogenes* to spread from cell-to-cell without exposure to the extracellular milieu [34].

The placenta has to protect the fetus from vertical transmission of pathogens while also providing an environment of immunological tolerance for the fetal allograft [52]. How the placenta accomplishes these contradictory tasks is unknown. It has long been postulated that the placenta is an immune-privileged organ that has diminished adaptive immune defenses in order to establish tolerance. However, low placental infection rates in the face of frequent pathogen exposure suggest that the organ itself must have defense mechanisms against infection.

What are the barriers of the placenta to infection and how is *L. monocytogenes* able to breach them? The placenta is comprised of maternal and fetal cells (Figure 1). Prior to implantation, the maternal uterine lining transforms into the receptive decidua. Shortly after, specialized fetally derived cells called trophoblasts differentiate into several subpopulations that perform critical placental functions. Specifically, invasive extravillous trophoblasts (EVT) anchor the placenta in the uterus and invade the decidua and maternal spiral arteries. Consequently, maternal blood flows into the intervillous space, bathing the fetally derived villous trees. These villi are covered by a continuous layer of multinucleate syncytium (SYN), a specialized trophoblast layer that mediates gas, nutrient and waste exchange between mother and fetus. The syncytium is

underlaid by progenitor cells called subsyncytial cytotrophoblasts (sCTB), which are separated by a basement membrane from the stroma of the villi where fetal capillaries are found.

We and others have previously shown that primary human placental organ cultures are relatively resistant to infection with *L. monocytogenes* [45, 50]. We utilized organ cultures from first trimester placentas to define where and how *L. monocytogenes* breaches the maternal-fetal barrier [45]. The syncytium that is in direct contact with maternal blood is highly resistant to infection. The other maternal-fetal interface is in the decidua where invasive EVT are in direct contact with maternal cells and tissues. Even though this interface has a much smaller surface area, it is the preferred site of initial placental infection. Indirect evidence suggested that EVT are capable of restricting intracellular growth and cell-to-cell spread of *L. monocytogenes* [101]. In this study, we further characterize the intracellular fate of *L. monocytogenes* in EVT*.*

We used a cell culture model system of primary human EVT [71] to understand how these specialized cells are able to delay or inhibit the intracellular life cycle of *L. monocytogenes*. We found that isolated EVT were able to restrict intracellular bacterial growth and spread. Furthermore, EVT prevented vacuolar escape and steered vacuolated bacteria towards degradation in lysozomes. This phenotype was strongest in invasive EVT, cells that *in vivo* are in contact with maternal tissues. Our results suggest that EVT have effective

51

defense mechanisms against intracellular pathogens and form a significant bottleneck in the transplacental transmission of pathogens.

Results

Culture of primary EVT

In order to examine the role of EVT in placental infection, we characterized the intracellular fate of *L. monocytogenes* in isolated primary human EVT. We used a well-established model system that has been previously used to study differentiation of progenitor cytotrophoblasts along the invasive pathway [72]. In this cell-culture system, cytotrophoblasts are isolated from second trimester placentas and induced towards differentiation along the invasive phenotype by culture on extracellular matrix such as Matrigel [69]. Tissue from the second trimester is used because the yield of cytotrophoblasts is higher than from first and term placentas [71]. Cytotrophoblasts are isolated by a series of enzymatic digestions and ficoll gradients. In order to assure a pure population of cytotrophoblasts, we performed a CD45-based depletion to remove any remaining immune cells prior to culture and differentiation. Cytokeratin 7, a cytotrophoblast marker [102], was used to determine the purity of the cell population. Generally our cell preparations contained over 95% cytotrophoblasts, with the remaining <5% being predominantly placental fibroblasts from the villous stroma (data not shown).

Intracellular fate of L. monocytogenes in EVT

EVT were infected with wild type *L. monocytogenes* at a multiplicity of infection (MOI) of 5. Gentamicin was added to the culture medium at 1 hour post-inoculation (p.i.) to eliminate extracellular bacteria. We observed a ~100-fold variation in susceptibility to infection across EVT from different placentas: 0.1-12% of EVT were infected, on average with one bacterium, at 2 hours p.i. This may be due to genetic differences between donors or heterogeneity in the condition of the placentas. We therefore normalized the growth of bacteria over time to the number of bacteria at the 2-hour time point for each placenta. Normalized data from 10 individual donor placentas was averaged to minimize the effects of individual differences. In contrast to almost all other previously studied cell types—which generally support *L. monocytogenes* growth [28]—intracellular bacteria in EVT decreased 2-fold between 2 and 5 hours p.i. and continued to decrease by 5-fold over the next 19 hours (Figure 8).

For comparison, the three commercially available human trophoblast-derived choriocarcinoma cell lines (BeWo, Jeg3, and Jar) were also infected at an MOI of 5, which resulted in significantly greater infection: ~14% of cells at 2 hours p.i. in BeWo (p = 0.004 by Student's T-test). Invasion of EVT and BeWo cells is InlA-dependent [44, 50, 101]. We observed lower levels of E-cadherin expression by immunofluorescence microscopy, the host cell receptor for InlA, in

isolated EVT in comparison to BeWo cells (data not shown), which most likely accounts for the difference in invasion between these two cell types.

In all of the choriocarcinoma cell lines *L. monocytogenes* grew with a similar doubling time of about 77 minutes between 2 and 5 hours p.i. (Figure 8 and data not shown). This is 2-fold slower than intracellular growth rates in murine macrophage cell lines [57], and in sharp contrast to the "halving time" of *L. monocytogenes* in EVT of about 310 min ($p < 10^{-4}$ by Student's T-test). In addition, we tested the fate of *L. monocytogenes* in primary human placental fibroblasts. These fibroblasts were isolated from a first trimester placenta [103] and propagated in culture for at least 10 generations before infection to ensure purity. To compare with EVT, placental fibroblasts were infected at an MOI of 60, which resulted in infection of ~1% of cells at 2 hours p.i. Subsequently, *L. monocytogenes* grew with a doubling time of 40 minutes between 2 and 5 hours p.i. (Figure 8).

Escape of L. monocytogenes into the cytosol

L. monocytogenes grows rapidly in the host cell cytosol [28], while mutants that are unable to access the cytosol generally do not replicate [57]. Therefore, the lack of intracellular growth of *L. monocytogenes* in EVT could be due to an inability to escape from the primary vacuole. We thus determined whether *L. monocytogenes* can escape from the primary vacuole in EVT and whether bacteria can be found in the host cell cytosol.

To determine vacuolar escape, we utilized a *L. monocytogenes* strain that expresses red fluorescent protein (RFP) under the *actA* promoter (p*actA*-RFP). ActA nucleates actin, and its transcription is up regulated 200-fold in the host cell cytosol [104, 105]. Therefore, the expression of RFP in this strain correlates with entry of bacteria into the cytoplasm [106]. In addition, polymerization of host actin filaments around bacteria indicates cytosolic localization of *L. monocytogenes* and can be visualized by staining fixed cells with fluorescently labeled phalloidin, a compound that binds F-actin [60].

First we analyzed vacuolar escape rates of *L. monocytogenes* in BeWo cells. We infected BeWo cells with p*actA*-RFP *L. monocytogenes* and fixed the cells for immunofluorescence microscopy at 2, 5, 8 and 24 hours. The preparation was counterstained with polyclonal anti-*Listeria* antibody to visualize the total number of bacteria per cell. Microscopic inspection of BeWo cells at 8 hours p.i. showed that the vast majority of bacteria expressed RFP (Figure 9A). The percentage of RFP-expressing bacteria increased from 17% to 95% between 2 and 8 hours p.i (Figure 9C). Consistent with high vacuolar escape rates in this cell line, the number of bacteria that co-localized with phalloidin steadily increased from 13% to 76% over the same time period (Figure 9C). Between 8 and 24 hours p.i. RFP expression remained at 95%, consistent with the long half-live of RFP [107], which led to RFP persistence in all bacteria that had escaped the primary vacuole. In contrast, phalloidin co-localization decreased to 53% at 24 hours p.i. The significant difference between RFP expression and phalloidin

co-localization at 8 hours p.i (p=0.04 by Student's T-test) and the observed decrease in phalloidin co-localization at 24 hours p.i. is most likely due to the fact that phalloidin staining provides a snapshot of intracellular bacteria that are in the actin-nucleating stage of their life cycle. In contrast to RFP expression, phalloidin does not co-localize with bacteria that have spread to neighboring cells and are still in the secondary vacuole. It is unlikely that host cell death at 24 hours p.i. contributes substantially to the decrease in phalloidin co-localization, because host cell death would lead to a significant decrease in intracellular bacteria as well [108], which we do not observe (Figure 8).

In contrast, infection of EVT with p*actA*-RFP *L. monocytogenes* counterstained with polyclonal anti-*Listeria* antibody revealed that the vast majority of bacteria did not express RFP at 8 hours p.i. (Figure 9B). Quantitation showed that less than 10% of *L. monocytogenes* expressed RFP over the 24-hour course of infection (Figure 9C), compared to nearly 100% in BeWo cells (p < 10^{-5} by Student's T-test). In addition, no co-localization of *L. monocytogenes* with phalloidin was observed in EVT (data not shown). Our results suggest that bacteria are unable to grow in EVT because they are trapped in the primary vacuole.

In the murine model of infection the virulence factor LLO, a cholesterol-dependent pore-forming cytolysin, is essential for vacuolar escape [109]. We evaluated the role of LLO in the intracellular fate of *L. monocytogenes* in EVT. We tested two bacterial strains: DP-L2161 which is deficient in LLO [99] and

unable to grow in BeWo cells (data not shown) and DP-L4057 which has a mutation in LLO (S44A) that increases phagosomal escape in murine bone marrow derived macrophages [91]. The outcome of infection did not differ from wild type infection - both strains were eliminated in EVT over 24 hours - although with slightly different kinetics (see Figure 20 in Chapter 4). These results suggest the possibility that LLO function is impaired in EVT.

The L. monocytogenes-containing vacuole in EVT

The maturation of *L. monocytogenes*-containing vacuoles has been studied in detail in murine macrophage cell lines (RAW 264.7 and J774A.1) [31]. Wild type *L. monocytogenes* escapes from a vacuolar compartment that includes the late endosomal marker Rab7. The early endosomal marker Rab5 does not associate with *L. monocytogenes* even at very early time points after phagocytosis. If the vacuole matures further and acquires the lysosomal marker Lamp1, the rate of vacuolar escape is minimal.

To characterize the vacuolar compartment that *L. monocytogenes* occupies in EVT, we examined these same markers. The early endosomal marker Rab5 was associated with less than 10% of bacteria at 2 and 5 hours p.i. (Figure 10A). The late endosomal marker Rab7 was found to co-localize with 55% of bacteria at 2 hours p.i. and with over 40% of bacteria at all other time points through 24 hours of infection (Figure 10B,C). Lamp1 co-localized with only

57

12% of bacteria at 2 hours p.i. and increased steadily to 40% at 24 hours p.i. (Figure 10B,D).

To test whether the *L. monocytogenes*-containing vacuole in EVT becomes acidified, we used the acidotropic dye Lysotracker. Lysotracker staining followed a similar trend to Lamp1 staining: 17% of bacteria were found in an acidified compartment at 2 hours p.i., increasing to 51% at 24 hours p.i. (Figure 10B,E).

While it is generally believed that *L. monocytogenes* replicates in the cytoplasm and not in vacuoles, there have been a few reports suggesting the possibility of slow replication in vacuolar compartments. Bhardwaj et al. described the presence of multiple bacteria in membrane-bound vacuoles in mononuclear cells in the liver of SCID mice with chronic listeriosis [110]. Furthermore, Birmingham et al. found that 13% of bacteria in a murine macrophage cell line were replicating slowly in autophagosome-like vacuolar compartments (LC3-positive, LAMP1-positive, non-acidified) and named these structures SLAPS (spacious *Listeria*-containing autophagosomes) [111]. We therefore evaluated whether *L. monocytogenes* co-localizes with the autophagy marker LC3, but found little to no co-localization in our system (Figure 10A). We concluded that bacteria in EVT are trapped in vacuoles that mature into acidified lysozomes, suggesting that *L. monocytogenes* is degraded in this compartment.

Vacuolar localization of L. monocytogenes

To look more closely at the subcellular localization of *L. monocytogenes* in EVT, transmission electron microscopy was performed. EVT were infected with wild type *L. monocytogenes* at an MOI of 60. This high inoculum was used to increase the number of infected cells and the number of bacteria/cell for better visualization. Because the most significant decrease in intracellular bacterial numbers occurred between 2 and 5 hours p.i. (Figure 8), infected EVT at those time points were examined (Figure 11A,B). The number of vacuolar *L. monocytogenes* was enumerated: at both time points, 81-86% of bacteria were confined to vacuoles (Figure 11C). These escape rates (14-19%) are slightly higher than those measured using the p*actA*-RFP strain above. This difference is significant ($p = 0.004$ by Student's T-test) and is likely due to differences in the infection (MOI of 5 versus 60) and/or due to a more limited detection threshold of RFP fluorescence as compared to electron microscopy. Furthermore, we enumerated the number of bacteria that appeared intact versus degraded. Intact appearing bacteria decreased from 67% to 50% between 2 and 5 hours p.i., and degraded bacteria increased from 33% to 50% during the same time interval (Figure 11D,E,F).

A vacuolar compartment derived from the primary vacuole consists of a single lipid bilayer, whereas secondary vacuoles (a result of infection via cell-to-cell spread) and autophagosomes typically consist of two lipid bilayers [34, 112]. With a membrane contrast-enhancing stain and at higher magnification the membranes of the *L. monocytogenes*-containing vacuoles were visualized and

59

appeared to consist of a single lipid bilayer (Figure 11E). These ultrastructural results are consistent with bacterial entrapment in the primary vacuole and degradation in lysozomes.

Vacuolar escape of L. monocytogenes in placental explants

We previously found that EVT are the preferred initial site of infection for *L. monocytogenes* in first trimester placental organ cultures [45]. Furthermore, we observed that *L. monocytogenes* is able to spread beyond the EVT along sCTB in some placentas. Under the conditions Robbins et al. used, such spread occurs in 50% of placentas over a time period of 72 hours. The inability of *L. monocytogenes* to escape from the primary vacuole in EVT could explain the delay or lack of listerial dissemination in placental organ cultures. Thus, we analyzed the rates of vacuolar escape in first trimester placental organ cultures infected with p*actA*-RFP *L. monocytogenes* and counterstained with polyclonal anti-*Listeria* antibody as described above (Figure 12A,B). At 8 hours p.i., only 14% of bacteria had escaped the vacuole, while 39% and 37% were in late endosomes and lysozomes respectively (Figure 12C). By 24 hours p.i. the percentage of RFP-expressing bacteria increased to 23% and the proportion of *L. monocytogenes* co-localizing with Rab7 and Lamp1 remained around 40% (Figure 12C).

Vacuolar escape rates in placental organ cultures were somewhat higher than those observed in isolated second trimester EVT (Figure 9C; p = 0.19 by

Student's T-test). We therefore decided to test whether vacuolar escape rates differ between distinct trophoblast subpopulations. When isolated cytotrophoblasts are grown on Matrigel they differentiate along the invasive pathway and therefore consist of a more homogeneous EVT population [71, 72]. In contrast, there are several distinct subpopulations of trophoblasts *in vivo* and *ex vivo* that are in different stages of differentiation ranging from progenitor cytotrophoblasts near the stroma to invasive EVT at the outer villus margin. Therefore, infection of placental organ cultures leads to infection of a mixed population of trophoblasts.

To test whether listerial escape rates differ in different trophoblast subpopulations, we compared escape rates in three distinct populations of trophoblasts: (1) trophoblasts that were in contact with Matrigel (invasive border EVT), (2) trophoblasts that were surrounded by other trophoblasts on all sides (middle EVT), and (3) those that were in contact with the basement membrane and its underlying stroma (parastromal trophoblasts) (Figure 13A-C). We increased the dose of *L. monocytogenes* to 2×10^7 bacteria/mL for 5 hours before addition of gentamicin in order to achieve infection of all three subpopulations within one placenta at 24 hours p.i., and compared escape rates between invasive border EVT, middle EVT and parastromal trophoblasts at 24 and 48 hours p.i. (Figure 13D,E). The average escape rate in invasive border EVT at 24 hours p.i. was 40% (range 11% to 55%). Because of this large variability between placentas from different donors, we normalized the escape rates in middle EVT

and parastromal trophoblasts to the escape rate in invasive border EVT from the same placenta. At 24 hours p.i. we determined the fold-difference in escape rates in middle EVT and parastromal trophoblasts in comparison to the escape rate in invasive border EVT from the same placenta. Vacuolar escape rates increased the closer the trophoblasts were to the core of the placental villus. The average increase in escape rates compared to invasive border EVT was 1.21-fold in middle EVT and 1.51-fold in parastromal trophoblasts (Figure 13E). At 48 hours p.i. we determined the fold difference in escape rates in all three subpopulations in comparison to the escape rate in invasive border EVT at 24 hours p.i., and found similar results. The average increase in escape rates was 1.14-fold (invasive EVT), 1.54-fold (middle EVT), and 1.76-fold (parastromal trophoblasts) ($p = 0.02$ by Student's T-test for combined 24- and 48-hour time points). We concluded that EVT at the invasive border—a cell type that is in direct contact with maternal cells *in vivo*—are especially prohibitive for listerial vacuolar escape. However, if *L. monocytogenes* is able to spread beyond the invasive EVT it can find a more hospitable environment.

Discussion

Much of the pioneering work on the *L. monocytogenes* life cycle and intracellular growth kinetics has been performed in murine bone marrow derived macrophages as well as various murine and human cell lines [28, 34, 113]. In these cells, *L. monocytogenes* vacuolar escape rates are 80% or higher [106,

114], and bacteria grow rapidly (generation time of ~40 min) in the nutrient-rich cytosol [57]. In contrast, the vacuolar escape rates in isolated primary EVT were less than 10%.

It is possible that vacuolar escape and growth rates vary depending on the specific cell type, especially in cells that play a role in host defense against infection. For example, primary murine dendritic cells are less hospitable to *L. monocytogenes* than primary bone marrow-derived mouse macrophages [114, 115]. Westcott et al. showed that bacterial doubling time is about 2-fold slower in primary murine dendritic cells (~70 min), and only ~40% of the bacteria escape into the cytosol. Specific endosomal maturation features in dendritic cells that are important for efficient processing and presentation of bacterial antigens to T cells are thought to be the underlying reason for these decreased vacuolar escape rates. Primary murine peritoneal macrophages are even more hostile to *L. monocytogenes*: Portnoy et al. has demonstrated that these cells kill ~80% of *L. monocytogenes* during the first 2 hours p.i. and that surviving bacteria grow at a generation time of ~120 min or longer [116]. Furthermore, if resident peritoneal macrophages are stimulated with IFNγ, bacterial growth is eliminated, and 95% of bacteria are found in vacuolar compartments [116]. While these activated professional immune cells are known to be critical in scavenging and containing infectious particles, it is more surprising that epithelial cells in the placenta, the EVT, would possess a similar bacteriocidal phenotype. In this context, it is interesting that IFNγ is crucial for a successful pregnancy and present at high

levels at the maternal-fetal interface [117]. IFNγ is produced by uterine natural killer cells, which comprise approximately 20-40% of the leukocytes in the decidua [118, 119], and IFNγ receptors are expressed on human trophoblast cells throughout pregnancy [120]. It is possible that residual effects of *in utero* IFNγ exposure contribute to decreased vacuolar escape and increased bacterial degradation in EVT.

Why are bacteria not able to escape the vacuole in EVT? In the murine model of infection the virulence factor LLO is essential for vacuolar escape [109]. We found that lack of LLO or increased hemolytic activity of LLO did not alter the outcome of infection in EVT, suggesting that LLO function is impaired in this cell type. LLO-mediated pore formation is a pH dependent process, with a pH optimum of 5.5 [121, 122]. Although the *Listeria*-containing vacuole in EVT acidifies, the kinetics or extent of acidification could present unfavorable conditions for LLO function. For example LLO loses its hemolytic activity at neutral pH in less than 10 min [123]. Another possibility is that the *Listeria*-containing vacuole has a different lipid composition that renders LLO non-functional. LLO is dependent on the presence of cholesterol, which is utilized by EVT for the synthesis of progesterone [124]. Specialized hormone synthesis in EVT could lead to differences in cholesterol metabolism and/or distribution in these cells, rendering it inaccessible to vacuolar LLO. Moreover, the active form of a host-derived thiol reductase (GILT) involved in antigen processing has been shown to be required for the activation of LLO [125], and may not be present or

64

accessible in the *Listeria*-containing vacuole in EVT. However, all of the above mentioned studies have been performed in the murine model of infection. In contrast, in many human cell types *L. monocytogenes* deficient in LLO is capable of vacuolar escape [57, 126, 127]. The mechanisms of LLO-independent vacuolar escape are poorly understood [128], but the existence of these examples opens up a myriad of other pathways that may be different in EVT, that ultimately could lead to vacuolar entrapment of *L. monocytogenes*. Further studies will be needed to assess these possibilities.

Work in several pregnant animal models of listeriosis supports our findings that *L. monocytogenes* has to pass several bottlenecks to infect the placenta and spread to the fetus. We have shown previously that the placenta in the pregnant guinea pig model is relatively protected from colonization, characterizing the kinetics of bacterial spread from maternal organs to the placenta and to the fetus [51]. The guinea pig placenta is colonized with 10^4-fold fewer bacteria than maternal liver and spleen after intravenous inoculation, and the bottleneck between placenta and fetus is again $1:10^4$ bacteria. Studies in the pregnant mouse and gerbil models also require high intravenous inoculums, $>10^6$ bacteria, to induce placental infection [43, 67].

Interestingly, there are several lines of evidence that suggest EVT are a suboptimal niche for the growth of intracellular pathogens in general. Human CMV infection, for example, is inefficient in trophoblasts, progresses slowly, and releases only small amounts of progeny virus [129]. Likewise, placentas infected

with CMV *in utero* show rare viral replication in EVT, with membrane-clustered virions [130]. Recent studies with HIV-1 indicate that EVT are also non-permissive to HIV-1 replication due to active degradation and/or passive inactivation of critical viral replication mechanisms [131]. Others have observed that the majority of HIV-1 virions are trapped within endosomal compartments [132]. The common thread in these studies is that vacuolar or endosomal trafficking is hindering the normal life cycles of pathogens and preventing growth and spread of the virus or bacterium. While little is known about EVT in general, ultrastructural studies of uninfected human placentas report many unidentified vesicles and vacuoles in EVT [133, 134]. It is possible that the invasive role of EVT and their active degradation of extracellular matrix may require unique degradative and/or endosomal pathways that interfere with the life cycle of intracellular pathogens. As a result, EVT create a significant barrier to infection, and pathogens must get past the bacteriocidal EVT into more permissive cells in the placenta for the infection to progress.

If the primary site of infection is an inhospitable cell-type, then how does placental infection progress to cause pregnancy complications and fetal infection? One possibility is that even though EVT are the preferred site of initial infection with *L. monocytogenes* [45] and *Toxoplasma gondii* [135] and can harbor CMV *in utero* [88], they are a dead end for pathogens. This seems unlikely because we have not observed placental infection without infection of EVT, and *L. monocytogenes* can spread beyond EVT in some placentas [101]. In

addition, other routes of crossing the trophoblast barrier appear even more difficult, since the syncytium is highly resistant to infection with *L. monocytogenes* [45] and *T. gondii* [135]. It is possible that EVT could differ in their resistance to infection due to host genotypic differences. This would mean that some people are simply more predisposed to placental infection and pregnancy complications than others. However, to our knowledge no genetic basis for differences in susceptibility to vertical transmission has ever been identified.

We hypothesize that EVT can either contain or eliminate an infection until a certain threshold of cellular damage or placental inflammation is surpassed. For instance, non-infectious pregnancy complications that influence oxygen tension or pH in the placenta could alter the biochemical and/or physiological condition of EVT and decrease their resistance to infection. Co-infection with other pathogens could similarly escalate an immune imbalance at the maternal-fetal interface. If these imbalances threaten the healthy progression of pregnancy, spontaneous abortion or preterm labor are initiated to avoid continuation of pregnancy with a compromised placenta.

The placenta has developed a marvelous defense against infection, most likely consisting of multiple layers of physical and biochemical barriers. Both subpopulations of trophoblasts—syncytium and EVT—that are in direct contact with maternal cells and tissues are effective barriers against infection. The syncytium is in direct contact with maternal blood and is highly resistant to infection. The EVT are in close contact to maternal cells and tissues in the

implantation site, and are the preferred initial sites for infection, but are inhospitable to a variety of intracellular pathogens. Both barriers can probably be breached by additional damage, resulting in infection of subsyncytial cytotrophoblasts, which appear to be more hospitable to intracellular replication of pathogens. Nevertheless, *L. monocytogenes* still has to pass another physical barrier: the basement membrane [45], to reach the villous stroma where the fetal capillaries are. *L. monocytogenes* will serve as an excellent model to characterize the precise molecular basis of the maternal-fetal barrier.

Methods

Ethics statement

This study was conducted according to the principles expressed in the Declaration of Helsinki. The study was approved by the Institutional Review Board at the University of California, San Francisco, where all experiments were performed (H497-00836-29). All patients provided written informed consent for the collection of samples and subsequent analysis.

Human tissue collection, cell isolation and culture

All chemicals were purchased from Sigma-Aldrich unless otherwise stated. For human placental organ cultures, placentas from elective terminations of pregnancy (gestational age 4 to 8 weeks) were collected and prepared as

68

previously described [90]. Briefly, fragments from the surface of the placenta were dissected into 1–3 mm tree-like villi, placed on Matrigel (BD Biosciences, San Jose, CA)-coated Transwell filters (Millipore, Bedirica, MA, 30-mm diameter, 0.4 um pore size) and cultured in Dulbecco's modified Eagle-F12 medium (DMEM-F12; 1:1, vol/vol) supplemented with 20% fetal bovine serum (FBS, Fisher Scientific), 1% L-glutamine and 1% penicillin/streptomycin (Invitrogen, Carlsbad, CA).

For EVT isolation, placentas from elective terminations of pregnancy (gestational age 14 to 24 weeks) were collected and prepared as previously described [72, 136]. Briefly, placentas from normal uncomplicated pregnancies were obtained immediately after aspiration and subjected to a series of enzymatic digestions followed by purification over a Percoll gradient. Remaining leukocytes were removed using a magnetic-bead-based EasySep CD-45 Depletion Kit with RoboSep device (Stem Cell Technologies, Vancouver, Canada). For growth curves, purified cells were plated on Matrigel-coated Transwell filters (Millipore, Bedirica, MA, 12-mm diameter, 0.4 um pore size) in serum-free DMEM-high glucose, with 2% Nutridoma (Roche Diagnostics, Indianapolis, IN), 1% L-glutamine, 1% sodium pyruvate, 1% 25mM HEPES, 1% penicillin/streptomycin at a concentration of 1.25×10^5 cells/transwell. For immunofluorescence microscopy, purified cells were plated on Matrigel-coated 6-well plates at a concentration of 2×10^6 cells/well.

Placental fibroblasts were isolated as described [103] from a placenta at gestational age 8 weeks, and were cultured in DMEM-high glucose with 10% FBS, 18% M-199, 1% penicillin/streptomycin. For growth curves and immunofluorescence microscopy, cells were plated on glass coverslips in 24-well plates at 2.5×10^5 cells/well.

Cell lines

The choriocarcinoma cell line BeWo (ATCC CCL-98) was cultured in Ham's F12 medium with 10% FBS, 1% L-glutamine, 0.15% sodium bicarbonate, 1% penicillin/streptomycin. For growth curves and immunofluorescence microscopy, cells were plated on glass coverslips in 24-well plates at 2.5×10^5 cells/well.

Pathogen strains and growth conditions

L. monocytogenes 10403S expressing GFP (strain DH-L1252) was a gift from Darren Higgins [137]. The p*actA*-RFP strain (PL512) was constructed as follows: The ORF encoding TagRFP from *Entacmaea quadricolor* [107] was codon optimized for expression in *L. monocytogenes* using Gene Designer software [138] and the gene was synthesized *de novo* (DNA2.0, Menlo Park, CA). The synthetic gene was cloned downstream of the *actA* promoter in the vector pPL2 and stably integrated at the *tRNA*^{Arg} locus of the bacterial chromosome in the wild type *L. monocytogenes* strain DP-L4056 as described

previously [139]. Molecular constructs were confirmed by DNA sequencing. For infections, bacteria were grown overnight to stationary phase in BHI (Brain Heart Infusion broth) at 30°C and washed once with PBS before dilution and infection.

L. monocytogenes infection

Cells were incubated in antibiotic-free medium for 1hour before infection. Bacteria were added for 30 minutes, followed by three washes with PBS and addition of antibiotic-free medium. For CFU determination gentamicin (50 µg/mL) was added at 60 minutes p.i. EVT were inoculated with 3×10^6 bacteria/mL (MOI 5), and placental fibroblasts with 4×10^7 bacteria/mL (MOI 60). At indicated times, cells were lysed with distilled water, aliquots were plated on BHI agar plates, and CFU were enumerated. Infection for immunofluorescence microscopy was performed as outlined above with following modification: at 60 minutes p.i. Matrigel was dissolved by incubation with BD Cell Recovery Solution (BD Biosciences, San Jose, CA) for 40 minutes, and cells were re-plated on fresh Matrigel on Transwell filters in media containing gentamicin (50 µg/mL). Therefore, gentamicin was added at 1 hour 45 minutes p.i. to infected cells that were analyzed by immunofluorescence microscopy. CFU after exposure to the enzymatic solution and gentamicin addition at 1 hour 45 min were not significantly different from those under standard CFU (gentamicin at 1 hour p.i.) conditions (data not shown). For electron microscopy, EVT were infected as above with the following alteration: the infectious dose was 4×10^7 bacteria/mL

(MOI 60). Infection of placental explants was performed as previously described [45] with the following alteration: the infectious dose was lowered to 3×10^6 bacteria/mL for 30 minutes.

Immunofluorescence

Explants were fixed in 3% paraformaldehyde, passed through a sucrose gradient and snap-frozen in OCT (Ted Pella, Redding, CA). Histological slicing was performed on a Hacker-Slee cryostat. Glass slides with sections were incubated in acetone, soaked in blocking solution (1% bovine serum albumin (BSA) in PBS), then incubated with primary antibodies, rinsed in PBS, incubated with secondary antibodies, and affixed over Vectashield mounting medium with DAPI (Vector Laboratories, Burlingame, CA).

Cultured cell lines and EVT were fixed in 3% paraformaldehyde. For Lysotracker visualization, the dye was added to cells for 30 minutes at 5 µM and washed in PBS before fixation. For Rab7 staining, cells were rinsed in glutamate lysis buffer (25 mM HEPES, 25 mM potassium chloride, 2.5 mM magnesium acetate, 5 mM EGTA, 150 mM K-glutamate), dipped into liquid nitrogen, rinsed in lysis buffer, and fixed in paraformaldehyde. Transwell filters were cut out of wells, blocked and permeabilized in 1% BSA and 0.1% Triton-X100, then stained as described above in BSA/TritonX-100/PBS solution.

Primary antibodies: polyclonal rabbit *Listeria* O antiserum (1:1000 BD Biosciences, San Jose, CA), mouse polyclonal Lamp1 antiserum (1:100 DSHB at University of Iowa), mouse monoclonal Rab5 antibody (1:100, BD Biosciences, San Jose, CA), mouse monoclonal LC3 antibody (1:100, gift from Dr. Jay Debnath), rabbit monoclonal Rab7 antibody (1:1000, gift from Dr. Suzanne Pfeffer). Secondary antibodies: Alexa Fluor 594 goat anti-mouse IgG (1:500, Invitrogen), Alexa Fluor 488 and 594 goat anti-rabbit IgG (1:1000 & 1:500, Invitrogen).

Slides were viewed using an inverted TE2000-E microscope (Nikon, Tokyo, Japan) equipped with a 12-bit cooled CCD camera (Q imaging, Surrey, Canada). Images were collected using Simple PCI software (Hamamats, Sewickley, PA).

Transmission Electron Microscopy

For the 2-hour time point, cells were fixed overnight at 4°C in 3% gluteraldehyde, 1% paraformaldehyde in 0.1 M cacodylate buffer. Fixed cells were post-fixed with 2% osmium tetroxide, dehydrated in ethanol and embedded in Epon. Thin sections (70 nm) were cut using a Leica Ultracut-UCT Microtome (Leica Microsystems, USA). Observations were made under a Philips Tecnai 10 transmission electron microscope (Department of Pathology, UCSF), and digital acquisition was performed with a CCD camera (Maxim DL Software, Cyanogen, Canada). For the 5-hour time point, cells were fixed as above, and post-fixed with

1% osmium tetroxide and 1.6% potassium ferrocyanide, stained with 5% uranyl acetate solution, dehydrated with ethanol and embedded. Sections were cut using a microtome (RMC MTX, Reichert Ultracut E, RMC MT6000) and observations made under a Philips Tectani 12 transmission electron microscope (EM lab, UC Berkeley). For quantification, 100 bacteria at each time point were counted and categorized by cytoplasmic versus vacuolar localization and intact versus degraded bacteria.

Image Processing

Images were prepared using ImageJ (RSB, Bethesda, MD), Photoshop and Illustrator (Adobe, San Jose, CA). RGB hues were linearly adjusted but no non-linear alterations were performed.
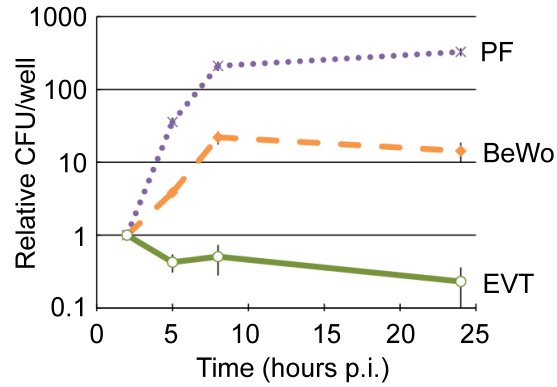
Figure 8. EVT restrict intracellular growth of *L. monocytogenes*. Intracellular growth curves of wild type *L. monocytogenes* in 3 cell types: primary placental fibroblasts (PF), choriocarcinoma cell line (BeWo), and primary extravillous trophoblasts (EVT). CFU/well were normalized to the 2-hour time point within each experiment. Each data point is an average of 3 independent experiments for PF and BeWo, and 10 independent experiments for EVT. Bars represent SEM.
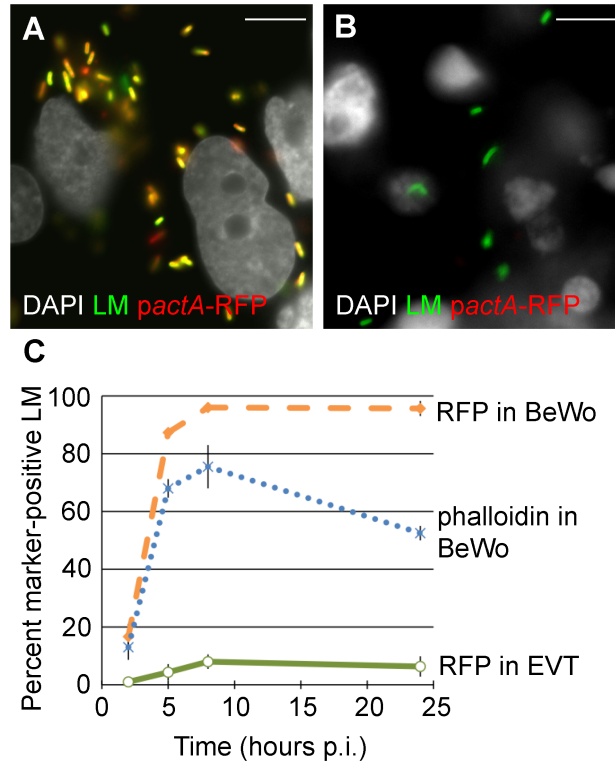
Figure 9. Vacuolar escape of *L. monocytogenes* (LM) is strongly impaired in EVT. BeWo cells and EVT were infected with p*actA*-RFP LM and counterstained with anti-LM antibody (green). **(A,B)** Representative images of BeWo **(A)** and EVT **(B)** 8 hours post-inoculation (p.i.). DAPI counterstain (white). Scale bar is 10 μm. **(C)** Percent RFP-expressing bacteria were enumerated and represent bacteria that escaped from the primary vacuole. Actin nucleation by wild type LM in BeWo cells was measured by co-localization with phalloidin. Bacterial RFP expression and phalloidin-co-localization are expressed as a percentage of the total number of intracellular bacteria. Each data point is an average of 3 independent experiments. Bars represent SEM.
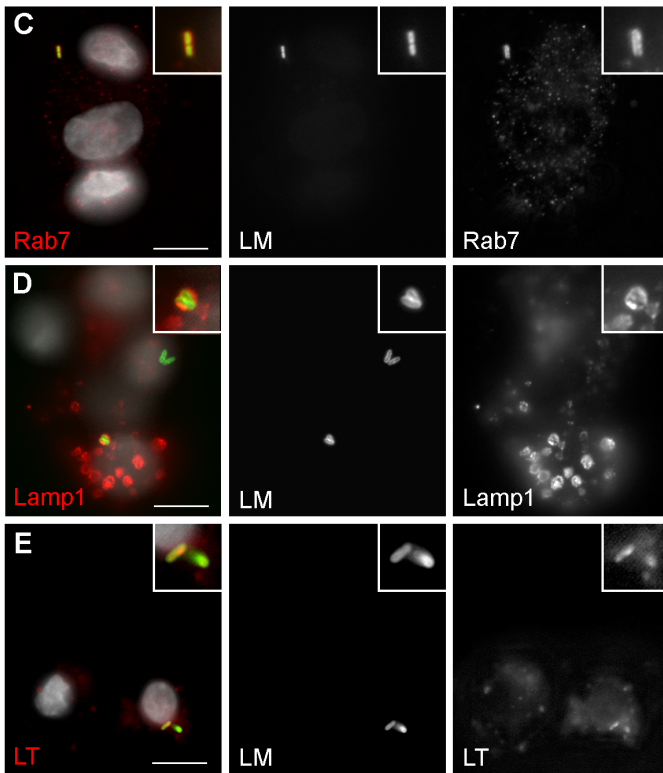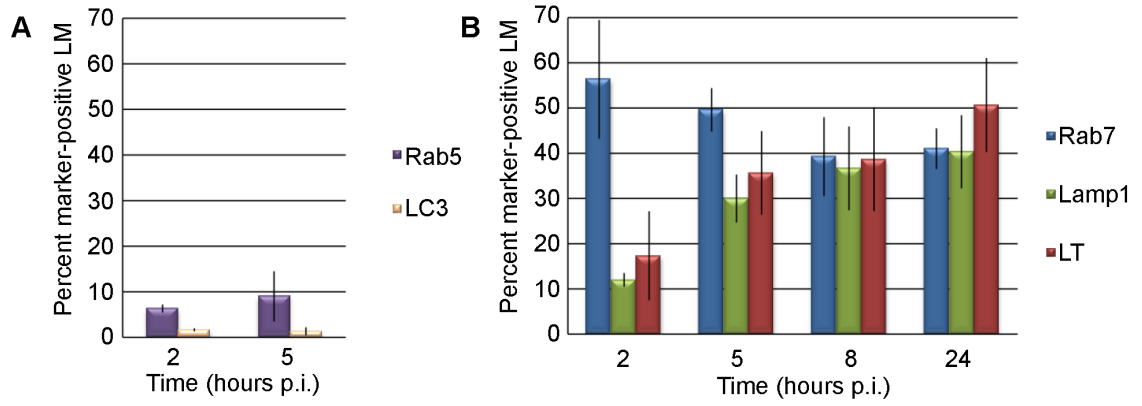
Figure 10. *L. monocytogenes* **(LM) is trapped in late endosomes and acidified lysozomes in EVT. (A)** Percent co-localization of early endosomal marker Rab5 and autophagosomal marker LC3 with LM. **(B)** Percent co-localization of late endosomal marker Rab7, lysosomal marker Lamp1 and acidotropic dye Lysotracker (LT) with LM. p.i. = post-inoculation. Each data point is an average of 3 independent experiments. Bars represent SEM. **(C-E)** Representative images of GFP-expressing LM (green) co-localizing with markers Rab7, Lamp1, and LT (red). The color-merged images also show DAPI counterstain (white). Scale bars are 10 μm.
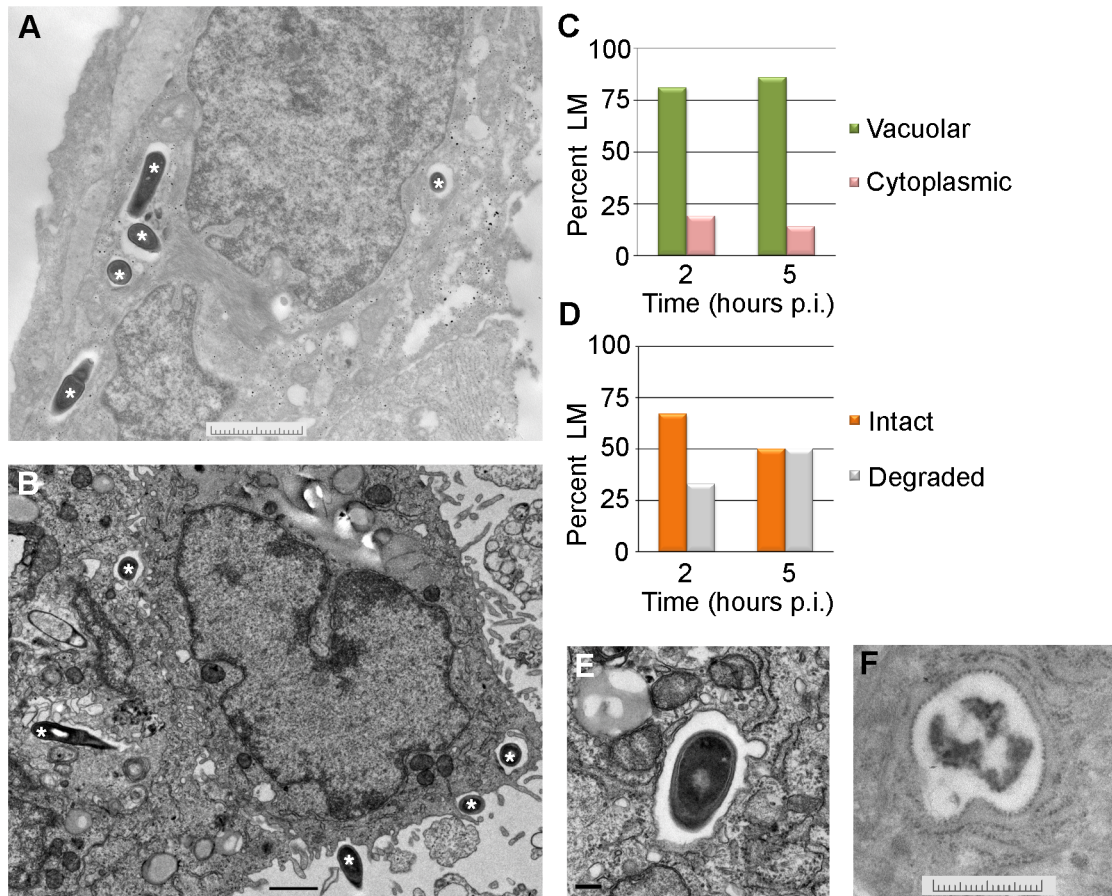
Figure 11. ***L. monocytogenes*** **(LM) in EVT is largely confined to vacuoles.**
(A,B) Representative transmission electron micrographs from 2 **(A)** and 5 **(B)** hours post-inoculation (p.i.). Bacteria are marked with asterisks. Scale bars are 2 and 1 µm respectively. **(C)** Quantification of subcellular localization of bacteria in EVT at 2 and 5 hours p.i. **(D)** Quantification of intact versus degraded bacteria in vacuoles in EVT at 2 and 5 hours p.i. **(E)** Close-up image at 5 hours p.i. shows a single membrane vacuole surrounding intact bacterium. Scale bar is 100 nm. **(F)** Close-up image of degraded bacterium in a vacuole in EVT at 5 hours p.i. Scale bar is 2 µm.
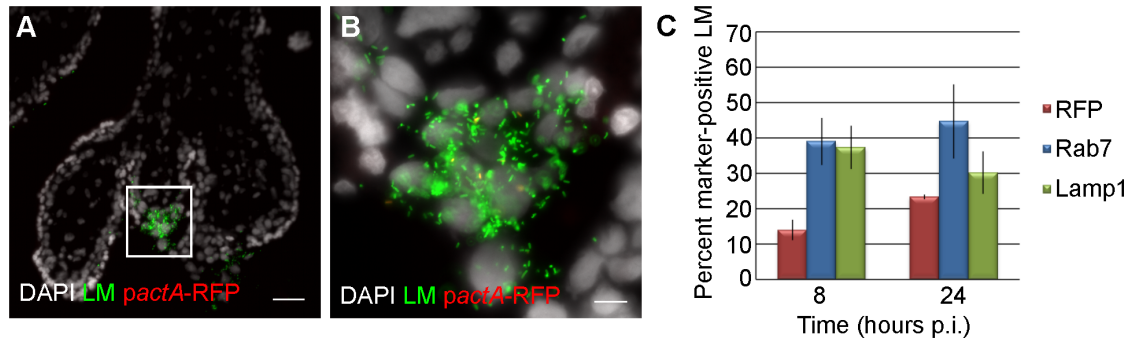
Figure 12. *L. monocytogenes* **(LM) is trapped in late endosomes and lysozomes in EVT of placental explants. (A)** Representative image of placental explant 8 hours post-inoculation (p.i.) with p*actA*-RFP LM counterstained with anti-LM antibody (green). DAPI counterstain (white). Scale bar is 50 µm. **(B)** Close-up of boxed area in panel A. Scale bar is 10 µm. **(C)** Vacuolar escape measured by percent RFP expression of p*actA*-RFP strain counterstained with anti-LM antibody (green). Percent co-localization of LM with late endosomal marker Rab7 and lysosomal marker Lamp1. Each data point is an average of 3 independent experiments. Bars represent SEM.
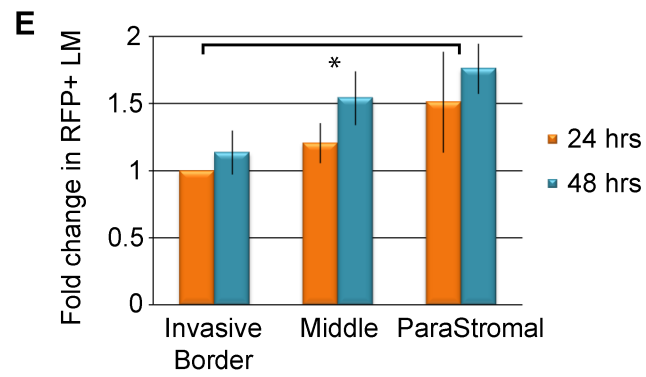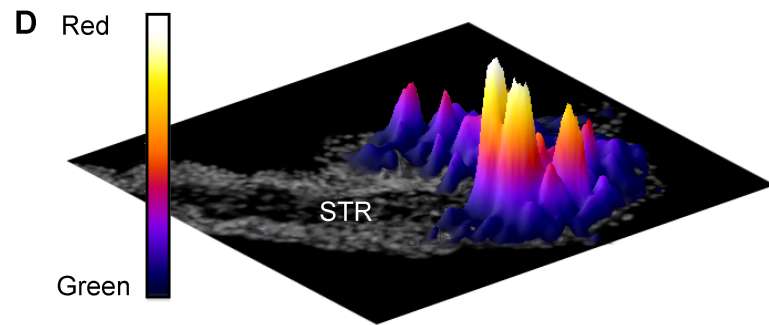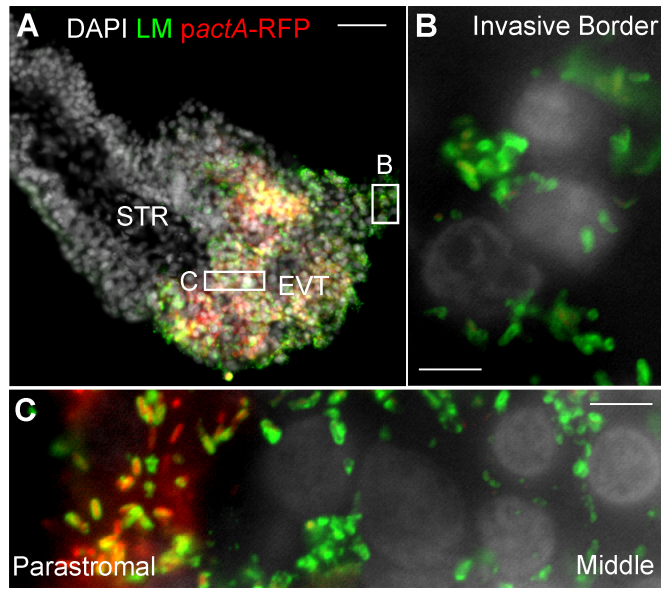
Figure 13. *L. monocytogenes* **(LM) vacuolar escape rates vary across subpopulations of trophoblasts. (A)** Representative image of placental explant 24 hours post-inoculation (p.i.) with p*actA*-RFP LM counterstained with anti-LM (green). DAPI counterstain (white). STR = stroma. **(B,C)** Close-up examples of Invasive Border EVT **(B)**, Parastromal trophoblasts and middle EVT **(C)**. **(D)** Rotated image of placental explant from panel A with superimposed surface plot representing areas of highest RFP expression in relation to total bacterial green signal. Highest peaks are in the parastromal trophoblast region, where vacuolar escape rates are highest. **(E)** Percent RFP-expressing bacteria in each trophoblast subpopulation were enumerated at 24 and 48 hours p.i. in villi where all 3 subpopulations were infected. RFP expression was normalized to the 24-hour time point in invasive border EVT from the same placenta. Results from 3 independent experiments were expressed as average fold-change in comparison to the escape rate in invasive border EVT at 24 hours. Bars are SEM. Asterisk represents significant difference (p=0.02).

Chapter 4

Cellular & Molecular mechanisms of EVT bacteriocidal phenotype

Introduction

We have shown above that EVT are the portal of entry for bacteria and parasites [135] into the placenta. We further showed that they create a barrier to bacterial spread by killing intracellular *Listeria monocytogenes*. We wanted to understand in more detail the bacteriocidal phenotype of these cells. Do the unique degradative and invasive properties of the EVT contribute to restricted intracellular bacterial growth? To address this question, we began by first ruling out external factors that may confound our phenotype, and then systematically looking at each step of the *Listeria* life cycle and determining the unique features of the bacterial interaction with EVT.

Results

External Conditions – Matrigel, Host Cell Density, Host Cell Replication

Because EVT are such uncharacteristic cells, they are cultured in a unique way - in media with serum-replacement solution (NutriDoma) and on a synthetic extracellular matrix called Matrigel. We wanted to eliminate these unique culture conditions as a possible explanation for the bacteriocidal phenotype in EVT.

We first looked at the extracellular matrix; Matrigel is a trademarked product that is supplied with added gentamicin. We had some initial concerns this gentamicin was affecting the invasion or replication of *L. monocytogenes* during infection of EVT. To address this, we dialyzed an aliquot of Matrigel to remove

the gentamicin, cultured EVT on this antibiotic-free matrix and performed bacterial growth curves as usual. No difference was seen in bacterial invasion or growth rates between dialyzed and non-dialyzed Matrigel (data not shown). We next sought to determine whether all cells cultured on Matrigel simply had different properties with respect to bacteria than those kept on normal cell-culture dishes. To this end, we performed bacterial growth curves on BeWo cells grown on Matrigel, and conversely we quantified bacterial growth in EVT grown on coverslips without Matrigel (Figure 14A, B). For both experimental conditions, the bacterial growth phenotype was characteristic to the cell type (growth in BeWo, demise in EVT) and did not appear to be significantly affected by extracellular matrix presence or absence.

The vacuolar stains defining the *Listeria*-containing endosomal compartment (Chapter 3) were performed on cells that were cultured on Matrigel overnight, infected, and then dispersed and re-plated on fresh Matrigel. To certify that this process did not alter the dynamics of infection and skew the vacuolar marker results, we performed a growth curve in cells under these conditions (dispersed and re-plated) (Figure 14B). We saw no appreciable difference and were satisfied that this was not a confounding factor. Next, we wanted to show that the bacteriocidal phenotype was not due to the lack of serum in EVT culture medium. We quantified bacterial growth in BeWo cultured in EVT media, and did not see a decrease in bacterial growth (Figure 14C), suggesting serum concentrations and sources are not responsible for the EVT phenotype.

Cytotrophoblasts in vivo differentiate toward the invasive trophoblast lineage in the context of densely packed cell columns [90]. It is possible that this density and cell-to-cell contact is important for correct differentiation. We wanted to assure that our cell culture system most closely mimics the high density of EVT in cell columns while also taking into consideration the scarce resource of primary cells available for experiments. We also wanted to ascertain that our observed EVT phenotype with respect to bacterial death is not an artifact of the plating method. To this end, we quantified bacterial growth in EVT cultured at several densities: 75,000 cells per 24-well transwell, 125,000 cells per 24-well transwell (all previous experiments done in this condition), and 250,000 cells per 24-well transwell. We were satisfied to see that at both lower and higher densities of EVT, we still observe a drop in bacterial numbers between 2 and 5 hours post-infection (Figure 15).

After ascertaining that the culture media, Matrigel, and cell density were not critical factors to our bacteriocidal phenotype, we continued all experiments with conditions described in Chapter 3.

L. monocytogenes is generally accepted as being able to replicate in a variety of host cell types; however, it has been noted that growth in primary macrophages is not as robust as in macrophage cell lines [140]. Because most of our understanding of bacterial growth comes from studies in cell lines, it is hard to understand the nature of this difference. One clear distinction between cell lines and primary cells is the former's ability to replicate. We hypothesized that

decreased bacterial survival in primary EVT was due to the metabolic status of these cells as differentiated and non-replicating. This would imply that the phenotype is not necessarily specific to these cells, but is a more generalized feature of primary cells. To test this hypothesis, we employed another type of primary cells – mouse embryonic fibroblasts. We compared bacterial growth in replicating fibroblasts to that in metabolically-arrested (mitomycin C-treated) fibroblasts. We did not observe a difference between intracellular bacterial growth in these two cell types (Figure 16) and concluded that replication status of cells does not significantly alter intracellular bacterial growth outcome.

Internalization

We previously showed that bacterial invasion of human placental explants is dependent on InlA [45], and it is known that EVT express E-cadherin [61] as they differentiate into the invasive phenotype in cell columns. Moreover, it has been previously described that invasion of primary EVT by *L. monocytogenes* is InlA-dependent, but this was done under different culture conditions [44]. We wanted to establish that in our cell culture system, *Listeria* invasion of EVT is also dependent on the Inl-A – E-cadherin interaction, so we infected primary EVT as described above with WT *L. monocytogenes* and the deletion mutants: ΔInlA, ΔInlB, and the combined mutant of ΔInlA&B. We collected CFU data at 2 hours post-infection (Figure 17) and showed that indeed invasion of primary EVT is InlA-dependent. While this data is consistent with all other observations, we want

to point out that this experiment was done only once and on cells that were not depleted of the CD45+ population as in previous chapters. This may also explain the difference in CFU between WT and ΔInlB; we did not expect to see such a large difference in these two strains, but it is possible that the effect is due to another population of cells in the prep. It has also been suggested that InlA and InlB work together in invasion of the feto-placental unit [43].

Escape from the Primary Vacuole

We established (Chapter 3) that EVT trap internalized *L monocytogenes* in the primary vacuole. However, it is entirely unclear why bacteria are unable to escape into the cytoplasm in EVT. In the murine model of infection, the virulence factor LLO is essential for vacuolar escape [109]. We sought to show that LLO protein is expressed by intracellular bacteria in EVT. This proved to be a more difficult venture than we had anticipated because LLO functions in a short window of time when bacteria are in the primary vacuole and is then rapidly degraded in the cytoplasm [108, 141]. Our attempts at performing a western blot for LLO were unsuccessful – only precipitated protein from broth cultures was observed with standard western blotting technique even at high inoculums in control BeWo cells (Figure 18A). We also used a published protocol that uses radioactive (S^{35}) labeled-methionine incorporation to detect the small amount of LLO protein produced by intracellular bacteria [141], but unknown technical difficulties abstracted these results as well (Figure 18B).

Despite being unable to detect direct LLO expression by intracellular bacteria in EVT, we decided to assume LLO was in fact expressed because the growth curve of ΔLLO *L. monocytogenes* is significantly different from that of WT *L. monocytogenes* (Figure 20). We then wanted to address the question: does LLO function to create pores in the primary vacuole. The kinetics of LLO-based pore formation has been elegantly studied in murine macrophages using a variety of fluorescent probes [142]. Lucifer Yellow (LY) is a small molecule with weight 522 g/mol that escapes the small initial pores formed in the primary vacuole by LLO. We sought to determine whether LLO is able to form pores in the primary vacuole in EVT, so we began by optimizing the concentration of LY and the time course of infection in primary placental fibroblasts. We infected cells with WT or ΔLLO LM as usual and fixed cells at 1, 2 and 5 hours post-infection as previously described. We observed that fewer WT bacteria co-localized with LY than ΔLLO bacteria over time; the difference was clearest at the 2 and 5 hour time points (Figure 19), and was a confirmation that this was an appropriate method. It would be interesting to follow up on this method of evaluating LLO function in EVT.

Our next foray into deciphering the role of LLO was to use *L. monocytogenes* strains that have altered LLO function. We quantified the intracellular growth of mutated or deleted copies of the *hly* gene: ΔLLO [143] and S44A, a version of the lysin that is more stable in the host cytoplasm and is cytotoxic [91]. In BeWo cells, (Figure 20A) the ΔLLO strain does not grow in the

89

first 8 hours and only is able to start replicating significantly by 24 hours, presumably because a few rare bacteria are able to escape from the primary vacuole. We were surprised to observe (Figure 20B) that the LLO deletion strain survived the first 5 hours of intracellular life in EVT better than the WT strain. This result is consistent with our hypothesis that there is an LLO-dependent initial defense response of the EVTs to bacteria. It is possible that membrane damage of the primary vacuole is sensed and initiates a response; it is also possible that LLO-based pores allow escape of an unknown antigen into the cytoplasm that is sensed and responded to by EVT. We address the role of LLO in the EVT response further in Chapter 5. The S44A mutant bacteria that has an overactive lysin showed even less growth over the time course than WT or the deletion mutant. In BeWo cells (Figure 20A), this mutant also dies very quickly presumably because it lyses its host cell and is then killed by extracellular gentamicin. This strain may be sensed and killed faster by EVT, or it could simply be cytotoxic to cells. A more in depth look at the role of LLO in EVT sensing would discern these two possibilities and is discussed in Chapter 5.

LLO-mediated pore formation is a pH dependent process, with a pH optimum of 5.5 [121, 122]. Although the *Listeria*-containing vacuole in EVT acidifies, the kinetics or extent of acidification could present unfavorable conditions for LLO function. For example LLO loses its hemolytic activity at neutral pH in less than 10 min [123]. To address the possibility that altered pH dynamics in EVT are responsible for decreased vacuolar escape, we used a

strain of L monocytogenes (L461T), whose LLO is engineered to have a much wider pH optimum [144]. If pH were a major barrier to vacuolar escape for bacteria, we would expect the L461T strain to grow much more rapidly in EVT. However, we did not observe such an increase in intracellular growth (Figure 21). We want to point out that this experiment was only done once and that the WT strain appears to grow over the time course in this particular preparation of EVT. Despite this unusual phenotype, we can make the internal comparison that the pH insensitive strain does not grow better in EVT, and thus pH sensitivity is likely not the sole reason for bacterial growth retardation in EVT.

Another possibility is that the *Listeria*-containing vacuole has a different lipid composition that renders LLO non-functional. LLO is dependent on the presence of cholesterol, which is utilized by EVT for the synthesis of progesterone [124]. Specialized hormone synthesis in EVT could lead to differences in cholesterol metabolism and/or distribution in these cells, rendering it inaccessible to vacuolar LLO. We sought to determine whether cholesterol plays a role in the EVT bacteriocidal phenotype with the hypothesis that the EVT plasma membrane does not have enough cholesterol for LLO to function properly. We quantified bacterial growth in EVT in the presence of added cholesterol (Figure 22). To address the possibility that cholesterol is being used up for progesterone synthesis in EVT, we added DL-aminoglutethimide, which blocks the enzymatic conversion of cholesterol to pregnenolone, the first step towards steroidogenesis [145]. We observed no marked difference in intracellular

91

bacterial growth in the presence or absence of these agents (Figure 22). However, we want to point out that this does not necessarily rule out a role for cholesterol in the mis-functioning of LLO in EVT. To further address this possibility we wanted to take a qualitative look at the cholesterol distribution in placental explants; we stained infected explants with filipin, a fluorescent molecule that binds free cholesterol. The staining appeared diffuse and often surrounding the nucleus; it was not was not remarkable in any way and was not quantified (data not shown).

In conclusion, we were unable to show the expression or function of LLO in infected EVT; however, we are fairly certain that LLO is in fact expressed and plays a role in the dynamics of the bacteriocidal phenotype because the deletion mutant has a strikingly different growth phenotype. It is possible that the pH and cholesterol dependencies of LLO are important factors in how LLO function is impaired in these cells, but we could not clearly show these with our methods.

Gentamicin in the Primary Vacuole

While mouse trophoblast giant cells (the murine analog of human EVT) are accepted to be highly phagocytic, human EVT are only somewhat phagocytic [146]. The large difference in internalization kinetics of WT vs. ΔInlA *L. monocytogenes* is consistent with the idea that phagocytosis is not highly active in our experimental system of primary cultured EVT. However, some concerns were raised that even a small level of phagocytosis may traffic gentamicin from

the extracellular medium into the Listeria-containing vacuole in EVT and be responsible for the observed bacterial killing. It is infeasible to execute an accurate intracellular bacterial growth curve in EVT without the use of gentamicin. This is in part due to the large number of *Listeria* that get trapped on Matrigel during initial seeding of EVT cultures with bacteria, replicate extracellularly through the time course and confound intracellular CFU results. In order to prove this, we performed such a growth curve without gentamicin and collected CFU over the course of 24 hours from lysed cells (theoretically intracellular bacteria) as well as from media supernatant (extracellular bacteria) (Figure 23A). The bacterial growth in cells without gentamicin highly resembles the CFU in the supernatant, suggesting that overgrowth is likely due to extracellular replication. To try to eliminate the factor of extracellular bacterial replication, we decided to execute a growth curve where bacteria were no longer replicating. Chloramphenicol is a bacteriostatic antibiotic for *Listeria* [147]. First, we wanted to make sure that the action of gentamicin is not epistatic to chloramphenicol, so we examined bacterial growth in extracellular media without antibiotics, with each antibiotic individually, and with both (Figure 23B). We concluded that gentamicin killed bacteria perfectly well in the presence of chloramphenicol, so we continued with a cell-culture experiment that combined the two antibiotics. Chloramphenicol was added to the culture media at concentrations ranging from 120-300 µg/mL. Gentamicin was added for either 1 hour (between 1-2 hours post-infection) or for the usual 4 hours (between 1-5

hours post-infection). The observed bacterial growth in the presence of these two bacteriostatic agents was surprising; but nevertheless, the two growth curves are quite similar (Figure 23C). If phagocytosis of gentamicin and its delivery to the primary vacuole in EVT was the main mechanism of bacterial killing in these cells, we would expect a shorter treatment with gentamicin (1 hour) to allow for higher CFU at 5 hours. This was not observed; the similarity in CFU between 1hours and 4 hours of gentamicin treatment alleviated our concerns that this antibiotic was the main source of bacterial killing in the EVT.

Death in the Primary Vacuole

Our immunofluorescence and EM evidence in Chapter 3 show that bacteria are dying in the primary vacuole. We were interested in identifying the molecular mechanisms of this killing. One of our hypotheses was that vacuolar killing of Listeria is mediated by reactive oxygen or nitrogen species. The feto-maternal interface is an area of local oxidative stress due to the production of these species. Nitric oxide is produced by nitric oxide synthases (NOS) including constitutively active synthases (eNOS) and inflammation-based inducible synthase (iNOS). eNOS expression in the placenta has been localized to endothelial cells, syncytiotrophoblast and EVT [148],[149]. iNOS expression has been shown in vascular endothelium and syncytium [150]. Superoxide can be produced enzymatically by several pathways including NADPH oxidases,

94

xanthine oxidase, and NOS, all of which have been described in the placenta [151].

The ability of ROI and RNI to protect against bacterial infections is well documented [152], [153]. In vivo challenges with *L. monocytogenes* have demonstrated that the NO-mediated response is critical for the host to survive the infection [154], [155]. Both ROI and RNI have been shown to be important for macrophage killing of *L. monocytogenes* in vitro [156], [157]. Specifically, macrophages activated prior to infection use largely ROI-based pathways to eliminate bacteria, whereas those activated after infection depend mainly on NO [158]. These observations allow us to postulate that *L. monocytogenes* restriction could be initiated by a rapid and toxic production of ROI and sustained by the bacteriocidal effects of NO.

Further evidence for the importance of NO in *L. monocytogenes* restriction is provided by the observation that *L. monocytogenes* grows well in nearly all published cell-types with the exception of two: IFNγ and IL-6 treated Caco-2 human intestinal epithelium cells [159], and IFNγ treated primary mouse hippocampal neurons [160]. In both cases, it was determined that NO production mediates bacterial killing. Moreover, Oadrhiri et al. found that "activated" Caco-2 cells sequestered about half of the bacteria within vacuoles [159]. Putting all of this together, we hypothesized that bacteria are internalized to a late endosome, and then killed through ROI and RNI mechanisms in this vacuole.

To test this hypothesis, we used inhibitors of these reactive species. L-NG-monomethyl arginine (L-NMMA), a well-accepted inhibitor of NO synthesis [161], was used to treat EVT prior to and during infection to determine if NO contributes to killing. Superoxide dismutase (SOD), an antioxidant enzyme that is commonly used to inhibit reactive oxygen species, was used to test the role of ROI. If addition of inhibitors to EVT infection time courses rescued bacterial replication, we could conclude that ROI and/or RNI are a primary mechanism of bacterial killing in EVT. We did not observe significant differences between bacterial growth dynamics with the addition of SOD; however, L-NMMA appeared to rescue bacterial growth to some degree (Figure 24). While these experiments are not significant enough to provide definitive proof for the involvement of reactive nitrogen species, it is an exciting suggestion we hope to pursue further.

Another hypothesis for the molecular mechanism behind vacuolar bacterial death is that antimicrobial peptides degrade bacteria. We chose to look specifically at lysozyme and cationic microbial peptides (CAMPs). Lysozyme is an antimicrobial peptide that is found in both host fluids such as saliva, tears, and serum, as well as in lysozomal granules of neutrophils and macrophages [162]. Although no reports exist documenting lysozyme production by trophoblast cells, it is possible that EVT express it or similar enzymes due to their unique degradative and invasive nature. CAMPs are a family of proteins normally produced at sites of infection or inflammation that have broad-spectrum antibacterial, antifungal or antiviral properties. In contrast to lysozyme, many

studies have detected CAMPs such as cathelicidin [163], β-defensins [164], and others in the placenta (for a review, see [165]). *Listeria monocytogenes* is naturally resistant to lysozyme thanks to the action of N-acetylglucosamine deacetylase (Pdg) and O-acetylmuramic acid transferase (Oat), which modify its peptidoglycan to avoid degradation by the enzyme [166-168]. Similarly, the MprF protein produced by *L. monocytogenes* confers bacterial resistance to CAMPs via lysinylation of phospholipids in bacterial membranes [169]. To address whether these antimicrobial peptides play a role in EVT killing of bacteria, we obtained *L. monocytogenes* strains with deletions at the Oat, Pdg, [170] and MprF [171] loci and quantified their growth in EVT . We first defined the growth of these mutants in control BeWo cells (Figure 25A). We observed decreased intracellular growth rates for the MprF deletion mutant as well as the Oat/Pdg double deletion mutant. We thus decided to go on to test these two strains in primary EVT. We observed a noticeable though not statistically significant decrease in MprF mutant bacterial growth suggesting CAMP may be present in EVT and affect bacterial survival (Figure 25B). On the other hand, the Oat/Pdg double mutant appeared to grow better intracellularly (though again, not a statistically significant difference). This was surprising since the mutation normally decreases bacterial survival; one possible explanation for this reverse phenotype is that the modified peptidoglycan in the WT strain is more immunogenic and elicits a stronger bacteriocidal response from the EVT.

Autophagy

It has been previously shown that autophagy plays a role in controlling *L. monocytogenes* infection in macrophages [172-174]. We thus wanted to investigate whether autophagy is at all responsible for bacterial death in EVT. Although we found no co-localization of vacuolar bacteria with LC3, a canonical marker of autophagosomes (Chapter 3), we took several more approaches to address this question. To first define whether autophagy machinery was even activated during infection, we compared LC3 expression in EVT infected with L. monocytogenes, with that in mock infected cells, and cells treated with Bafilomycin-A, an inhibitor of vacuolar ATPase [175] . Treatment of cells with Bafilomycin-A blocks fusion of the lysozomes with autophagosomes, which inhibits autophagy as a process and results in the accumulation of autophagosomes in the cytoplasm [176]. We observed an increase in punctate LC3 staining in BafA-treated EVT when compared to untreated cells as expected (Figure 26A). EVT infected with L. monocytogenes showed increased LC3 staining as well, indicating that autophagy is induced by bacterial infection. We want to point out that this does not imply that bacterial death is necessarily caused by this induced autophagy response. To address this question more directly, we compared bacterial growth in EVT under normal conditions to growth in EVT treated with Bafilomycin-A (wherein autophagosomes are not able to acidify and function correctly). We observed no difference in infection progress between the two conditions (Figure 26B). This data along with the lack of LC3 on

98

the Listeria-containing vacuole in EVT convinced us that autophagy is not a key cellular process in our phenotype.

Cell-to-Cell Spread

We next sought to determine if actin-based motility and cell-to-cell spread have a role in EVT infection. Because such a small proportion of L. monocytogenes (10-20%) manage to escape the primary vacuole, it is difficult to tease out the importance of a downstream life cycle event. Nevertheless, to address this idea, we infected EVT with bacteria lacking the ActA gene and measured their replication. Normally, differences in intracellular growth between these strains are seen beginning around 8 hours post-infection [177]. We observed that CFU at 5 hours post-infection are quite similar, but by 8 hours diverge with the deletion mutant dropping in CFU significantly (Figure 27). A caveat of this set of experiments is that the average growth in EVT appears to be much higher than seen previously (Chapter 3), meaning the tissue may have inherently different susceptibility to L. monocytogenes than the average EVT. More experiments would need to be done to tease out the meaning of this phenotype.

Conclusions & Future Directions

We investigated a variety of cellular aspects of bacterial interaction with EVT during infection to elucidate the nature of the unique bacterial growth defect inside these cells. Because the main feature of the phenotype is the bacterium's inability to escape the primary vacuole, we first looked at the bacterial virulence factor LLO. We were unable to show intracellular LLO expression even in the control cell line BeWo. Immunofluorescence staining-based detection of the protein was unsuccessful (data not shown). To amplify the signal, we used radioactive amino acid incorporation and immunoprecipitation of LLO; nevertheless, these efforts at detecting the protein in cell lysates were foiled. This was in part due to the short half-life of LLO inside the eukaryotic cytoplasm, and in part due to technical difficulties of working with radioactive materials and challenging protocols. It may be useful in the future to show that LLO is in fact expressed inside EVT, and the best method is certainly the immunoprecipitation of radioactively-labeled protein. Other options for showing LLO expression indirectly includes 1. placing a fluorescent protein under the LLO promoter and measuring fluorescent signal, or 2. detecting RNA transcript for LLO using qPCR or FISH. Another possibility to assess the bacterial state more globally during infection would be to isolate intracellular bacterial RNA and perform *Listeria* microarray analysis. While the bacterial state would provide us with some clues to their intracellular environment, a major caveat to this experiment is that the majority of bacteria are dead by 5 hours post-infection and thus may not show useful information; an early time course would best suit this approach.

While we did not show LLO expression directly, we were certain that it is expressed because the LLO deletion mutant has significantly different intracellular growth dynamics when compared to the wild type strain (Figure 20). We considered factors that may be inhibiting proper LLO function in EVT, and found that improper pH is not likely to be the limitation, as the strain with a pH insensitive LLO protein did not have altered growth dynamics. Overall cholesterol levels or hormone production were also not identified to be critical for LLO function in EVT. The active form of a host-derived thiol reductase (GILT) involved in antigen processing has recently been shown to be required for the activation of LLO [125], and may not be present or accessible in the *Listeria*-containing vacuole in EVT.

In terms of how bacteria are killed inside the primary vacuole in EVT – we looked at a few methods that other eukaryotic cells use: autophagy, reactive oxygen and nitrogen species, and antimicrobial peptides. We concluded that while autophagy is activated in EVT upon bacterial invasion, it does not contribute to bacterial demise. Reactive nitrogen species may indeed play a role, though reactive oxygen is not as effective. It would be interesting to look into how the production of reactive nitrogen species is induced. Namely, is NO production a consistent feature of these cells, or is it a response to bacteria? Because EVT *in vivo* are in a hypoxic environment, it is possible that NO is produced by these cells without pathogen stimulation [93]. Interestingly, Myers et al. suggests reactive oxygen and nitrogen may inactivate LLO [161], so aside from

generalized degradation of the bacteria, NO may contribute to LLO dysfunction. Finally, using bacterial mutants with differential susceptibilities to antimicrobial peptides, we found that cationic antimicrobial peptides (CAMPs) may play a role in bacterial death. To pursue this avenue further, it would be interesting to look at EVT expression of CAMPs previously detected in the placenta such as cathelicidin or β-defensins.

Overall, our cellular methods did not provide a satisfying answer to how or why EVT are killing bacteria. The implication of reactive nitrogen species and antimicrobial peptides point to interesting possibilities that we hope to explore in the future. We plan to use a more global approach to understand how EVT sense bacteria and respond.

Methods & Materials

All human tissue collection, cell isolation, culture of primary cells and cell lines, bacterial growth and quantification, immunofluorescence staining, visualization and image processing was performed as described in previous chapters. Novel strains and conditions are described below.

Materials & Stock Solutions

Anisomycin (EMD, San Diego, CA) was dissolved in DMSO for a stock concentration of 3mg/mL. Cycloheximide (EMD, San Diego, CA) was dissolved in 100% Ethanol for a stock concentration of 16.66 mg/mL. S-35-labeled L-methionine/cysteine was purchased as EXPRE^{35}S^{35}S Protein Labeling mix in 50mM tricine, 10mM 2-mercaptoethanol (Perkin-Elmer, Santa Clara, CA). Protease Inhibitor Cocktail (Fermentas, Lithuania) was used for all western blot protocols. Recombinant Protein A-Sepharose 4B Conjugate (Invitrogen, Carlsbad, CA) was used for immunoprecipitation of LLO. ENHANCE (Perkin-Elmer, Santa Clara, CA) autoradiography enhancer was used for radioactive LLO western visualization. LLO protein (Abcam, San Francisco, CA) was used at 0.7 mg/mL as positive control for some western blots. LLO protein was also a generous gift from Dr. Jen Robbins and Dr. Julie Theriot at a concentration of 2.86μg/mL. Chloramphenicol (Sigma-Aldrich) was dissolved in 100% Ethanol for a stock concentration of 20mg/mL. Lucifer Yellow CH dilithium salt (Sigma-Aldrich) was dissolved in distilled water for a stock concentration of 100 mg/mL. Cholesterol (Water-soluble, Sigma-Aldrich) was dissolved in distilled water for a 5mM stock solution. DL-Aminoglutethimide (Sigma-Aldrich) was dissolved in DMSO for a stock concentration of 90mM. N^G-Methyl-L-arginine acetate salt (L-NMMA, Sigma-Aldrich) was dissolved in distilled water for a stock concentration of 100mM. Superoxide dismutase (SOD, from human erythrocytes, Sigma-Aldrich) was dissolved in distilled water for a stock solution of ~1965 units/mL. Filipin (complex from *Streptomyces filipinesis*, Sigma-Aldrich) was dissolved in

DMSO for a stock concentration of 25mg/mL. Mitomycin-C (Sigma-Aldrich) was dissolved in distilled water for a stock concentration of 1mg/mL. Bafilomycin-A, at 25µM, was a gift from Dr. Jay Debnath. All other basic chemicals were purchased from Sigma-Aldrich unless otherwise noted.

Strains

S44A strain (DP-L4057) [91], L461T strain (DP-L4017) [144], and Oat-, Pdg-, Oat-/Pdg-, MprF- strains [170] were a generous gift from Dr. Dan Portnoy.

Dialysis of Matrigel

Slide-A-Lyzer 10,000 MWCO Gamma Irradiated Dialysis Cassette (Thermo Scientific) were used as per instructions provided. Briefly, all materials including Matrigel was allowed equilibrate to 4°C, Matrigel was injected into the dialysis cassette and floated in DMEM as the dialysis buffer for 2 hours at 4°C, fresh DMEM replaced for overnight dialysis. Matrigel was then removed from the cassette and used in culture as previously described.

Mouse Embryonic Fibroblasts

Mouse Embryonic Fibroblasts (MEF) from CD-1 mice were a gift from Dr. Yuki Oho. Cells were grown on gelatin-coated dishes in DMEM-high glucose with 10% FBS, 1% L-glutamine, 1% sodium pyruvate, 1% nonessential amino acids (UCSF CCF), 1% penicillin/streptomycin, and 10 µM β-mercaptoethanol. For

mitomycin-C treated cells, fibroblasts were incubated with 10 µg/mL mitomycin-C for 4 hours, washed with PBS, trypsinized and frozen in 10% DMSO, 90% FBS solution. For growth curves, MEFS were thawed onto gelatin and infection performed the following day.

TCA Precipitation of LLO from Broth Cultures

Overnight cultures (2mL BHI, 30°C, no shaking) of *L. monocytogenes* were diluted 1:100 in LB and grown shaking at 37°C for 2-4 hours (OD_{600} 0.4-0.6) with 2mM Glucose-1-Phosphate (Sigma-Aldrich) to mimic intracellular conditions. Culture was pelleted, re-suspended in distilled water. 6.1 N trichloroacetic acid (Sigma-Aldrich) was added to 10%, and mixture incubated on ice for 30 minutes. The solution was pelleted at 4°C for 15 minutes at >10Kg, supernatant removed. The pellet was dried by addition of acetone and centrifugation. The pellet was then re-suspended in half volume PBS, half volume 2x gel loading buffer (100 mM Tris-Cl, 4% SDS, 0.2% bromophenol blue, 20% glycerol, 200mM β-mercaptoethanol). The sample was then boiled for 5 minutes, aliquoted and stored at -20°C for use as control for western blotting of LLO.

Western Blot for LLO

6-well dishes of BeWo cells, Placental fibroblasts, or EVT on transwells were infected with WT or ΔLLO *L. monocytogenes* as previously described. At 5 hours post-infection, cells were washed in PBS, and 2mL of lysis buffer added to

each flask (Lysis buffer: 100 µL 1M tris-Cl, 300uL 1M NaCl, 400 µL 5% TritonX-100, 80µL 25x Protease inhibitor cocktail (Fermentas), 4µL 0.5M EDTA, 1200 µL distilled water), and incubated for 15 minutes at 4°C. Cells were then scraped off the dish and centrifuged 10 minutes at full speed at 4°C, supernatants collected and frozen for running on polyacrylamide gel. Gel was transferred onto standard nitrocellulose paper. Polyclonal rabbit α-LLO antibody (DP2813, gift from Dr. Dan Portnoy) was used at 1:5000 overnight at 4°C in 5% de-fatted milk block in TBST buffer. Goat α-rabbit HRP (gift from Dr. Joanne Engel) was used at 1:5000 for 1 hour at room temperature. ECL Western Blotting Detection System (Amersham) was used to visualize blot.

S^{35}-Methionine Incorporation and Immunoprecipitation of LLO

Approximately 1.5 million BeWo cells and primary EVT per condition were plated in 6 well dishes and allowed to settle overnight. Cells were infected as previously described at MOI of ~25. At 30 minutes post-infection cells were washed 3x in PBS and starvation media (standard media with substitutions of dialyzed FBS for FBS, and DMEM without methnionine and cysteine for standard DMEM) was added to cells with protein synthesis inhibitors (225 µg/mL cycloheximide & 30 µg/mL anisomycin). At 1 hour post-infection, gentamicin was added to cells as usual, as well as 200µCi of S^{35}labelled cysteine/methionine mix. At 2 hours post-infection, cells were washed 3x with ice-cold PBS, and 1mL ice-cold KD lysis buffer with 1x protease inhibitors was added to each sample

(KD Lysis buffer: PBS, 0.02% Saponin, 2% Triton-X100, 10mM EDTA). Cells were incubated on ice for 30 minutes, scraped off plate, pelleted for 15 min at 4°C at >10kG and supernatant collected. Monoclonal B3-19 αLLO antibody (gift from Dr. Dan Portnoy) was added at 1:5000 to each supernatant and incubated at 4°C for 1.5 hours. 100µL per sample of Protein-A beads were washed 3x in KD lysis buffer, re-suspended in buffer with protease inhibitors and incubated with sample overnight at 4°C. Samples were washed to remove non-precipitated proteins, and 2x gel running buffer was added to remaining beads. Immunoprecipitation was performed similarly for broth (in cell culture medium) cultures of WT and ΔLLO *L. monocytogenes*. Polyacrylamide gels were run and stained either with InstantBlue (Fisher Scientific) as a coomassie stain, or fixed for radioactive detection. Fixation was accomplished with 10% glacial acetic acid, 30% methanol for 30 minutes. Gel was incubated with ENHANCE autoradiographic enhancement solution for 1 hour at room temperature and then incubated with 10% PEG8000 solution for 30 minutes on ice. Gel was dried and exposed to film for 1 week at -80°C.

Novel infection conditions

For Lucifer Yellow-based assays for LLO function, placental fibroblasts were infected at MOI ~50 with WT or ΔLLO *L. monocytogenes* in the presence of 0.5 mg/mL Lucifer Yellow. At 30 minutes post-infection, cells were washed with PBS and media without Lucifer Yellow replaced. Cells were fixed at 45, 60, 120,

300 minutes post-infection in 4% Paraformaldehyde as previously described. Bafilomycin A was added to cells at the same time as bacteria at 50nM. Cholesterol was added at 50μM, and inhibitor of progesterone synthesis DL-AGTE was added at 90μM for 4 hours prior to infection and kept in the media throughout the time course. Inhibitors of reactive oxygen and nitrogen species L-NMMA (1mM) and SOD (100 u/mL) were added at 1 hour post-infection and kept in the media throughout the time course.

A

BeWo

B

EVT

C

BeWo

109
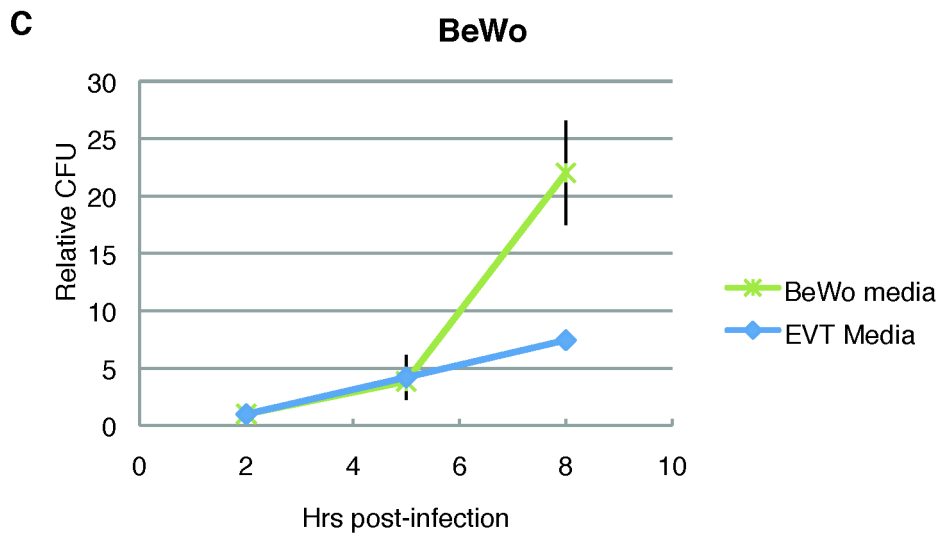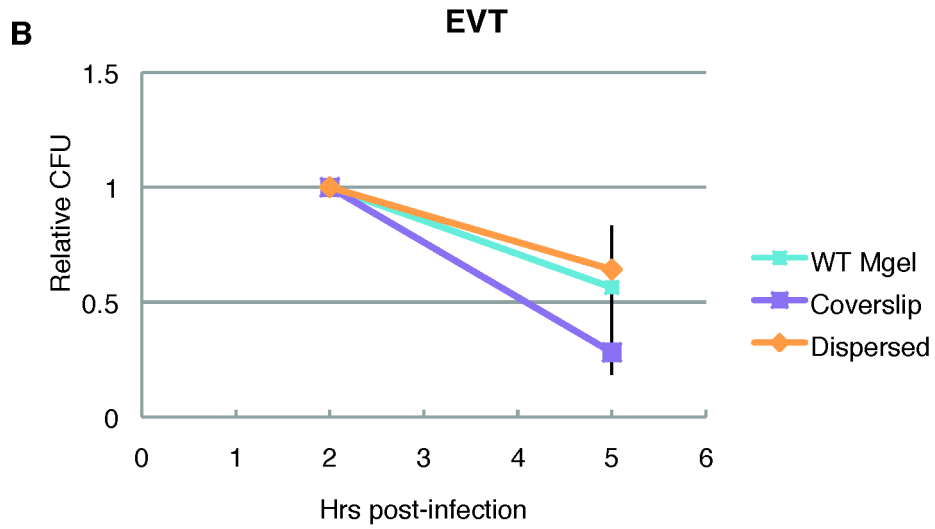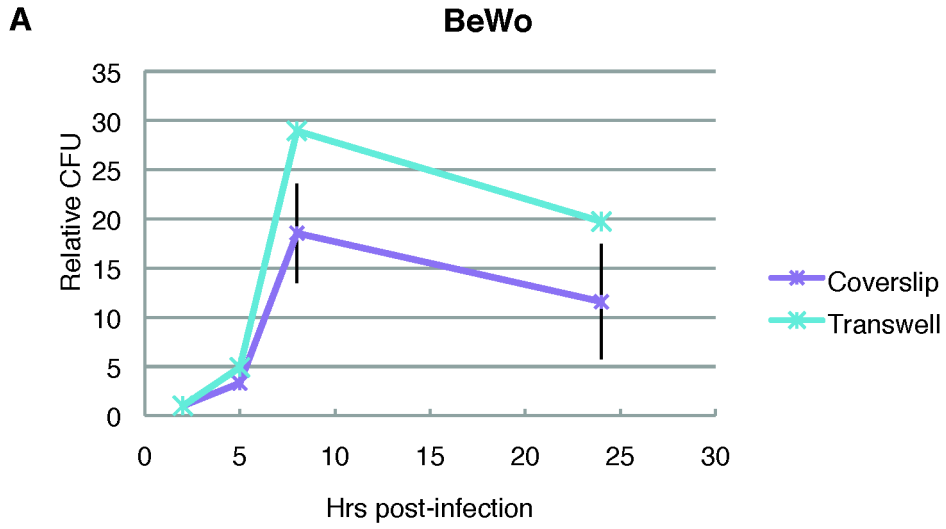
Figure 14. Effects of Matrigel and media on intracellular bacterial growth in BeWo. EVT Matrigel and media are not responsible for bacterial demise in EVT. CFU/well were normalized to the 2-hour time point within each experiment. Bars represent SEM. Lack of error bars means n = 1 for that condition. **(A)** Intracellular bacterial growth in BeWo cultured on coverslips (n=3) vs. transwells with Matrigel (n=1). **(B)** Intracellular bacterial growth in EVT cultured on transwells with Matrigel (WT Mgel) (n=10) vs. on a glass coverslip (n=2) vs. dispersed at t=1hr and re-plated on fresh Matrigel (see Chapter 3 methods for details) (n=1) **(C)** Intracellular bacterial growth in BeWo grown in standard BeWo (n=3) media vs. in EVT media (n=1).
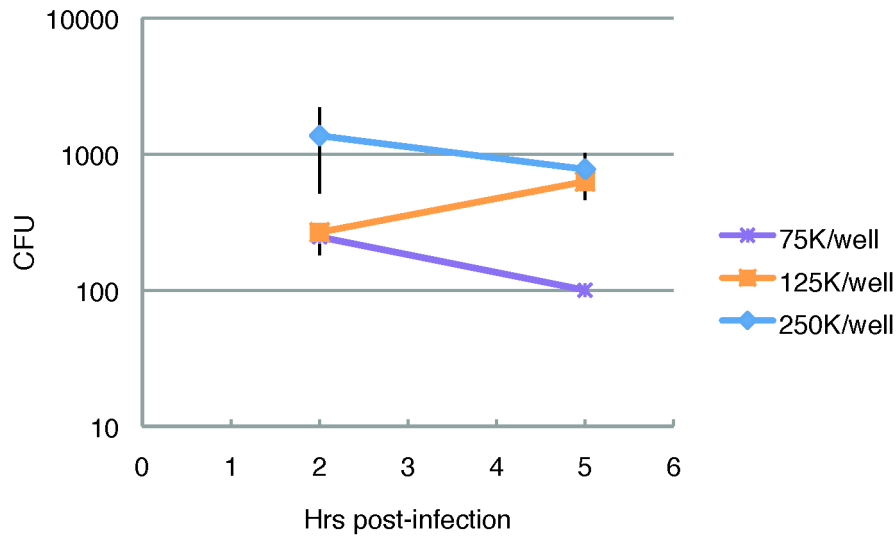
Figure 15. Effects of EVT cell density on intracellular bacterial growth There is no coherent bacterial growth difference between varying densities of host cell culture. Bars represent SEM. Lack of error bars means n = 1 for that condition. Intracellular bacterial growth in EVT plated at different densities on 24-well transwell: 75,000 cells/well (n=1), 125,000 cells/well (n=10), 250,00 cells/well (n=2).
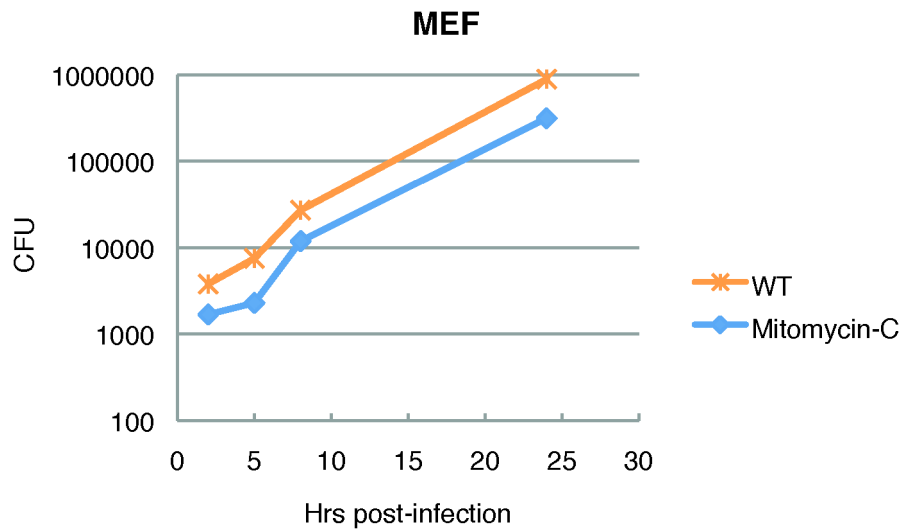
Figure 16. Effect of host cell replication on intracellular bacterial growth
Host cell replication does not alter intracellular bacterial growth. Intracellular bacterial CFU in mouse embryonic fibroblasts (MEF, WT) and mouse embryonic fibroblasts treated with Mitomycin-C. N=1 for both conditions.
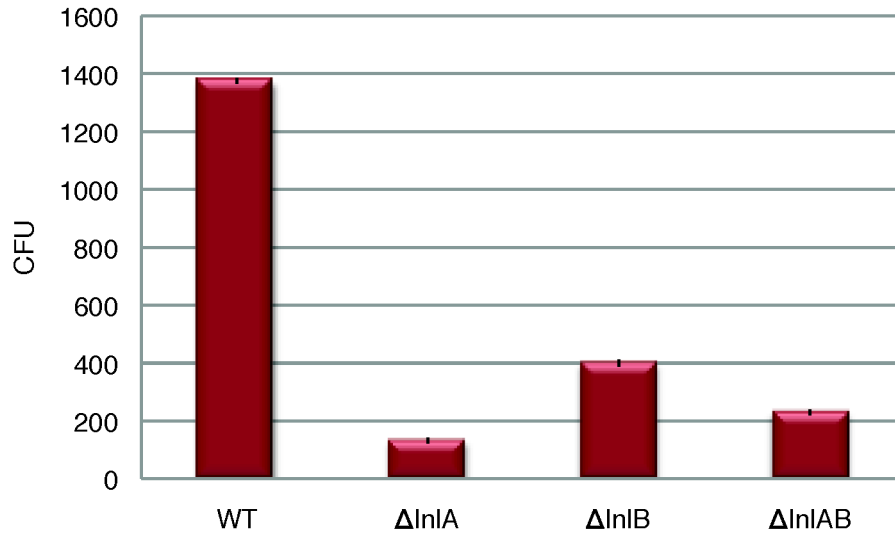
Figure 17. Role of InlA & InlB in invasion of primary EVT Bacterial invasion of

EVT is dependent on InlA and partially on InlB. CFU in EVT (not depleted of

CD45-positive population) at 2 hours post-infection. N=1 for all conditions.
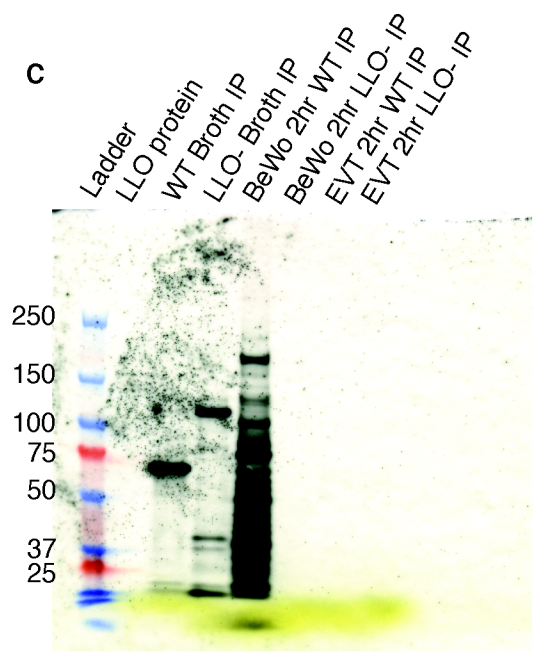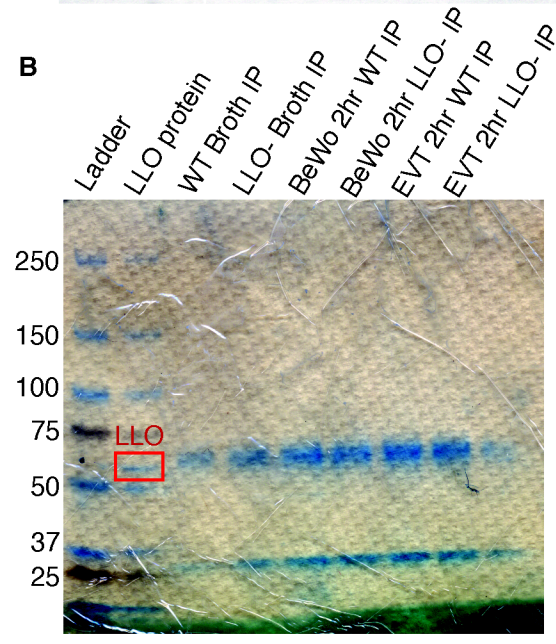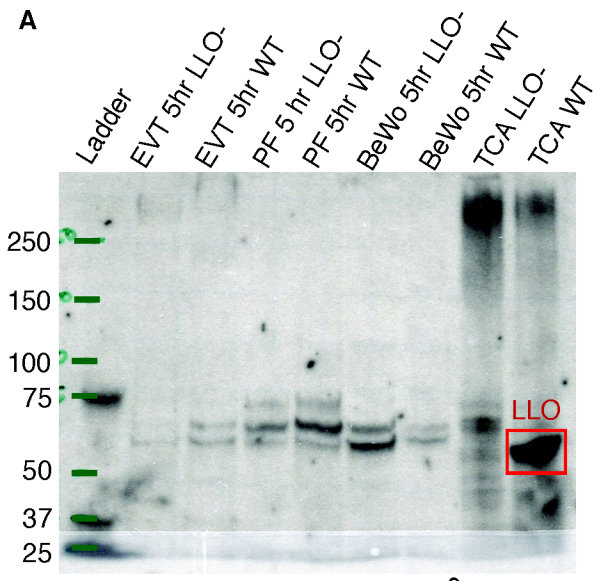
Figure 18. Expression of LLO by intracellular bacteria in BeWo, EVT Failure to detect intracellular LLO in EVT, BeWo, Placental Fibroblasts (PF). Representative blots shown **(A)** Western blot for LLO protein from 5 hour post-infection cell lysates of EVT, BeWo, PF infected with wild type *L. monocytogenes* or ΔLLO *L. monocytogenes* (LLO-), and trichloroacetic acid – precipitated protein from broth cultures (TCA). Red box highlights predicted location of LLO protein. **(B,C)** Immunoprecipitation (IP) of LLO protein from 2 hours post-infection cell lysates of BeWo & EVT, and from broth cultures. **(C)** Autoradiograph of immunopreciptated LLO protein from 2 hour post-infection cell lysates of (S^{35})-methionine treated BeWo & EVT, and (S^{35})-methionine treated broth cultures. See Chapter 4 methods for details.
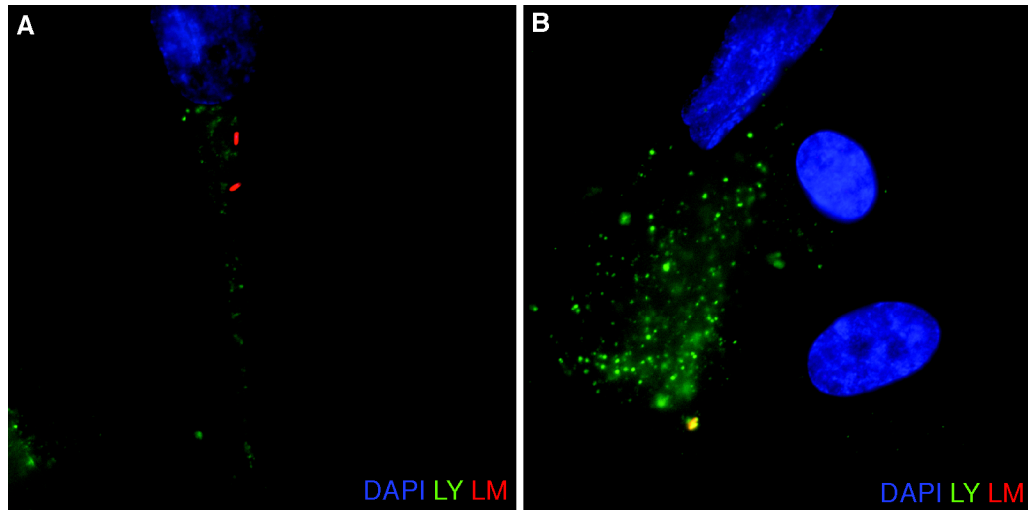
Figure 19. Lucifer Yellow assay as a measure of intracellular LLO function

Small molecule dye Lucifer Yellow (LY, green) is internalized with *L. monocytogenes* and co-localizes with bacteria (red) when LLO does not function and both are trapped in the same vacuole. Representative images of placental fibroblasts 5 hours post-infection with WT **(A)** and ΔLLO *L. monocytogenes* **(B)**. LY was added to cells at the same time as bacteria for 30 minutes. Bacteria are counter-stained with anti-*Listeria* antibody in red and DAPI in blue.

A

BeWo
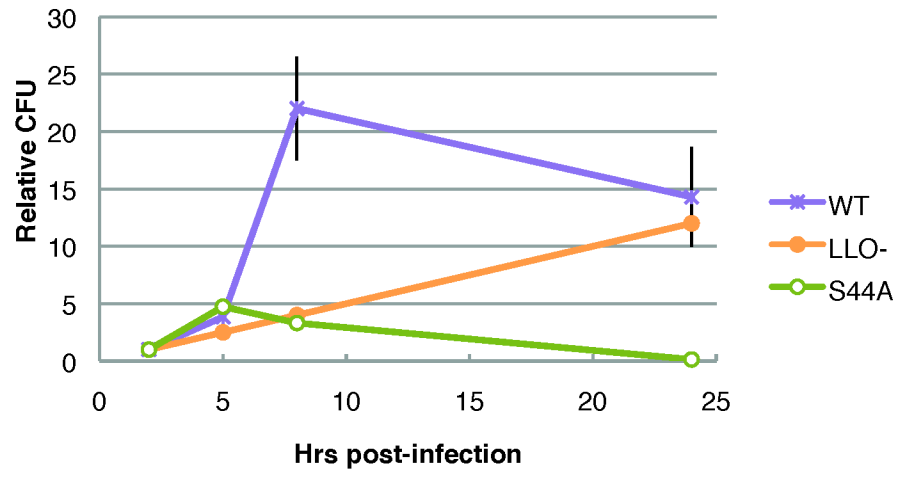
B

EVT
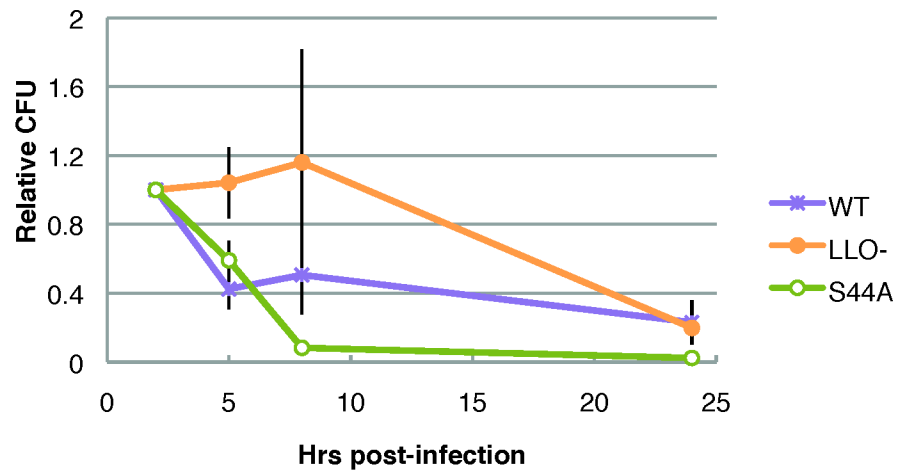
Figure 20. Intracellular growth of LLO mutant strains in BeWo (A) , EVT (B)

Comparison of intracellular bacterial growth of wild type (WT) *L. monocytogenes* ΔLLO *L. monocytogenes* (LLO-), and a strain that has increased hemolytic activity in comparison to wild type LLO (S44A). CFU/well were normalized to the 2-hour time point within each experiment. Each data point is an average of multiple independent experiments: WT: n=10, LLO-: n=5, S44A: n=2. Bars represent SEM.
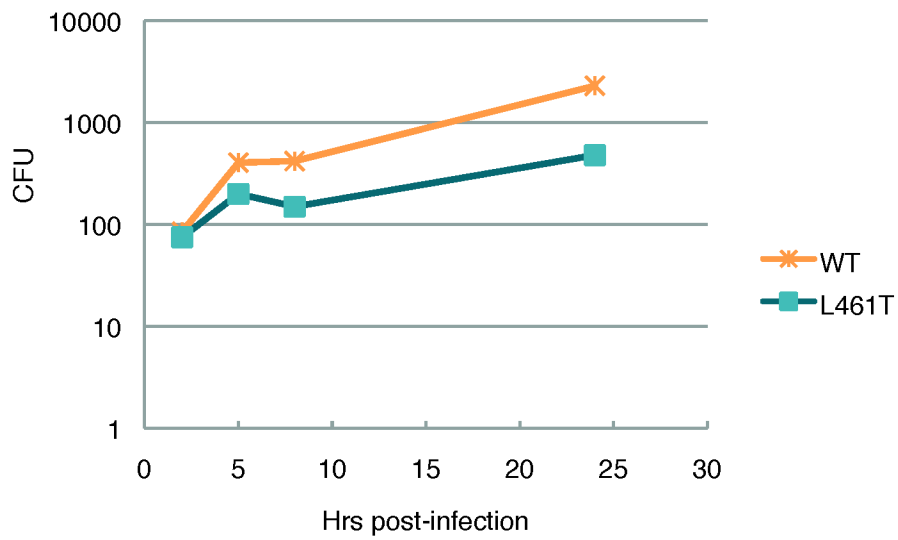
Figure 21. Intracellular growth of pH-insensitive LLO mutant strain in EVT

No marked difference between intracellular bacterial growth of wild type (WT) *L. monocytogenes* and a strain that has a pH-insensitive copy of LLO (L461T). N=1 for each condition.
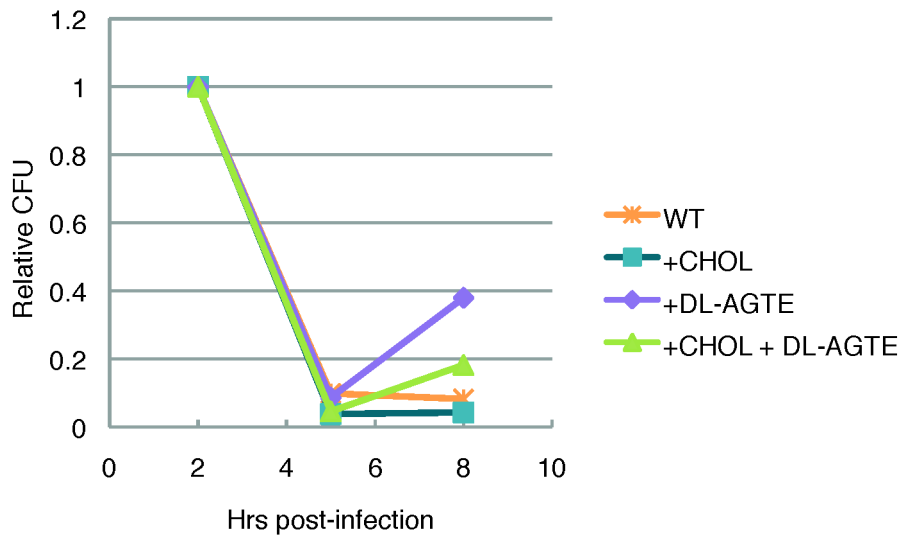
Figure 22. Effect of cholesterol on intracellular bacterial growth in EVT (A)

No marked difference in intracellular bacterial growth is observed when EVT are treated with extracellular cholesterol (+CHOL), with an inhibitor of the first step of enzymatic conversion of cholesterol to progesterone (+DL-AGTE), or with both (+CHOL + DL-AGTE). Cholesterol and DL-AGTE were added to cells 4 hours prior to infection. CFU/well were normalized to the 2-hour time point within each experiment. N=1 for each condition.
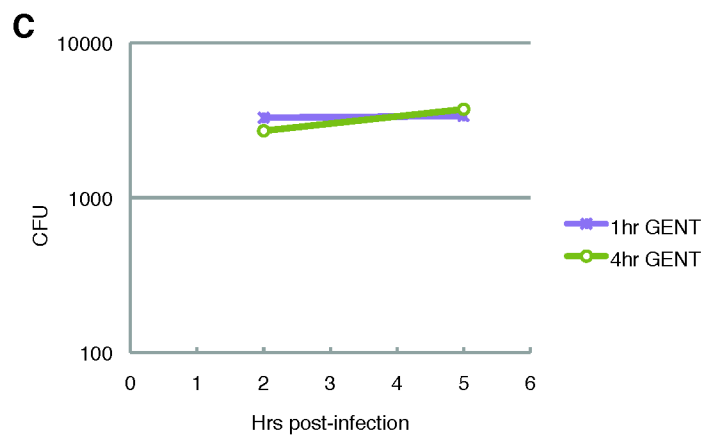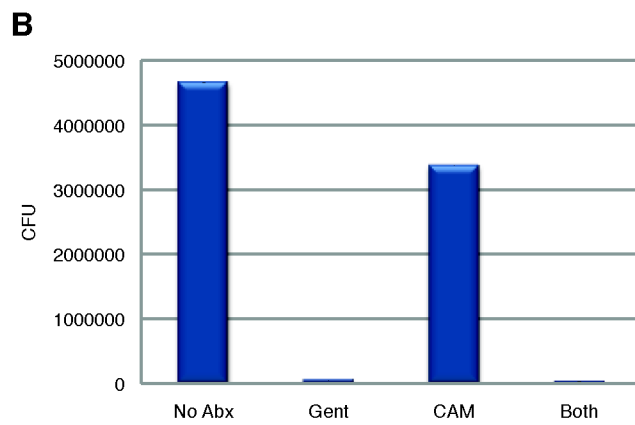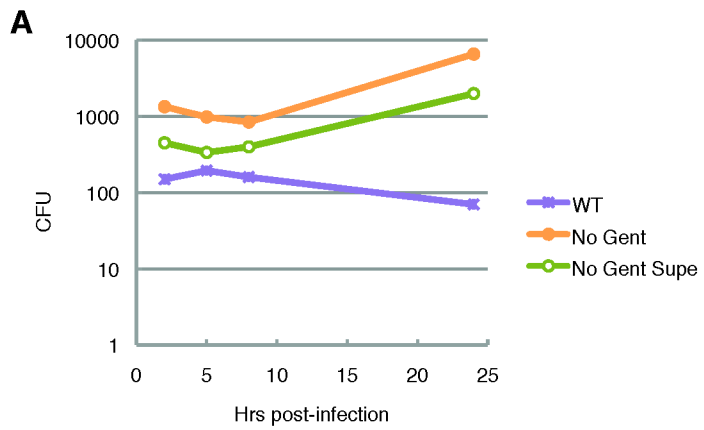
Figure 23. Effect of gentamicin on intracellular bacterial growth in EVT

(A) Intracellular bacterial growth in EVT in the presence of gentamicin (WT), without gentamicin (No Gent), and supernatant of infected EVT without gentamicin (No Gent Supe). CFU of No Gent resemble supernatant more than WT infection, suggesting extracellular bacterial replication confound these results. N=1 for each condition **(B)** Gentamicin is not epistatic to chloramphenicol. Bacterial growth in EVT culture medium without antibiotics (No Abx), in the presence of 50μg/mL gentamicin (Gent), 150 μg/mL chloramphenicol (CAM), or both. N=1 for each condition. **(C)** Intracellular bacterial growth in EVT in presence of 150 μg/mL chloramphenicol, and gentamicin for 1 hour post-infection or for entire time course (4 hours). N=1 for each condition. No marked difference between conditions suggests gentamicin is not critical for intracellular bacterial demise.
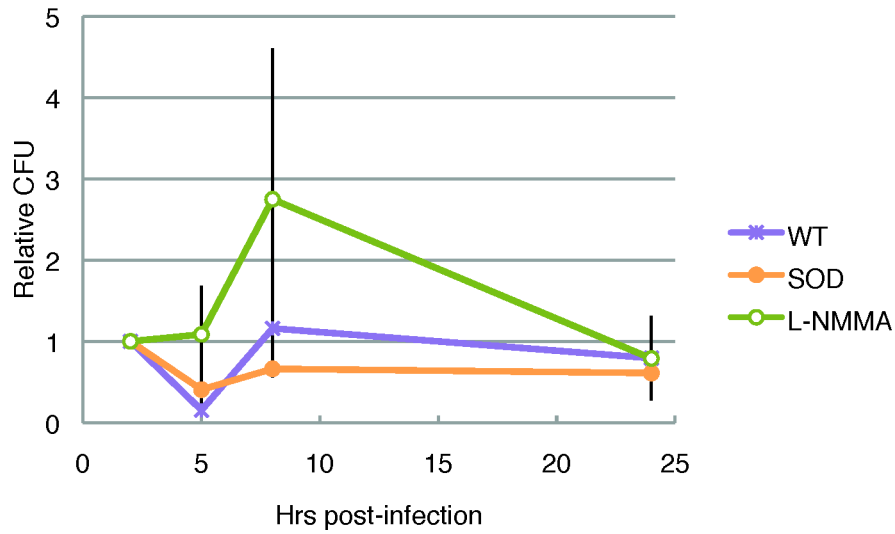
Figure 24. Role of reactive oxygen and nitrogen species in bacteriocidal phenotype of EVT Comparison of intracellular bacterial growth under standard conditions (WT) and in the presence of an inhibitor of reactive oxygen intermediates (SOD) or an inhibitor of reactive nitrogen species (L-NMMA). Inhibitors were added 1 hour post-infection. WT: n=3, SOD: n=2, L-NMMA: n=3. Bars represent SEM.

A

BeWo

B

EVT
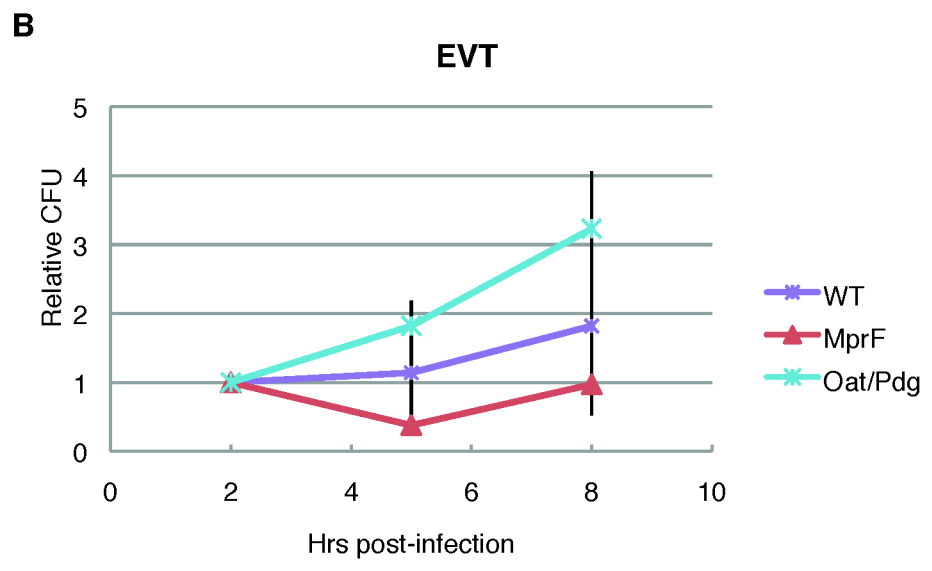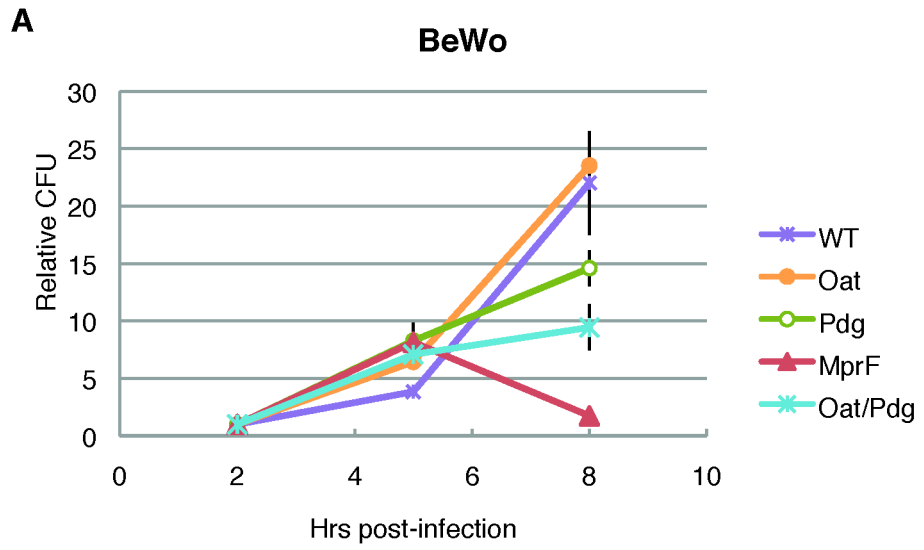
Figure 25. Effects of lysozyme and CAMPs on bacterial growth in BeWo, EVT Comparison of intracellular bacterial growth of wild type (WT) *L. monocytogenes* and strains with deletion(s) in genes responsible for modification of cell wall components that render bacteria resistant to lysozyme (Oat,Pdg, Oat/PDG double mutant) and cationic microbial peptides (CAMPs) (MprF). CFU/well were normalized to the 2-hour time point within each experiment. Bars represent SEM. **(A)** Infection in BeWo, n=3 for all conditions. **(B)** Infection in EVT, WT: n=2, Oat/Pdg: n=3, MprF: n=3.
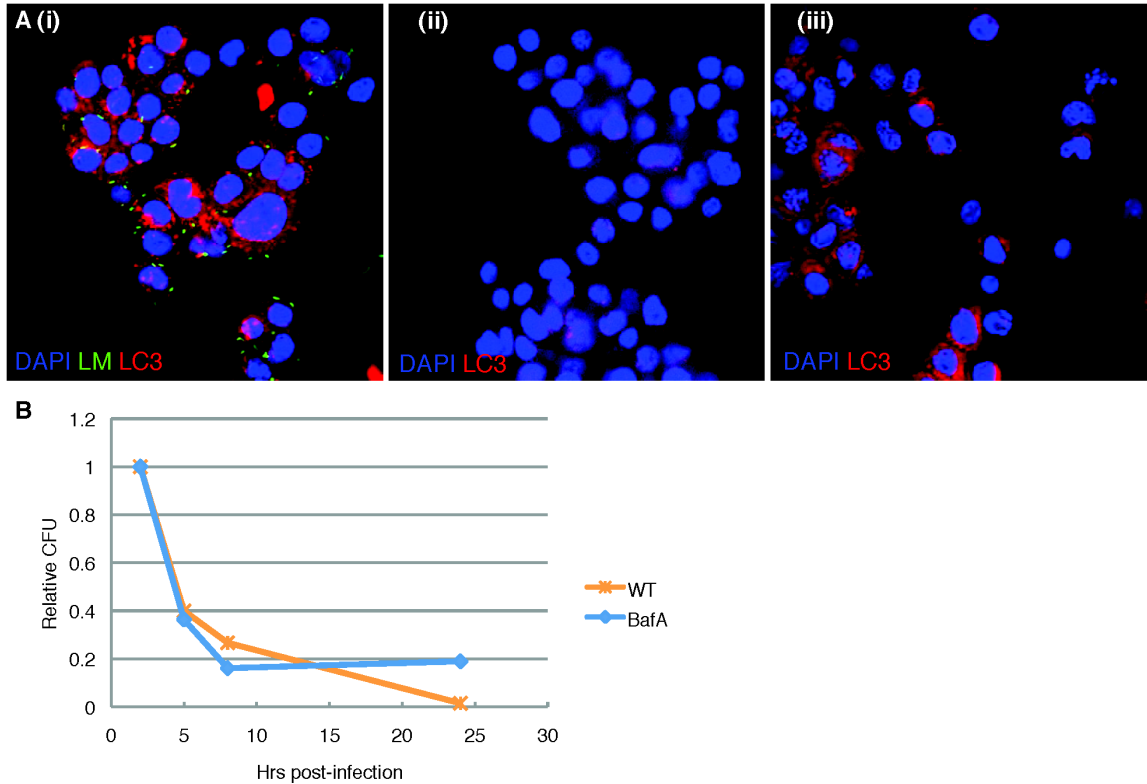
Figure 26. Role of autophagy in EVT bacteriocidal phenotype Autophagy is induced in EVT upon infection, but is not responsible for bacterial demise. **(A)** Representative image of EVT 24 hours post-treatment with **(i)** *L. monocytogenes* counter-stained in green, **(ii)** no treatment, and (iii) Bafilomycin A. Stained for LC3 in red. **(B)** Intracellular bacterial growth in EVT under standard conditions (WT) and in the presence of Bafilomycin A (BafA). Bafilomycin A was added at initiation of infection. CFU/well were normalized to the 2-hour time point. N=1 for both conditions.
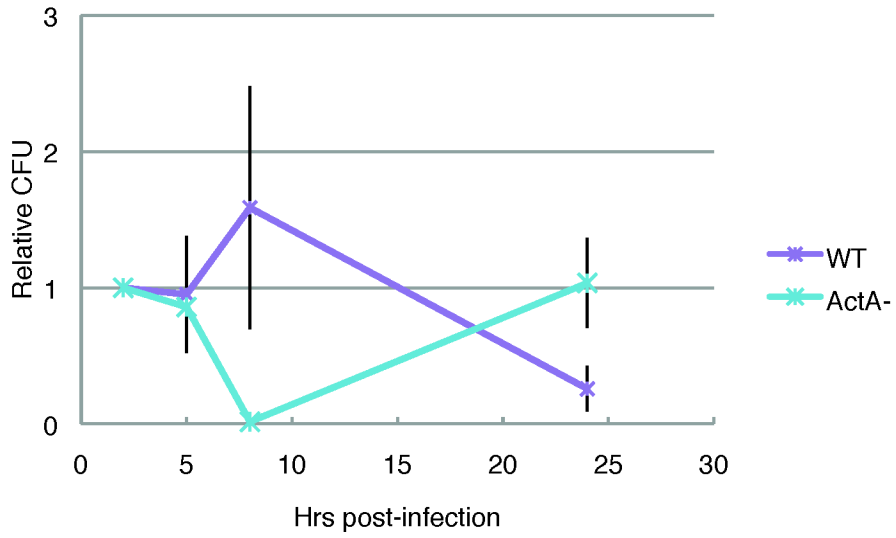
Figure 27. Role of ActA in bacterial growth in EVT Intracellular bacterial growth in EVT of wild type *L. monocytogenes* (WT) and the ΔActA deletion mutant (ActA-). CFU/well were normalized to the 2-hour time point within each experiment. Bars represent SEM. N=2 for both conditions.

Chapter 5

EVT Response to Infection

Introduction

We have shown that placental infection is initiated in specialized invasive cells called extravillous trophoblasts (EVT) at the feto-maternal interface, and that EVT have the unique ability to restrict bacterial growth by trapping and degrading them in the lysozomes. Our main aim in this chapter was to determine the cellular and molecular processes responsible for this unique bacteriocidal phenotype, as well as to speculate on how these responses fit into the larger picture of infection evolving into pregnancy complications. Luckily, *L. monocytogenes* has long been used as a model pathogen to study the host cell response to bacteria as well as broader immune signaling systems during infection.

Host Cell Response to L. monocytogenes

The host cell response to *L. monocytogenes* has been extensively defined in macrophages. It is generally accepted that *L. monocytogenes* infection induces type I interferons in an LLO-dependent manner [178-180]. In fact, macrophages have two waves of response to bacteria. The first response to vacuolar bacteria begins through bacterial sensing via TLRs and through MyD88 induces genes dependent on NF-κB such as IL-1 TNFα and other cytokines; the secondary, cytosolic response includes the type I interferons (IFNs) and their downstream signaling cascades including pro-inflammatory cytokines IL12 and IL18. This secondary response is mediated by NOD2 family of pattern recognition receptors sensing bacterial DNA and MDP [181-183] as well as cytosolic sensing of c-di-

129

AMP [184]. Type I IFNs are usually thought of as an anti-viral response, and actually may be beneficial to the bacteria more than to the host during *L. monocytogenes* infection [185, 186]. The location of the bacterium inside (and not the specific presence of the LLO molecule) macrophages is key for determining the type of response the host cell initiates [179]. On the other hand, Induction of IFNγ expression is dependent on LLO specifically [187]. Surprisingly, in Caco2 cells, the same program is initiated for both WT and ΔLLO *L. monocytogenes* [188]. It is important to remember that any dependence on LLO can mean either dependence on cytosolic bacterial localization or on another result of LLO function. For instance, LLO-based loss of membrane integrity may be sensed by cells. Extracellular LLO can induce Fas-FasL mediated apoptosis in T cells possibly by damaging mitochondrial membranes and releasing cytochrome C [189]. Pore formation can also create an avenue for delivery of other antigens such as LTA (lipoteicoic acid), MDP (muramyl dipeptide), bacterial DNA or PGN (peptidoglycan). For instance, it was shown that in activated macrophages, degraded bacteria creates ligands that induce the cytosolic response [190]. Furthermore, in HUVEC cells LLO has been shown to induce a strong LLO-dependent response of NO release and up-regulation of pro-inflammatory cytokines that was attributed to LLO-elicited Ca^{2+} flux [191].Finally, it is also possible for LLO to be directly sensed by pattern recognition receptors; intravenously-delivered LLO has been shown to induce NF-κB activation in

endothelial cells *in vivo* [192], and is able to induce IL-12 and IL-18 production by macrophages in vitro [187].

Trophoblast signaling at the feto-maternal interface

The implantation site is a highly controlled, active, and functional immune environment. The decidua contains a large number of immune cells such as macrophages, dendritic cells, NK and regulatory T cells [14, 193] that are essential to the implantation process and successful pregnancy. It has been shown that trophoblasts cells secrete chemokines that recruit immune cells to the implantation site [194, 195]. Furthermore, trophoblasts can modulate the differentiation of immune cells [196] and these immune cells then respond in unique ways to create the niche environment for implantation [197]. The features involved in this dynamic crosstalk between trophoblasts and the decidua have been relatively well studied [198] [199]. For instance, decidually produced cytokines such as IL-1β and TGFβ regulate trophoblast invasion, and in turn process signals from the trophoblast in order to correctly guide implantation [200, 201].It stands to reason that infection of EVT at this delicate immune interface, especially early in gestation, would affect the development and progression of pregnancy overall.

Trophoblast Response to Infection

We are specifically interested in understanding how these non-immune EVT cells of the placenta respond to infectious challenge. Many groups have studied the effects of bacterial and viral infection on trophoblast cells, though nearly all of these studies have used trophoblast cell lines or the mouse model. Generally, the focus of studies has been on determining how infection affects 1. the cell-cycle state and general health of trophoblasts, 2. innate immune signaling by trophoblasts, or 3. hormone production by the trophoblast. All these aspects can be understood to directly affect the maintenance and progression of a healthy pregnancy.

In terms of the general survival of the cells, it has been shown that parasite [202] and viral infection, or stimulation with viral ligands can cause apoptosis in trophoblast cells such as BeWo [203].Unsurprisingly, trophoblast apoptosis correlates with preterm delivery in mice [204]. Similarly, bacterial ligands such as peptidoglycan have been shown to induce necrosis in mouse trophoblasts [205]. Furthermore, studies with cytomegalovirus suggest that infection of trophoblasts reduce their invasive qualities, which can impair proper placentation [206]. The health and normal function of invading trophoblasts is clearly important for the correct function of the placenta as a whole.

The Abrahams lab has studied the role of trophoblasts in the innate immune system extensively. The placenta been demonstrated to express many TLRs [207]. TLR2 and TLR4 have been specifically defined as highly expressed by extravillous trophoblast cells throughout gestation [208-212]. These TLRs as

132

well as NODs [213] can sense a variety of microbial ligands. However, it is not entirely clear from the literature how different levels or types of infections affect the level or type of inflammation induced. For instance, LPS and PDG have been shown to induce pro-inflammatory IL-6 and IL-8 production by EVT [213, 214], while *Chlamydia trachomatis* infection induced a strong IL-1β response in another system [215]. Overall, infection of trophoblasts can certainly result in inflammation, though the details of which pathways are stimulated in response to which ligands is not clear. Furthermore, it is difficult to speculate which responses are important for the downstream development of pregnancy complications.

The production of hormones by the placenta is critical for maintenance of a pregnancy. Stimulation of trophoblast TLRs has been shown to increase trophoblast secretion of chorionic gonadotropin (hCG) [216]. Similarly, *Chlamydia trachomatis* infection can affect the synthesis of progesterone and estrogen synthesis in trophoblasts [217]. Interestingly, hCG has been demonstrated to increase macrophage functions such as phagocytosis, reactive oxygen and nitrogen species production, and cytokine secretion [218], tying hormone production into the innate immune system. It is reasonable to assume that infection-based changes in hormone levels at the feto-maternal interface would have an effect on the success and health of a pregnancy.

It is likely that infection results in pregnancy complications via a combination of effects on trophoblast survival, innate immune function and signaling, and hormone production. As the literature shows, infection can skew a

133

myriad of delicate processes in the development of the placenta and fetus. We hope to define some of these processes that are affected by *L. monocytogenes* infection in our system of primary human placental tissue.

Results

We have shown that invasion of EVT by *L. monocytogenes* does not cause an overwhelming infection; these specialized cells are able to trap and degrade bacteria in lysozomes. We hypothesized that the ability of these cells to contain infection without causing inflammation are critical for preserving the delicate immunological balance at the feto-maternal interface while protecting the pregnancy from complications. To address this hypothesis, we aimed to define the global response of EVT to bacterial infection.

We first characterized the cytokine response of EVT to infection with *L. monocytogenes* using the SABiosciences qPCR array system. RNA was isolated from primary cells at 5 hours post-infection (and 5 hours post-mock infection as control). Analysis tools provided online by SABiosciences were used to check the quality of data: reverse transcription, PCR, and housekeeping gene controls were in the appropriate range, and the genomic DNA control was negative; all data with unusual dissociation or melting curves was eliminated. All ratios were normalized to the uninfected control and those with over 2.8-fold change in the infected condition were plotted (Figure 28). The most dramatic results were the induction of BMP8 (a TGFβ family member) 9-fold, CSF2 (granulocyte &

macrophage colony-stimulating factor) 8-fold, and IFNβ 7-fold. Down-regulated genes included IL-16 (chemo-attractant of CD4+ cells) and GDF10 (another member of the TGFβ superfamily), and IL-1β (pro-inflammatory cytokine precursor). These results were somewhat difficult to interpret, as similar families of cytokines appear to be up- and down-regulated. For example, the up-regulation of CSF2 would recruit innate immune cells to the infected EVT, while down-regulation of IL-16 would signal the opposite effect. The up-regulation of IFNβ is especially perplexing as this cytokine is typically associated with the cytosolic response to bacteria. It is possible that in EVT, IFNβ is induced by the 10-20% of bacteria that manage to escape the vacuole, or that EVT have a unique response to vacuolar and cytoplasmic pathogens unlike the previously described macrophage systems. The main caveat of these results is that the experiment was done only once; especially because primary cells are so variable in comparison to cell lines, generalizable conclusions are much more difficult to make in this system.

Despite the limited conclusions of these results, we hypothesized that the bacteriocidal phenotype is a result of an "activated" state of the EVT. This proposed state of activation could be due to their unique environment *in vivo* (for instance, the implantation site is known to be IFNγ rich [117], or it could be induced in a paracrine fashion by initially infected EVT. To address the second hypothesis of paracrine activation, we infected BeWo cells with *L. monocytogenes* in the presence of infected EVT and quantified intracellular

135

bacterial growth over 24 hours (Figure 29). Bacteria appeared to grow slower inside BeWo cells in the presence of infected EVT, suggesting infected EVT secrete something like a cytokine to stimulate BeWo cells to become less hospitable to intracellular bacteria. We next hypothesized that this secreted effector is IFNβ, because IFNβ was identified as one of the most up-regulated cytokines in EVT infection (Figure 28). We went on to test this theory by incubating EVT with neutralizing antibodies against IFNβ during infection, and quantifying intracellular bacterial growth (Figure 30). We did not observe a coherent difference between EVT treated with increasing amount of anti-interferon antibody, suggesting this is not the main paracrine signal between EVT during infection.

We next decided to take a more unbiased approach to understanding the EVT response to infection. Microarrays are an invaluable tool in evaluating global transcriptional changes in response to a stimulus. In addition to all the previously published microarray studies with *L. monocytogenes* - infected cells (see Introduction to the Chapter), the Fisher lab has performed array-based transcriptional analyses of primary human EVT (unpublished). These previously collected data sets would allow us to make novel comparisons to understand why EVT are such distinctive cells.

One of our initial concerns with performing microarray analysis on EVT was the resistance of these cells to bacterial invasion. We first calculated the rate of infection of EVT at different MOIs (Figure 31). We quantified that with MOIs

above 25, cells had taken up multiple bacteria. Our goal in optimizing the MOI was to maximize the percentage of cells infected without going over 2 bacteria per infected cell, thus we settled on an MOI of 25 for microarray experiments. Another issue in designing our experimental setup for the microarray experiment was eliminating donor-to-donor variability. To address this concern, we decided to collect infected and mock-infected RNA from each donor in order to be able to normalize each data point to its own donor-specific mock-infected control. We also decided on 4 as a reasonable number of donors. Finally, we were very interested in dissecting the role of LLO and the intracellular location of the bacteria in EVT infection. While macrophages are known to have distinct responses to vacuolar vs. cytoplasmic bacteria, it is unclear whether EVT react similarly. One hypothesis is that keeping bacteria vacuolar is one way for EVT to stay non-inflammatory in a delicate immune environment. Perplexingly, our preliminary cytokine array data shows a typically cytoplasmic response of IFNβ induction by EVT. To elucidate the role of LLO in EVT response to infection, we collected RNA from WT and ΔLLO *L. monocytogenes* – infected EVT (data not shown). At the time of writing, 4 experiments have been carried out with different donors and 4 complete sets of RNA have been collected. Each set contains 5 samples: 2 hours post - WT infection, 2 hours post - ΔLLO infection, 5 hours post - WT infection, 5 hours post - ΔLLO infection, 5 hours post – mock infection. These samples will next be submitted to the Microarray Processing Core for amplification, hybridization and analysis.

Conclusions & Future Directions

In attempting to dissect EVT response to infection, we hoped to answer two main questions. The first was mechanistic - how do EVT sense and kill bacteria? Is this an active process or an accident of other unique cell functions? Secondly - what is the role of EVT in the development of pregnancy complications? Is their ability to contain infection critical for preventing inflammation at the feto-maternal interface?

While our cytokine array study proved relatively inconclusive due to the small sample size, it opened avenues for further investigation. The induction of IFNβ during infection was surprising because it is typically a response to cytoplasmic pathogens. The down-regulation of some chemokines and up-regulation of others suggests that infected EVT recruit specific subsets of innate immune cells. It would be interesting to discern which decidual cells respond to these signals. A fascinating experiment would involve co-culturing primary decidual cells with infected vs. uninfected EVT.

Our results suggest that EVT do in fact secrete factors that affect nearby cells to be less hospitable to bacterial growth. We showed that this factor is likely not IFNβ, and the nature of this effector remains an exciting open question we hope to address in the future. Our current plans to profile the transcriptional response of EVT to infection will identify the variety of cellular processes that are affected by bacterial invasion. We are most interested in looking at immune

pathways that would lead to the bacteriocidal phenotype as well as those that may play a role in recruiting or activating the innate immune system in the decidua. One of the caveats with our experimental setup is that only ~50% of cells collected for RNA analysis are infected, and this will make it difficult to discern small transcriptional changes, especially that of down-regulated genes. Furthermore, we recognize that within the infected dish, two populations (infected and uninfected but exposed to pathogen) will contribute individual changes that we cannot discriminate. To address the differences between infected cells and those simply exposed to pathogens but not invaded, we have developed a system to isolate infected cells using Laser Capture Microdissection (LCM). We hope to use this system along with qPCR to differentiate between these two populations with regard to specific gene expression changes. Moreover, we will be able to use the LCM-qPCR system to isolate and analyze infected EVT from whole placental explants infected with bacteria. One of our main goals for global transcriptional analysis is to generate a signature profile that we can then use to easily (using qPCR for a few key factors) in studying infection and its interaction with a variety of conditions related to pregnancy complications – e.g. other pathogens, immune or hormonal changes, varying oxygen concentrations.

We expect that EVT will respond to bacteria more like immune cells rather than epithelial cells in their recognition of the bacteria in an LLO-dependent manner. However, we do not expect to see up-regulation of the standard set of IFN-inducible genes, as EVT are unlikely to be pro-inflammatory. Instead, we

expect NF-κB signaling pathways to be engaged and downstream targets to be affected. For instance, stimulation of microbial ligand receptors triggers a classical pathway leading to iNOS transcription that involves p38 MAPK, NF-κB, and the JAK-STAT-IRF1 pathways [153]. Neuronal killing of *L. monocytogenes* mediated by NO production was found to be dependent on the STAT-1 pathway [160], so we may expect to see a similar mechanism in EVT. The unbiased scope of the array will reveal the presence of other defense mechanisms. For instance, TBK1, an angiogenesis-related kinase, has recently been found to regulate vacuolar integrity during bacterial infection either by initiating autophagy or modulating the flux of ions and water through the pathogen-containing vacuole [219], and may be involved in vacuolar sequestration in EVT. The depletion of L-tryptophan by up-regulation of IDO is another transcriptionally-controlled antimicrobial mechanism. Other possibilities include the deprivation of iron from endocytic vacuoles by the up-regulation of lactoferrin or down-regulation of trasferrin receptors, or NRAMP1, a membrane protein that exerts a bacteriostatic effect by extruding divalent cations from the phagosome [220].

One of the main challenges of working with primary cells is the difficulty in genetically modifying them. We hope to nevertheless follow up on interesting hits from our microarray data set with several alternative methods. There has been some inspiring evidence suggesting siRNA knockdown in primary EVT and even placental explants is possible [221]. We also hope to be able to study the details of specific pathways by knocking down genes in the more amenable and

available BeWo cells. Lastly, we plan to use the vast acumen of knowledge about *L. monocytogenes* genes and use mutants with well-known effects on eukaryotic pathways we are interested in.

Methods & Materials

All human tissue collection, cell isolation, culture of primary cells and cell lines, bacterial growth and quantification, immunofluorescence staining, visualization and image processing was performed as described in previous chapters. Novel methods and conditions are described below.

Neutralizing antibody against IFNβ

Monoclonal Anti-human IFNβ antibody (R&D Systems) was reconstituted in PBS to a stock concentration of 0.5mg/mL and added to standard experimental conditions at 30 minutes post-infection to final concentrations of 5μg/mL, 20μg/mL and 50μg/mL.

RNA Collection for Cytokine Arrays & Microarrays

EVT were plated on 6-well transwells at 1-2 million cells per sample and infected at MOI 25 as previously described. The RNEasy kit (Qiagen) and an altered RNA Isolation protocol were used. Briefly, cells were washed with cold PBS, and 500uL ice-cold RLT buffer (Qiagen) with β-mercaptoethanol (10μL/mL buffer) was added to each sample and cells scraped off into 12mL round-bottom

tubes. An upright tissue homogenizer (T25 digital Ultra-Turrax IKA, Staufen, Germany) was used to disrupt cells for 25 seconds at setting 3. Between samples, homogenizer was rinsed with RNase-Away (Molecular BioProducts, San Diego, CA), 100% Ethanol, and nuclease-free water for 5 seconds each. 1mL of nuclease-free water was added to each sample followed by 10uL Proteinase K (50µg/mL stock, Epicentre). Mixture was incubated for 10 minutes at 55°C, then pelleted for 3 minutes at room temperature at 10Kg. The supernatant was collected and 750uL 100% ethanol was added and mixed by pipetting. This mixture was put on the Qiagen column, and provided protocol followed exactly, including on-column DNAse treatment. Finally, RNA was eluted form the column in 30µL of 65°C nuclease-free water, quantified via NanoDrop, and stored at -80°C.

SABiosciences qPCR Arrays

cDNA was made from isolated RNA following the SABiosciences protocol and the provided RT^2 First Strand Kit, and verified for integrity by agarose gel electrophoresis (data not shown). The protocol for qPCR Arrays was followed exactly with thermal profile provided by SABiosciences. Analysis was done via online tools provided by the company as well.
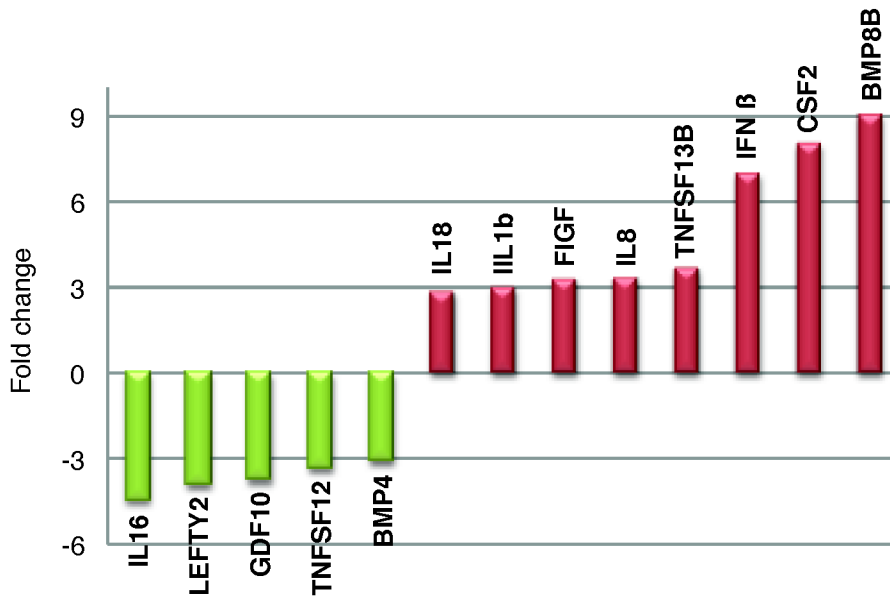
Figure 28. EVT cytokine response to infection EVT were infected under standard conditions and RNA was collected at 5 hours post-infection, reverse transcribed into cDNA and assayed for expression of cytokine genes using SABiosciences qPCR Array System. Fold changes were calculated as compared to 5-hour post mock-infection control. All assayed genes with >2.8 fold change were plotted.
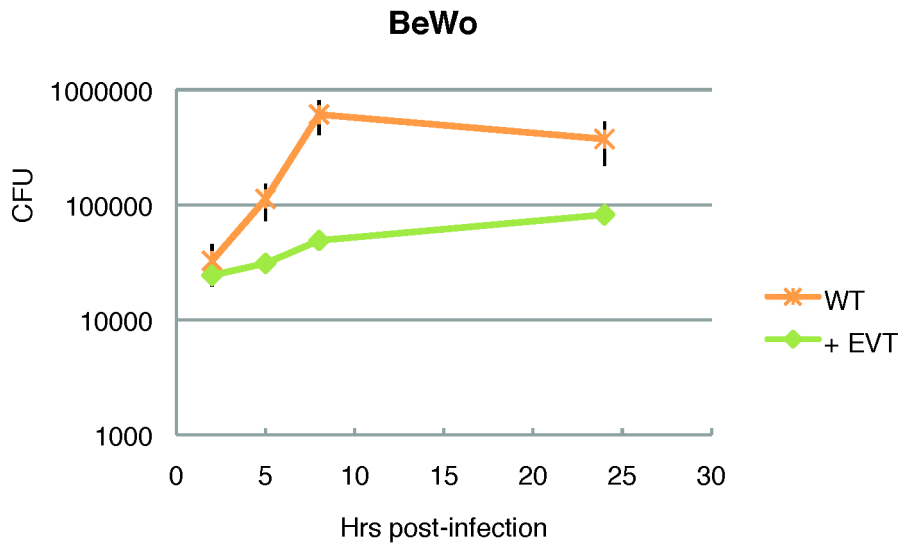
Figure 29. Paracrine effect of infected EVT in bacterial growth in BeWo
BeWo cells were grown on coverslips and assayed for intracellular bacterial growth under standard conditions (WT) or in the presence of infected EVT (+ EVT) in transwells floating above BeWo in the same well. EVT were infected 1 hour prior to BeWo, treated with gentamicin for 15 minutes, and transferred to well with BeWo. Infection was then immediately initiated in BeWo in EVT media. Bars represent SEM. WT: n=3, +EVT: n=1.
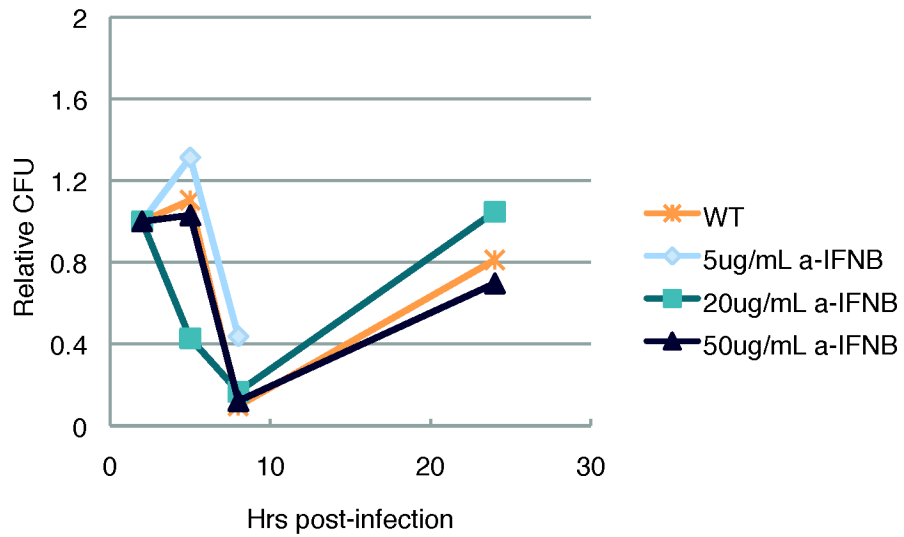
Figure 30. Role of IFNβ in bacteriocidal phenotype of EVT No marked difference was observed between intracellular bacterial growth in standard conditions (WT) and in the presence of increasing concentrations of neutralizing antibody against IFNβ (a-IFNB). Antibody was added at 30 minutes post-infection. N=1 for all conditions.

MOI	Dilution of original bacterial culture	Percent of cells infected	Average number of bacteria per cell
8	1:600	12	1.3
17	1:300	23	1.2
25	1:200	33	2
34	1:150	44	2.2
50	1:100	35	4.8
100	1:50	69	5.2

Figure 31. Infection rates of EVT at different MOIs EVT at 2 hours post-infection were fixed, antibody-stained for *L. monocytogenes*, and percentage of cells infected, as well as average number of bacteria per cell, counted microscopically.

Chapter 7

Developing methods to study syncytial resistance mechanisms

Introduction

Infection of the multinucleate syncytium covering fetal villi has seldom been observed. This is surprising because it represents an enormous surface area (12 m^2) that receives up to 20% of the maternal blood volume at term [16] and is thus exposed to many blood borne maternal microbes. Several systems describe the resistance of the syncytium to invasion. We recently demonstrated that in primary placental organ cultures, the syncytium is resistant to invasion by the bacterium *L. monocytogenes* [45]. Syncytial infection by the parasite *Toxoplasma gondii* is similarly restricted [135]. In terms of viruses, CMV is rarely found in the syncytium in histopathological analyses of in utero-infected tissue [130]. Supporting studies using human placental organ cultures show the syncytium to be spared during ex vivo CMV infection as well [88]. HSV entry into the syncytium is similarly inefficient in a primary cultured trophoblast system [86].

One reason the syncytium is likely protected from invasion on the apical surface is its profuse branched microvilli, which prevent pathogen adherence and invasion. Moreover, invasion is certainly thwarted by the syncytium's overall paucity of surface receptors. This has been definitively shown for *L. monocytogenes* entry receptor E-caderin [45, 62], and HSV receptors HveA, HveB and HveC [86]. Furthermore, the syncytium's lack of intercellular junctions serves as a protective measure, as many pathogens take advantage of these sites to enter tissues and cells. Lastly, the basal surface may also be guarded

against invasion by the dense cytoskeletal network that supports the laterally vast syncytium [82].

The syncytium appears to be a formidable barrier to infection; it resists invasion likely by virtue of its lack of junctions, receptors, and its intra- and extracellular physical features. In fact, its function as a protective layer may be the reason almost all mammalian placentas have evolved a syncytium [222].

We sought to study the biophysical properties of the syncytium that may be responsible for its resistance to pathogens. We began by looking at the cytoskeletal features of the syncytium in primary human placenta. We next explored different methods of syncytializing the placental cell line BeWo as well as primary human cytotrophoblasts. Finally, we moved into using the mouse trophoblast system, which has many more available tools and appears to more clearly mimic the syncytial features we'd like to investigate.

Results

Cytoskeletal Features of the Human Trophoblast

Previous studies of placental cytoskeletal structures have described the major syncytioskeletal structures [79-82, 223]. Strands of keratin form a thick basal layer and a thinner apical mat; others stretch across the syncytium linking the two layers at intervals and connecting to desmosomes at the basal surface of the syncytium that is in contact with underlying cytotrophoblasts or the basal

lamina. An open lattice-like network of microtubules that is oriented parallel to the syncytial surface supports an apparently disordered mesh of actin microfilaments. This mesh of actin reaches up into the microvilli with a distinct polarity. Desmoplakin and cytokeratin has been identified in this apical zone, whereas the intermediate filaments desmin and vimentin have not observed in the syncytium at all.

We sought to replicate some of these findings in our system of cultured primary human placental explants and in our hands. Our immunofluorescence stains for vimentin and desmin did confirm the absence of these intermediate filaments in the syncytium (data not shown). Staining of actin showed a relatively disorganized network of smaller filaments as compared to the long strands of actin stretching across underlying cytotrophoblasts (Figure 32). With this understanding of the structures of syncytium, we went on to optimize a system where these cytoskeletal features would be replicated.

Syncytialization of BeWo & Primary Cytotrophoblasts

One of the most widely used models of syncytium uses differentiation of BeWo cells [224, 225]. Specifically, this type of differentiation is accomplished by analogs of cyclic AMP or the chemical forskolin, an adenylate cyclase activator [224]. Increased levels of cyclic AMP trigger a cascade that induces actual fusion of cells, which is followed by up-regulation of proteins specific for the syncytium such as beta-hCG [226]. We followed Coutifaris' and Wice's protocols

for differentiating BeWo cells with 8-bromo-cAMP and forskolin respectively and looked at actin distribution in the cells at 24, 48, 72 and 96 hours of treatment. At 72 and 96 hours, all treated cells appeared unhealthy, many of them floating or with blebbing nuclei (data not shown). At 24 and 48 hours, treated cells still appeared intact and did develop more diffuse actin networks as compared to untreated cells. In Both treatments (cAMP and forskolin), fewer and fewer long actin filaments outlining the cells were observed over time, consistent with cell fusion and disappearance of cell boundaries (Figure 33). Despite these definite changes in the direction of syncytium formation, we were not satisfied with the proportion of cells that appeared to be fusing – the treated coverslip appeared to have patches of syncytialized cells surrounded by well-outlined apparently un-fused BeWo cells. We next tried another protocol wherein primary cytotrophoblasts are treated with epidermal growth factor (EGF) to induce syncytialization [227]. However, the resulting syncytium was even spottier than that of cAMP-based methods (data not shown). We decided that studying bacterial growth dynamics and their relationship to the cytoskeletal structures would be too difficult in a mixed population, so we went on to the more robust mouse model of syncytialization.

Mouse Syncytiotrophoblast Model

The mouse model of trophoblast differentiation is based on the well-established protocol of isolating mouse trophoblast stem cells (TSCs) [228]. These stem cells can be propagated indefinitely, or differentiated into one of two fates: syncytium, or invasive giant cells – the mouse analog the human EVT [229]. One of the most attractive features of this system is the possibility of deriving TSCs from genetically engineered mice in order to characterize any number of molecular mechanisms [230]. The Maltepe lab here at UCSF has developed a robust system of producing syncytiotrophoblast in cell culture based on their findings that the oxygen-sensitive transcriptional regular HIF inhibits syncytialization of TSCs [231, 232]. Upon removal of growth factors from TSC culture, cells will differentiate into syncytiotrophoblast unless treated with a HIF-stabilizing agent, DMOG to inhibit cell fusion. DMOG treatment pushes TSCs to differentiate into the invasive giant cells. We decided to use this new system to study the resistance of syncytium to bacterial infection.

The system functioned fairly well in our hands – a 6-7 day differentiation protocol produced large patches of syncytialized cells (Figure 34), although some portions of the coverslip still contained stem cells, giant cells, and other precursor cell types. We were able to identify syncytialized portions by their diffuse actin staining over a multi-nucleated space (Figure 34B, star). Next, we wanted to establish that this syncytial system recapitulates our observation that the syncytium is resistant to infection. We first quantified bacterial growth in trophoblast giant cells using WT 10403S *L. monocytogenes* as well as an EGD-E

strain with an engineered version of InlA that interacts more efficiently with mouse E-cadherin [67]. We were surprised to see that the WT and engineered strains were equally proficient at invading and replicating inside mouse trophoblast giant cells (Figure 35A). This suggests that either the engineered InlA is not as efficient as previously thought, or that bacteria are invading giant cells independent of the E-cadherin-InlA interaction; it is possible that invasion occurs through phagocytosis. For consistency with previous data, we used WT 10403S *L. monocytogenes* for all subsequent experiments.

We went on to quantify bacterial growth in giant cells as compared to syncytialized cells. The mouse giant cells do not replicate the human EVT phenotype of restricting bacterial replication and spread (Figure 35A). Furthermore, we did not observe decreased bacterial growth in syncytialized cells (Figure 35B). We hypothesized that this could be the result of bacterial replication in undifferentiated cells, which are present in the dish due to incomplete syncytialization of the stem cells. We estimated visually that approximately 70% of the syncytialized dish appears to be truly fused cells. We went on to inspect the distribution of bacteria among these subpopulations of cells in the syncytialized dish. We noted that fewer bacteria were present in the syncytialized areas as compared to those with more stem cell or giant cell –like morphology (Figure 35C). One issue we have faced in quantifying this difference has been the difficulty in distinguishing intracellular versus extracellular bacteria.

Conclusions & Future Directions

Our hypothesis for this work states that the syncytium's resistance to pathogen invasion is a result of its unique biophysical properties including its cytoskeletal features and microvillous surface. We began to address this hypothesis by developing systems to study placental syncytium in vitro. Our efforts in syncytializing BeWo cells and primary cytotrophoblasts were unsatisfactory, so we moved into the mouse trophoblast system. Although the mouse system does not recapitulate the bacterial growth defect seen in human invasive trophoblasts, we believe it represents a good model of syncytiotrophoblast. The mouse model is also powerful because of the available genetic tools that would allow for a more in dept analysis of molecular pathways.

Unfortunately, we did not observe a quantifiable defect in bacterial invasion or growth in mouse syncytiotrophoblast as compared to mouse giant cell cytotrophoblast. We believe this may be an artifact of the incomplete syncytialization of mouse trophoblast stem cells into syncytium. Microscopically, it did appear as though fewer bacteria are present in syncytialized areas of the sample dish. Microscopy-based quantification would give credence to this phenotype and is the first step to validating this system.

We plan to test the biophysical properties of the syncytium by probing the rigidity of the mouse syncytiotrophoblast via atomic force microscopy in Dan Fletcher's lab at UC Berkeley. We will then compare this with previous biophysical studies of *L. monocytogenes* protrusions during cell-to-cell spread

[233]. We have collected this type of data from control BeWo cells and are ready to look at syncytium. We expect syncytialized cells to be more rigid than cytotrophoblast or trophoblast stem cells; this would be consistent with our idea that bacterial protrusions are more difficult to achieve into the syncytium as compared to other cell types, making it less susceptible to pathogen invasion.

Lastly, we plan to use the mouse trophoblast system to investigate the effect of bacteria on the differentiation of trophoblasts. It is plausible that one of the pathways from pathogen invasion to pregnancy complications involves incorrect differentiation of trophoblast into different cell lineages causing improper implantation. For instance, improper implantation is a major factor in the development of pre-eclampsia [234]. We have infected mouse trophoblast stem cells with *L. monocytogenes* and have some preliminary evidence that it indeed skews the differentiation of stem cells towards the invasive phenotype (data not shown). We hope to follow up on this idea by quantifying these changes and looking into what cellular and molecular factors are involved.

Methods & Materials

All human tissue collection, cell isolation, culture of primary cells and cell lines, bacterial growth and quantification, immunofluorescence staining, visualization and image processing was performed as described in previous chapters. Novel materials, methods and conditions are described below.

Materials & Stock Concentrations

CellStart Humanized Substrate for Cell Culture (Cell Therapy Systems) was used for culture of mouse trophoblast stem cells. Fibroblast Growth Factor-4 (FGF-4, Sigma-Aldrich) was dissolved in distilled water for a 25µg/mL stock solution. U0126 solution (10µM) was a gift from Dr. Emin Maltepe. DMOG (Sigma-Aldrich) was diluted in DMSO to 570mM. Heparin sodium salt (Sigma-Aldrich) was dissolved in PBS for a 1mg/mL stock solution). Gelatin (Sigma-Aldrich) was purchased and stored as a 2% solution in water. 8-bromo-cAMP (Sigma-Aldrich) was dissolved in distilled water for a 0.15M stock solution. Forskolin (Sigma-Aldrich) was dissolved in 95% ethanol to a stock concentration of 0.01M. Human Epidermal Growth Factor (EGF, GIBCO) was dissolved in 0.1% BSA in PBS for a stock solution of 10µg/mL

Strains

L. monocytogenes with murinized InlA replacing WT InlA [67] was a gift from Dr. Dan Portnoy.

Antibodies

Mouse monoclonal α-Vimentin antibody (Thermo Scientific) was used at 1:100, and rabbit polyclonal α-Desmin antibody (Thermo Scientific) was used at 1:200.

Syncytialization of BeWo, EVT

Cells were plated at 200,000 cells per 24-well coverslip or transwell. 8-bromo-cAMP was added to BeWo cells at 1.5mM for 24-96 hours; forskolin was added to BeWo cells at 0.1mM for 24-96 hours. EGF was added to EVT at 100ng/mL for 24-72 hours.

Mouse Trophoblast Stem Cell (TSC) Culture

To prepare dishes for culture of TSCs, CellStart was diluted 1:20 in PBS and 60mm^2 dishes were coated with the dilution and incubated for 2hours at 37°C. Excess liquid was aspirated and cells plated onto the dish. TSCs were cultured in RPMI-1640 with 20% FBS, 1% sodium pyruvate, 100μM β-mercaptoethanol, 1% L-glutamine, 1% penicillin/streptomycin. FGF4 (25ng/mL) and Heparin (1μg/mL) was added fresh to media each time cells were thawed, split, or fed. Cells were split every day at 1:4 or every 2 days at 1:8.

Differentiation of TSC into Giant Cells

Dishes were prepared as described above for TSCs except with Gelatin (1:20 dilution in PBS) instead of CellStart. After trypsinization, TSCs were re-suspended in media without FGF4, without Heparin, and instead with DMOG (3mM). Cells were fed with fresh media every 2 days and allowed to differentiated for 7 days.

Differentiation of TSC into Syncytiotrophoblast

Differentiation into syncytiotrophoblast was identical to the protocol for giant cells except for addition of U0126 at 10nM instead of DMOG. This novel Mek-inhibitor has been characterized by Dr. Emin Maltepe to better induce syncytialization of mouse TSCs (personal communication).
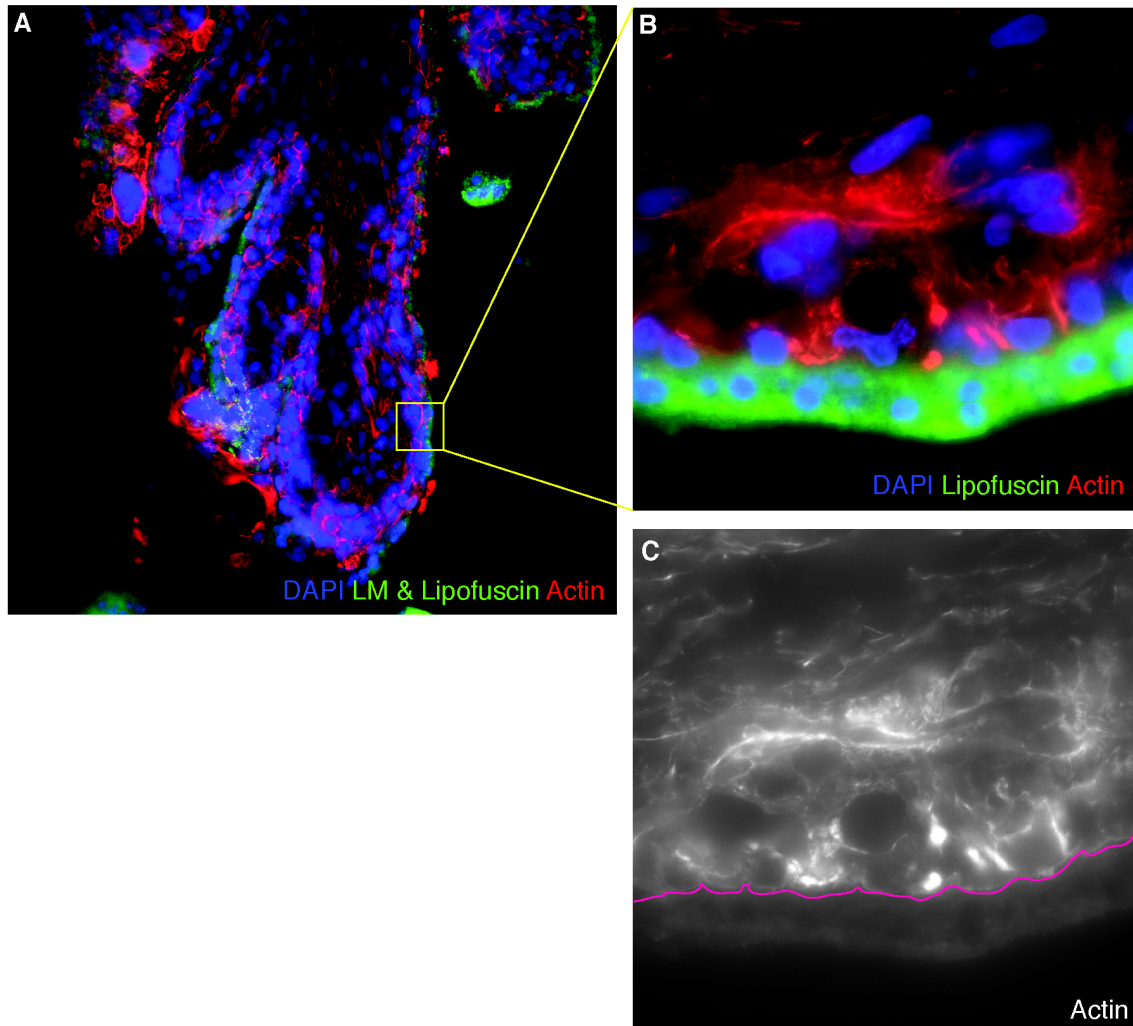
Figure 32. Actin structure in human placental explants Syncytial actin structure is diffuse as compared to underlying cytotrophoblasts and stromal cells. **(A)** Human placental explant 24 hours post-infection with GFP-expressing *L. monocytogenes* was fixed, frozen, sectioned, and stained for actin (red) and nuclei (DAPI, blue). **(B)** Zoom into part of explant with clear syncytial boundary, demarcated by lipofuscin (green). **(C)** Actin (red) channel from **(B)** shown in white, with syncytial boundary drawn in pink.
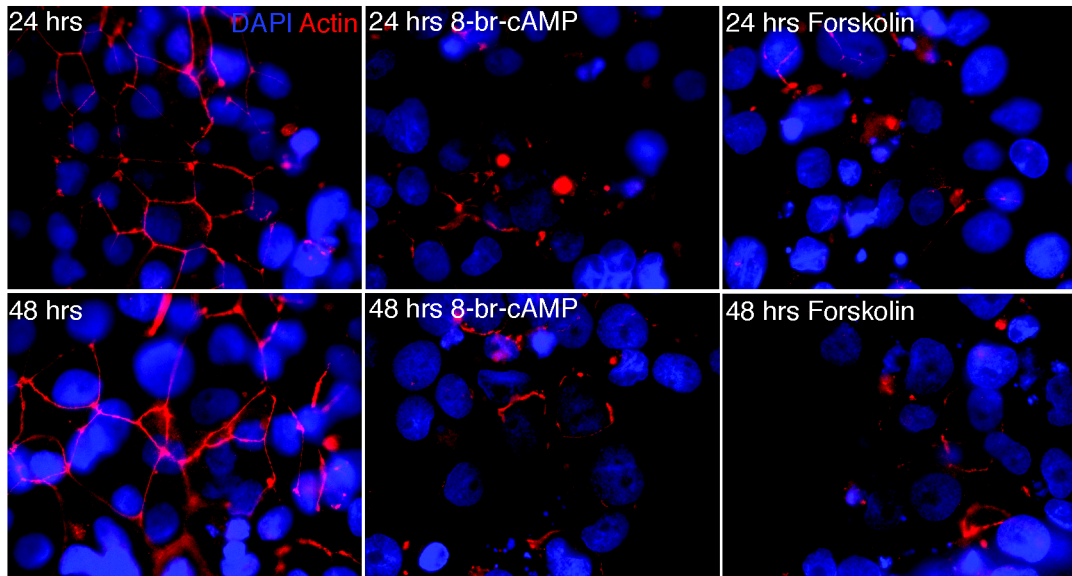
Figure 33. Syncytialization of BeWo using cyclic AMP and Forskolin BeWo
after 24 and 48 hours of treatment with syncytializing agents Forskolin and cyclic
AMP analog (8-br-cAMP) as compared to culture without treatment (two left-most
panels). Cells are stained for actin (red) and nuclei (blue). A decrease in actin-
demarcated cell boundaries in treated cells suggests cell fusion/syncytialization.
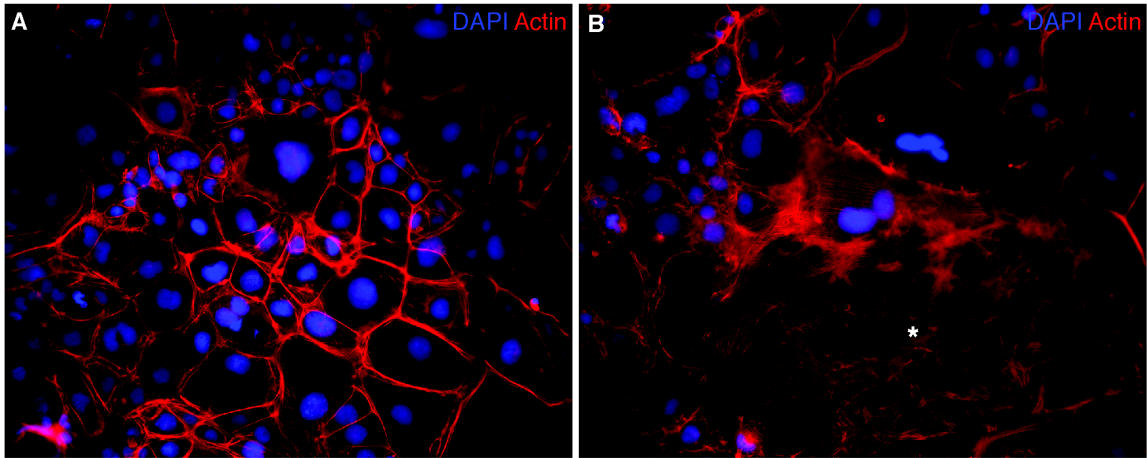
Figure 34. Differentiation & syncytialization of mouse trophoblast stem cells (mTSCs) mTSCs were differentiated into Giant cells **(A)** or syncytiotrophoblasts **(B)**. See Chapter 6 methods for details. Syncytialization was observed in ~70% of cells on treated dishes, identified by areas of diffuse actin (*).
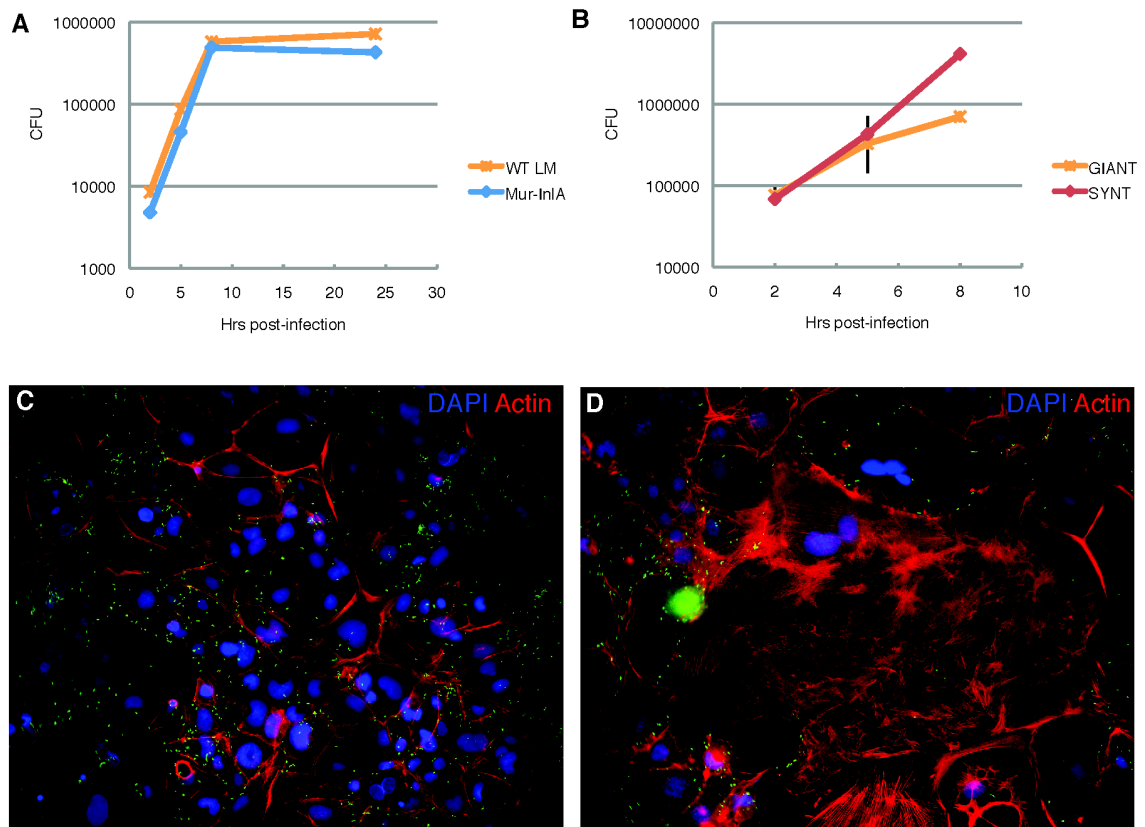
Figure 35. *L. monocytogenes* **growth in mouse trophoblast** **(A)** Intracellular bacterial growth of wild type L. monocytogenes (WT LM) and a strain with engineered InlA designed to bind more efficiently to mouse E-cadherin (Mur-InlA). **(B)** No significant difference between intracellular bacterial growth in syncytialized mouse trophoblasts (SYNT) as compared to trophoblast giant cells (GIANT). Representative image mouse trophoblast giant cells **(C)** and syncytialized trophoblasts **(D)** 2 hours post-infection with *L. monocytogenes* (green). Counterstained for actin (red) and nuclei (blue). Note relative absence of bacteria in syncytialized area as compared to neighboring un-fused cells **(D)**.

Chapter 8

Overall Conclusions and Future Directions

The placenta is an incredible organ that creates a unique immunological environment to protect the fetus from invading pathogens while avoiding maternal immune rejection. How these critical and contradictory tasks are accomplished is a major immunological paradox. Though many questions remain unanswered, we have been fortunate to contribute to the field by dissecting some of the intrinsic defense mechanisms of the placenta. We have had the privilege of studying these processes in primary human tissue and cells.

The human placental structure creates two points of direct contact between mother and fetus: 1. the large surface area of the syncytium that is bathed in maternal blood and 2. the EVT that invade the decidua where they are juxtaposed to maternal immune cells. Both of these sites have been hypothesized to be a crossing avenue for vertically transmitted pathogens. But in fact, these two cell types have several unique properties making them resistant to infection.

Our first experiments with whole tissue placental explants showed that the syncytium is a formidable barrier to infection. We found the syncytium to be resistant to invasion by *L. monocytogenes* (Chapter 2) as well as by *Toxoplasma gondii* [135]. This is consistent with previous studies showing rare viral invasion and replication in this cell type [86, 88, 130]. This resistance is likely due to the syncytium's lack of junctions, receptors, and its intra- and extracellular physical features. We hypothesize that its rigid cytoskeletal network and microvillous

164

surface prevent pathogen adhesion and protrusion/invasion. We hope to test this hypothesis using the mouse system of syncytialized trophoblast. We have preliminary data showing this system recapitulates the resistance to *L. monocytogenes* we observe in human syncytium. We plan to measure the physical resistance of the syncytium to protrusion using Atomic Force Microscopy and correlate it to previously studied forces of L. monocytogenes cell-to-cell spread [233].

The resistance of the syncytium to invasion may explain why most transplacental pathogens have facultative or obligate intracellular life cycles. Dissemination through the blood is not a major route of infection. Rather, pathogens are more likely to travel inside cells to the implantation site and infect fetal extravillous trophoblasts (EVT).

Using *L. monocytogenes* and *T. gondii* in a primary placental organ culture system, we have shown that EVT are the preferred site of entry for these pathogens into the placenta (Chapter 2, [135]). However, infection even with high doses of *L. monocytogenes* was difficult to achieve and highly variable, suggesting these cells are inhospitable to some pathogens. In fact, we further showed (Chapter 3) that isolated primary human EVT entrap *L. monocytogenes* in lysosomal compartments where they are degraded. Previous studies support the notion of EVT as a barrier cell: for instance CMV and HIV infection has been shown to be inefficient in trophoblasts [129], [130], [131]. In fact, HIV-1 virions have been reported to be trapped within endosomal compartments in

trophoblasts [131]. Lastly, we have some preliminary evidence that *Chlamydia trachomatis* infection in EVT is unproductive and results in aberrant reticulate bodies (data not shown), suggesting the phenotype may be true for a variety of intracellular pathogens.

Several experimental systems, including ours, demonstrate EVT endosomal trafficking hindering the normal life cycles of pathogens and preventing growth and spread of the bacterium or virus. It is possible that the invasive role of EVT and their active degradation of extracellular matrix may require unique degradative and endolysosomal pathways that interfere with the life cycle of intracellular pathogens. We investigated the bacteriocidal phenotype of EVT further, addressing a number of hypotheses with respect to its origin. We have yet to discern the specific mechanism of killing, though cationic microbial peptides and reactive nitrogen species may play a role. In fact, placental production of antimicrobials like β-defensins, indoleamine 2,3-dioxygensase, cathelicidin, and reactive oxygen and nitrogen species has been established [164], and would be interesting factors to look at more closely.

We observed that infected EVT are able to affect neighboring cells to become less hospitable to bacterial replication, suggesting a paracrine signaling factor that may put cells in an "activated" state. We saw an up-regulation of IFNβ during infection; however, we concluded this was not the signaling factor. We now hope to dissect the mechanisms of bacterial killing using a broader approach – transcriptional profiling with microarrays. We have collected samples of infected

166

and mock-infected primary EVT for whole genome microarray analysis with the UCSF Genomics Core.

To follow up on the global screen, we will pick the most promising candidate genes - those significantly up-regulated during infection. We will use newly worked out RNAi delivery techniques [221] to knock down these mediators and assess their importance in EVT control of infection. We can also inspect these pathways in the more amenable systems of BeWo cells or our newly developed mouse trophoblast system. Lastly, the unbiased characterization of the EVT response to infection may open avenues for further investigation into placental immunity and into the roots of pregnancy complications associated with infection

Despite the effectiveness of the placental barrier, infections can nevertheless progress to cause pre-term labor or colonization of the fetus. What factors contribute to the occasional success of feto-placental infection? It is possible that rare infection is a result of patient predisposition or of strains that possess enhanced colonization capacities to overcome the bottlenecks. To our knowledge, no host genetic basis for differences in susceptibility to pre-term labor or vertical transmission has been identified. There is little work to date identifying placental-specific pathogen virulence factors, and this remains an interesting and open area of research.

We hypothesize that both the syncytial and EVT barriers are effective until a certain threshold of cellular damage or placental inflammation is surpassed.

This can occur due to co-infection with other pathogens or non-infectious changes that influence oxygen tension or pH in the placenta. These could alter the biochemical and physiological condition of the syncytium and the EVT to decrease their resistance to infection. An uncontrolled infection can escalate inflammation to trigger pre-term labor, or spread enough to reach the fetus. Cardenas et al. has dubbed this model the "Double Hit Hypothesis," and demonstrated that subclinical viral infection sensitizes pregnant mice to bacterial infection leading to pre-term delivery [235]. Further support for this hypothesis comes from histopathological analyses of in utero CMV infections that reveal the virus is more often found in placentas with concurrent bacterial infections [236]. This idea is also an attractive explanation for the long-documented predisposition of women with gum disease to pre-term labor [237]; exposure to temporarily bloodborne oral bacteria may intensify placental responses to a subclinical infection and lead to the inflammation-based initiation of labor. More studies are needed to establish these connections between multiple pathogens and the pregnant host. We hope to pursue this avenue specifically with the sexually transmitted pathogen *Chlamydia trachomatis*; Chlamydia has been associated with pregnancy complications [238] such as preterm labor and is a likely candidate for the "Double Hit" scenario.

The placenta has developed a powerful defense against infection consisting of multiple layers of physical and biochemical barriers. Both

subpopulations of trophoblasts—syncytium and EVT—that are in direct contact with maternal cells and tissues are effective barriers against infection. These barriers can likely be breached by additional infectious or non-infectious damage to the placenta. Such damage can impair intrinsic defenses to allow pathogen growth and transmission or escalate an immune imbalance at the fetal-maternal interface leading to pre-term labor.

References

1. Goldenberg, R.L., et al., *Epidemiology and causes of preterm birth.* Lancet, 2008. **371**(9606): p. 75-84.

2. Goldenberg, R.L., J.C. Hauth, and W.W. Andrews, *Intrauterine infection and preterm delivery.* N Engl J Med, 2000. **342**(20): p. 1500-7.

3. Faye-Petersen, O.M., *The placenta in preterm birth.* J Clin Pathol, 2008. **61**(12): p. 1261-75.

4. Beck, S., et al., *The worldwide incidence of preterm birth: a systematic review of maternal mortality and morbidity.* Bull World Health Organ. **88**(1): p. 31-8.

5. Arechavaleta-Velasco, F., et al., *Viral infection of the trophoblast: time to take a serious look at its role in abnormal implantation and placentation?* J Reprod Immunol, 2002. **55**(1-2): p. 113-21.

6. von Dadelszen, P. and L.A. Magee, *Could an infectious trigger explain the differential maternal response to the shared placental pathology of preeclampsia and normotensive intrauterine growth restriction?* Acta Obstet Gynecol Scand, 2002. **81**(7): p. 642-8.

7. Hsu, C.D. and F.R. Witter, *Urogenital infection in preeclampsia.* Int J Gynaecol Obstet, 1995. **49**(3): p. 271-5.

8.	von Dadelszen, P., et al., *Levels of antibodies against cytomegalovirus and Chlamydophila pneumoniae are increased in early onset pre-eclampsia.* BJOG, 2003. **110**(8): p. 725-30.

9.	Romero, R., et al., *Inflammation in pregnancy: its roles in reproductive physiology, obstetrical complications, and fetal injury.* Nutr Rev, 2007. **65**(12 Pt 2): p. S194-202.

10.	Vrachnis, N., et al., *Intrauterine inflammation and preterm delivery.* Ann N Y Acad Sci. **1205**: p. 118-22.

11.	Brosens, I., et al., *The "Great Obstetrical Syndromes" are associated with disorders of deep placentation.* Am J Obstet Gynecol. **204**(3): p. 193-201.

12.	Munoz-Suano, A., A.B. Hamilton, and A.G. Betz, *Gimme shelter: the immune system during pregnancy.* Immunol Rev. **241**(1): p. 20-38.

13.	Warning, J.C., S.A. McCracken, and J.M. Morris, *A balancing act: mechanisms by which the fetus avoids rejection by the maternal immune system.* Reproduction. **141**(6): p. 715-24.

14.	Mor, G., et al., *Inflammation and pregnancy: the role of the immune system at the implantation site.* Ann N Y Acad Sci. **1221**: p. 80-7.

15.	Carter, A.M., *Animal models of human placentation--a review.* Placenta, 2007. **28 Suppl A**: p. S41-7.

16.	Benirschke, K., P. Kaufmann, and R.N. Baergen, *Pathology of the human placenta.* 2006, Springer: New York. p. xx, 1050 p.

17. Cantle, S.J., et al., *Interpretation of syncytial sprouts and bridges in the human placenta.* Placenta, 1987. **8**(3): p. 221-34.

18. Schiebler, T.H. and P. Kaufmann, *Reife Placenta.* Die Plazenta des Menschen, ed. V. Becker, T.H. Schiebler, and F. Kubli. 1981, Stuttgart: Thieme.

19. Benirschke, K., P. Kaufmann, and R.N. Baergen, *Pathology of the human placenta.* 5th ed. 2006. 30-41.

20. Red-Horse, K., et al., *Trophoblast differentiation during embryo implantation and formation of the maternal-fetal interface.* J Clin Invest, 2004. **114**(6): p. 744-54.

21. Drevets, D.A. and M.S. Bronze, *Listeria monocytogenes: epidemiology, human disease, and mechanisms of brain invasion.* FEMS Immunol Med Microbiol, 2008.

22. Swaminathan, B. and P. Gerner-Smidt, *The epidemiology of human listeriosis.* Microbes Infect, 2007. **9**(10): p. 1236-43.

23. Lecuit, M., *Human listeriosis and animal models.* Microbes Infect, 2007. **9**(10): p. 1216-25.

24. Pamer, E.G., *Immune responses to Listeria monocytogenes.* Nat Rev Immunol, 2004. **4**(10): p. 812-23.

25. Portnoy, D.A., *Manipulation of innate immunity by bacterial pathogens.* Curr Opin Immunol, 2005. **17**(1): p. 25-8.

26. Cossart, P. and A. Toledo-Arana, *Listeria monocytogenes, a unique model in infection biology: an overview.* Microbes Infect, 2008. **10**(9): p. 1041-50.

27. Pizarro-Cerda, J. and P. Cossart, *Listeria monocytogenes membrane trafficking and lifestyle: the exception or the rule?* Annu Rev Cell Dev Biol, 2009. **25**: p. 649-70.

28. Portnoy, D.A., V. Auerbuch, and I.J. Glomski, *The cell biology of Listeria monocytogenes infection: the intersection of bacterial pathogenesis and cell-mediated immunity.* J Cell Biol, 2002. **158**(3): p. 409-14.

29. Bierne, H., et al., *Internalins: a complex family of leucine-rich repeat-containing proteins in Listeria monocytogenes.* Microbes Infect, 2007. **9**(10): p. 1156-66.

30. Mengaud, J., et al., *E-cadherin is the receptor for internalin, a surface protein required for entry of L. monocytogenes into epithelial cells.* Cell, 1996. **84**(6): p. 923-32.

31. Henry, R., et al., *Cytolysin-dependent delay of vacuole maturation in macrophages infected with Listeria monocytogenes.* Cell Microbiol, 2006. **8**(1): p. 107-19.

32. Ray, K., et al., *Life on the inside: the intracellular lifestyle of cytosolic bacteria.* Nat Rev Microbiol, 2009. **7**(5): p. 333-40.

33. Schnupf, P. and D.A. Portnoy, *Listeriolysin O: a phagosome-specific lysin.* Microbes Infect, 2007. **9**(10): p. 1176-87.

34.   Tilney, L.G. and D.A. Portnoy, *Actin filaments and the growth, movement, and spread of the intracellular bacterial parasite, Listeria monocytogenes.* J Cell Biol, 1989. **109**(4 Pt 1): p. 1597-608.

35.   Notermans, S., et al., *Studies on the risk assessment of Listeria monocytogenes.* J Food Prot, 1998. **61**(2): p. 244-8.

36.   Mylonakis, E., et al., *Listeriosis during pregnancy: a case series and review of 222 cases.* Medicine (Baltimore), 2002. **81**(4): p. 260-9.

37.   Kajii, T., et al., *Anatomic and chromosomal anomalies in 639 spontaneous abortuses.* Hum Genet, 1980. **55**(1): p. 87-98.

38.   Kirkbride, C.A., *Bacterial agents detected in a 10-year study of bovine abortions and stillbirths.* J Vet Diagn Invest, 1993. **5**(1): p. 64-8.

39.   Kaur, S., et al., *Listeria monocytogenes in spontaneous abortions in humans and its detection by multiplex PCR.* J Appl Microbiol, 2007. **103**(5): p. 1889-96.

40.   Lallemand, A.V., et al., *Fetal listeriosis during the second trimester of gestation.* Pediatr Pathol, 1992. **12**(5): p. 665-71.

41.   Teberg, A.J., et al., *Clinical manifestations of epidemic neonatal listeriosis.* Pediatr Infect Dis J, 1987. **6**(9): p. 817-20.

42.   Abram, M., et al., *Murine model of pregnancy-associated Listeria monocytogenes infection.* FEMS Immunol Med Microbiol, 2003. **35**(3): p. 177-82.

43.   Disson, O., et al., *Conjugated action of two species-specific invasion proteins for fetoplacental listeriosis.* Nature, 2008. **455**(7216): p. 1114-8.

44.   Bakardjiev, A.I., et al., *Listeriosis in the pregnant guinea pig: a model of vertical transmission.* Infect Immun, 2004. **72**(1): p. 489-97.

45.   Robbins, J.R., et al., *Placental syncytiotrophoblast constitutes a major barrier to vertical transmission of Listeria monocytogenes.* PLoS Pathog. **6**(1): p. e1000732.

46.   Smith, M.A., et al., *Dose-response model for Listeria monocytogenes-induced stillbirths in nonhuman primates.* Infect Immun, 2008. **76**(2): p. 726-31.

47.   Le Monnier, A., et al., *ActA is required for crossing of the fetoplacental barrier by Listeria monocytogenes.* Infect Immun, 2007. **75**(2): p. 950-7.

48.   Bakardjiev, A.I., B.A. Stacy, and D.A. Portnoy, *Growth of Listeria monocytogenes in the guinea pig placenta and role of cell-to-cell spread in fetal infection.* J Infect Dis, 2005. **191**(11): p. 1889-97.

49.   Lecuit, M., *Understanding how Listeria monocytogenes targets and crosses host barriers.* Clin Microbiol Infect, 2005. **11**(6): p. 430-6.

50.   Lecuit, M., et al., *Targeting and crossing of the human maternofetal barrier by Listeria monocytogenes: role of internalin interaction with trophoblast E-cadherin.* Proc Natl Acad Sci U S A, 2004. **101**(16): p. 6152-7.

51.   Bakardjiev, A.I., J.A. Theriot, and D.A. Portnoy, *Listeria monocytogenes traffics from maternal organs to the placenta and back.* PLoS Pathog, 2006. **2**(6): p. e66.

52.   Moffett, A. and C. Loke, *Immunology of placentation in eutherian mammals.* Nat Rev Immunol, 2006. **6**(8): p. 584-94.

53.   Trowsdale, J. and A.G. Betz, *Mother's little helpers: mechanisms of maternal-fetal tolerance.* Nat Immunol, 2006. **7**(3): p. 241-6.

54.   Medawar, P.B. *Some immunological and endocrinological problems raised by the evolution of viviparity in vertebrates.* in *Symp Soc Exp Biol.* 1953.

55.   Shen, Y., et al., *InlB-dependent internalization of Listeria is mediated by the Met receptor tyrosine kinase.* Cell, 2000. **103**(3): p. 501-10.

56.   O'Riordan, M. and D.A. Portnoy, *The host cytosol: front-line or home front?* Trends Microbiol, 2002. **10**(8): p. 361-4.

57.   Portnoy, D.A., P.S. Jacks, and D.J. Hinrichs, *Role of hemolysin for the intracellular growth of Listeria monocytogenes.* J Exp Med, 1988. **167**(4): p. 1459-71.

58.   Robbins, J.R., et al., *Listeria monocytogenes exploits normal host cell processes to spread from cell to cell.* J Cell Biol, 1999. **146**(6): p. 1333-50.

59.   Kocks, C., et al., *L. monocytogenes-induced actin assembly requires the actA gene product, a surface protein.* Cell, 1992. **68**(3): p. 521-31.

60. Theriot, J.A., et al., *The rate of actin-based motility of intracellular Listeria monocytogenes equals the rate of actin polymerization.* Nature, 1992. **357**(6375): p. 257-60.

61. Zhou, Y., et al., *Human cytotrophoblasts adopt a vascular phenotype as they differentiate. A strategy for successful endovascular invasion?* J Clin Invest, 1997. **99**(9): p. 2139-51.

62. Coutifaris, C., et al., *E-cadherin expression during the differentiation of human trophoblasts.* Development, 1991. **113**(3): p. 767-77.

63. Brown, L.M., et al., *E-cadherin in the assessment of aberrant placental cytotrophoblast turnover in pregnancies complicated by pre-eclampsia.* Histochem Cell Biol, 2005. **124**(6): p. 499-506.

64. Vicovac, L. and J.D. Aplin, *Epithelial-mesenchymal transition during trophoblast differentiation.* Acta Anat (Basel), 1996. **156**(3): p. 202-16.

65. Floridon, C., et al., *Localization of E-cadherin in villous, extravillous and vascular trophoblasts during intrauterine, ectopic and molar pregnancy.* Mol Hum Reprod, 2000. **6**(10): p. 943-50.

66. Lecuit, M., et al., *A single amino acid in E-cadherin responsible for host specificity towards the human pathogen Listeria monocytogenes.* Embo J, 1999. **18**(14): p. 3956-63.

67. Wollert, T., et al., *Extending the host range of Listeria monocytogenes by rational protein design.* Cell, 2007. **129**(5): p. 891-902.

68.   Drevets, D.A., T.A. Jelinek, and N.E. Freitag, *Listeria monocytogenes-infected phagocytes can initiate central nervous system infection in mice.* Infect Immun, 2001. **69**(3): p. 1344-50.

69.   Fisher, S.J., et al., *Degradation of extracellular matrix by the trophoblastic cells of first-trimester human placentas.* J Cell Biochem, 1985. **27**(1): p. 31-41.

70.   Miller, R.K., et al., *Human placental explants in culture: approaches and assessments.* Placenta, 2005. **26**(6): p. 439-48.

71.   Hunkapiller, N.M. and S.J. Fisher, *Chapter 12. Placental remodeling of the uterine vasculature.* Methods Enzymol, 2008. **445**: p. 281-302.

72.   Fisher, S.J., et al., *Adhesive and degradative properties of human placental cytotrophoblast cells in vitro.* J Cell Biol, 1989. **109**(2): p. 891-902.

73.   Drake, P.M., et al., *Human placental cytotrophoblasts attract monocytes and CD56(bright) natural killer cells via the actions of monocyte inflammatory protein 1alpha.* J Exp Med, 2001. **193**(10): p. 1199-212.

74.   Huang, Y., et al., *Human trophoblasts recruited T lymphocytes and monocytes into decidua by secretion of chemokine CXCL16 and interaction with CXCR6 in the first-trimester pregnancy.* J Immunol, 2008. **180**(4): p. 2367-75.

75.   Red-Horse, K., P.M. Drake, and S.J. Fisher, *Human pregnancy: the role of chemokine networks at the fetal-maternal interface.* Expert Rev Mol Med, 2004. **6**(11): p. 1-14.

76.   Forner, L., et al., *Incidence of bacteremia after chewing, tooth brushing and scaling in individuals with periodontal inflammation.* J Clin Periodontol, 2006. **33**(6): p. 401-7.

77.   Cobe, H.M., *Transitory bacteremia.* Oral Surg Oral Med Oral Pathol, 1954. **7**(6): p. 609-15.

78.   Pentecost, M., et al., *Listeria monocytogenes invades the epithelial junctions at sites of cell extrusion.* PLoS Pathog, 2006. **2**(1): p. e3.

79.   Ockleford, C.D., J. Wakely, and R.A. Badley, *Morphogenesis of human placental chorionic villi: cytoskeletal, syncytioskeletal and extracellular matrix proteins.* Proc R Soc Lond B Biol Sci, 1981. **212**(1188): p. 305-16.

80.   Berryman, M., R. Gary, and A. Bretscher, *Ezrin oligomers are major cytoskeletal components of placental microvilli: a proposal for their involvement in cortical morphogenesis.* J Cell Biol, 1995. **131**(5): p. 1231-42.

81.   Beham, A., H. Denk, and G. Desoye, *The distribution of intermediate filament proteins, actin and desmoplakins in human placental tissue as revealed by polyclonal and monoclonal antibodies.* Placenta, 1988. **9**(5): p. 479-92.

82.   King, B.F., *The organization of actin filaments in human placental villi.* J Ultrastruct Res, 1983. **85**(3): p. 320-8.

83.   Vacek, Z., *Electron microscopic observations on the filaments in the trophoblast of the human placenta.* Folia Morphol (Praha), 1969. **17**(4): p. 382-8.

84.   Scheuner, G., et al., *[Submicroscopic detection of oriented protein filaments in the plasmoditrophoblast of the human placenta (author's transl)].* Anat Anz, 1980. **147**(2): p. 145-51.

85.   Rajabian, T., et al., *The bacterial virulence factor InlC perturbs apical cell junctions and promotes cell-to-cell spread of Listeria.* Nat Cell Biol, 2009. **11**(10): p. 1212-8.

86.   Koi, H., et al., *Syncytiotrophoblast is a barrier to maternal-fetal transmission of herpes simplex virus.* Biol Reprod, 2002. **67**(5): p. 1572-9.

87.   Maidji, E., et al., *Maternal antibodies enhance or prevent cytomegalovirus infection in the placenta by neonatal Fc receptor-mediated transcytosis.* Am J Pathol, 2006. **168**(4): p. 1210-26.

88.   Fisher, S., et al., *Human cytomegalovirus infection of placental cytotrophoblasts in vitro and in utero: implications for transmission and pathogenesis.* J Virol, 2000. **74**(15): p. 6808-20.

89.   Sooranna, S.R., et al., *Characterization of human placental explants: morphological, biochemical and physiological studies using first and third trimester placenta.* Hum Reprod, 1999. **14**(2): p. 536-41.

90.   Genbacev, O., S.A. Schubach, and R.K. Miller, *Villous culture of first trimester human placenta--model to study extravillous trophoblast (EVT) differentiation.* Placenta, 1992. **13**(5): p. 439-61.

91.   Glomski, I.J., A.L. Decatur, and D.A. Portnoy, *Listeria monocytogenes mutants that fail to compartmentalize listerolysin O activity are cytotoxic, avirulent, and unable to evade host extracellular defenses.* Infect Immun, 2003. **71**(12): p. 6754-65.

92.   Genbacev, O., M.T. McMaster, and S.J. Fisher, *A repertoire of cell cycle regulators whose expression is coordinated with human cytotrophoblast differentiation.* Am J Pathol, 2000. **157**(4): p. 1337-51.

93.   Genbacev, O., et al., *Regulation of human placental development by oxygen tension.* Science, 1997. **277**(5332): p. 1669-72.

94.   Barnes, P.D., et al., *Yersinia pseudotuberculosis disseminates directly from a replicating bacterial pool in the intestine.* J Exp Med, 2006. **203**(6): p. 1591-601.

95.   Kim, K.S., *Mechanisms of microbial traversal of the blood-brain barrier.* Nat Rev Microbiol, 2008. **6**(8): p. 625-34.

96.   Bishop, D.K. and D.J. Hinrichs, *Adoptive transfer of immunity to Listeria monocytogenes. The influence of in vitro stimulation on lymphocyte subset requirements.* J Immunol, 1987. **139**(6): p. 2005-9.

97.   Skoble, J., D.A. Portnoy, and M.D. Welch, *Three regions within ActA promote Arp2/3 complex-mediated actin nucleation and Listeria monocytogenes motility.* J Cell Biol, 2000. **150**(3): p. 527-38.

98.   Shen, A. and D.E. Higgins, *The 5' untranslated region-mediated enhancement of intracellular listeriolysin O production is required for Listeria monocytogenes pathogenicity.* Mol Microbiol, 2005. **57**(5): p. 1460-73.

99.   Jones, S. and D.A. Portnoy, *Intracellular growth of bacteria.* Methods Enzymol, 1994. **236**: p. 463-7.

100.   Sundstrom, C. and K. Nilsson, *Establishment and characterization of a human histiocytic lymphoma cell line (U-937).* Int J Cancer, 1976. **17**(5): p. 565-77.

101.   Robbins, J.R., et al., *Placental syncytiotrophoblast constitutes a major barrier to vertical transmission of Listeria monocytogenes.* PLoS Pathog, 2010. **6**(1): p. e1000732.

102.   Maldonado-Estrada, J., et al., *Evaluation of Cytokeratin 7 as an accurate intracellular marker with which to assess the purity of human placental villous trophoblast cells by flow cytometry.* J Immunol Methods, 2004. **286**(1-2): p. 21-34.

103.   Ilic, D., M. Kapidzic, and O. Genbacev, *Isolation of human placental fibroblasts.* Curr Protoc Stem Cell Biol, 2008. **Chapter 1**: p. Unit 1C 6.

104. Smith, G.A., et al., *The two distinct phospholipases C of Listeria monocytogenes have overlapping roles in escape from a vacuole and cell-to-cell spread.* Infect Immun, 1995. **63**(11): p. 4231-7.

105. Shetron-Rama, L.M., et al., *Intracellular induction of Listeria monocytogenes actA expression.* Infect Immun, 2002. **70**(3): p. 1087-96.

106. Freitag, N.E. and K.E. Jacobs, *Examination of Listeria monocytogenes intracellular gene expression by using the green fluorescent protein of Aequorea victoria.* Infect Immun, 1999. **67**(4): p. 1844-52.

107. Merzlyak, E.M., et al., *Bright monomeric red fluorescent protein with an extended fluorescence lifetime.* Nat Methods, 2007. **4**(7): p. 555-7.

108. Decatur, A.L. and D.A. Portnoy, *A PEST-like sequence in listeriolysin O essential for Listeria monocytogenes pathogenicity.* Science, 2000. **290**(5493): p. 992-5.

109. Palmer, M., *The family of thiol-activated, cholesterol-binding cytolysins.* Toxicon, 2001. **39**(11): p. 1681-9.

110. Bhardwaj, V., et al., *Chronic Listeria infection in SCID mice: requirements for the carrier state and the dual role of T cells in transferring protection or suppression.* J Immunol, 1998. **160**(1): p. 376-84.

111. Birmingham, C.L., et al., *Listeriolysin O allows Listeria monocytogenes replication in macrophage vacuoles.* Nature, 2008. **451**(7176): p. 350-4.

112. Xie, Z. and D.J. Klionsky, *Autophagosome formation: core machinery and adaptations.* Nat Cell Biol, 2007. **9**(10): p. 1102-9.

113. Gaillard, J.L., et al., *In vitro model of penetration and intracellular growth of Listeria monocytogenes in the human enterocyte-like cell line Caco-2.* Infect Immun, 1987. **55**(11): p. 2822-9.

114. Westcott, M.M., et al., *Differential susceptibility of bone marrow-derived dendritic cells and macrophages to productive infection with Listeria monocytogenes.* Cell Microbiol, 2007. **9**(6): p. 1397-411.

115. Westcott, M.M., et al., *Dendritic cells inhibit the progression of Listeria monocytogenes intracellular infection by retaining bacteria in major histocompatibility complex class II-rich phagosomes and by limiting cytosolic growth.* Infect Immun. **78**(7): p. 2956-65.

116. Portnoy, D.A., et al., *Gamma interferon limits access of Listeria monocytogenes to the macrophage cytoplasm.* J Exp Med, 1989. **170**(6): p. 2141-6.

117. Murphy, S.P., et al., *Interferon gamma in successful pregnancies.* Biol Reprod, 2009. **80**(5): p. 848-59.

118. Hunt, J.S., *Stranger in a strange land.* Immunol Rev, 2006. **213**: p. 36-47.

119. Koopman, L.A., et al., *Human decidual natural killer cells are a unique NK cell subset with immunomodulatory potential.* J Exp Med, 2003. **198**(8): p. 1201-12.

120. Banerjee, S., et al., *Placental expression of interferon-gamma (IFN-gamma) and its receptor IFN-gamma R2 fail to switch from early hypoxic*

to late normotensive development in preeclampsia. J Clin Endocrinol Metab, 2005. **90**(2): p. 944-52.

121. Geoffroy, C., et al., *Purification, characterization, and toxicity of the sulfhydryl-activated hemolysin listeriolysin O from Listeria monocytogenes.* Infect Immun, 1987. **55**(7): p. 1641-6.

122. Portnoy, D.A., et al., *Capacity of listeriolysin O, streptolysin O, and perfringolysin O to mediate growth of Bacillus subtilis within mammalian cells.* Infect Immun, 1992. **60**(7): p. 2710-7.

123. Schuerch, D.W., E.M. Wilson-Kubalek, and R.K. Tweten, *Molecular basis of listeriolysin O pH dependence.* Proc Natl Acad Sci U S A, 2005. **102**(35): p. 12537-42.

124. Bonenfant, M., et al., *Localization of type 1 17beta-hydroxysteroid dehydrogenase mRNA and protein in syncytiotrophoblasts and invasive cytotrophoblasts in the human term villi.* J Endocrinol, 2000. **165**(2): p. 217-22.

125. Singh, R., A. Jamieson, and P. Cresswell, *GILT is a critical host factor for Listeria monocytogenes infection.* Nature, 2008. **455**(7217): p. 1244-7.

126. Paschen, A., et al., *Human dendritic cells infected by Listeria monocytogenes: induction of maturation, requirements for phagolysosomal escape and antigen presentation capacity.* Eur J Immunol, 2000. **30**(12): p. 3447-56.

127.   Grundling, A., M.D. Gonzalez, and D.E. Higgins, *Requirement of the Listeria monocytogenes broad-range phospholipase PC-PLC during infection of human epithelial cells.* J Bacteriol, 2003. **185**(21): p. 6295-307.

128.   Burrack, L.S., J.W. Harper, and D.E. Higgins, *Perturbation of vacuolar maturation promotes listeriolysin O-independent vacuolar escape during Listeria monocytogenes infection of human cells.* Cell Microbiol, 2009. **11**(9): p. 1382-98.

129.   Hemmings, D.G., et al., *Permissive cytomegalovirus infection of primary villous term and first trimester trophoblasts.* J Virol, 1998. **72**(6): p. 4970-9.

130.   Maidji, E., et al., *Developmental regulation of human cytomegalovirus receptors in cytotrophoblasts correlates with distinct replication sites in the placenta.* J Virol, 2007. **81**(9): p. 4701-12.

131.   Ross, A.L., et al., *Proteasome-independent degradation of HIV-1 in naturally non-permissive human placental trophoblast cells.* Retrovirology, 2009. **6**: p. 46.

132.   Vidricaire, G. and M.J. Tremblay, *Rab5 and Rab7, but not ARF6, govern the early events of HIV-1 infection in polarized human placental cells.* J Immunol, 2005. **175**(10): p. 6517-30.

133.   Yeh, I.T., D.M. O'Connor, and R.J. Kurman, *Vacuolated cytotrophoblast: a subpopulation of trophoblast in the chorion laeve.* Placenta, 1989. **10**(5): p. 429-38.

134. Jones, C.J. and H. Fox, *Ultrastructure of the normal human placenta.* Electron Microsc Rev, 1991. **4**(1): p. 129-78.

135. Robbins, J.R., et al., *Tissue barriers of the human placenta to infection with Toxoplasma gondii.* Infect Immun.

136. Kliman, H.J., et al., *Purification, characterization, and in vitro differentiation of cytotrophoblasts from human term placentae.* Endocrinology, 1986. **118**(4): p. 1567-82.

137. Lieberman, L.A. and D.E. Higgins, *Inhibition of Listeria monocytogenes infection by neurological drugs.* Int J Antimicrob Agents. **35**(3): p. 292-6.

138. Villalobos, A., et al., *Gene Designer: a synthetic biology tool for constructing artificial DNA segments.* BMC Bioinformatics, 2006. **7**: p. 285.

139. Lauer, P., et al., *Construction, characterization, and use of two Listeria monocytogenes site-specific phage integration vectors.* J Bacteriol, 2002. **184**(15): p. 4177-86.

140. de Chastellier, C. and P. Berche, *Fate of Listeria monocytogenes in murine macrophages: evidence for simultaneous killing and survival of intracellular bacteria.* Infect Immun, 1994. **62**(2): p. 543-53.

141. Schnupf, P., D.A. Portnoy, and A.L. Decatur, *Phosphorylation, ubiquitination and degradation of listeriolysin O in mammalian cells: role of the PEST-like sequence.* Cell Microbiol, 2006. **8**(2): p. 353-64.

142.   Shaughnessy, L.M., et al., *Membrane perforations inhibit lysosome fusion by altering pH and calcium in Listeria monocytogenes vacuoles.* Cell Microbiol, 2006. **8**(5): p. 781-92.

143.   Jones, S. and D.A. Portnoy, *Characterization of Listeria monocytogenes pathogenesis in a strain expressing perfringolysin O in place of listeriolysin O.* Infect Immun, 1994. **62**(12): p. 5608-13.

144.   Glomski, I.J., et al., *The Listeria monocytogenes hemolysin has an acidic pH optimum to compartmentalize activity and prevent damage to infected host cells.* J Cell Biol, 2002. **156**(6): p. 1029-38.

145.   Kawai, M., et al., *Placental endocrine disruption induced by cadmium: effects on P450 cholesterol side-chain cleavage and 3beta-hydroxysteroid dehydrogenase enzymes in cultured human trophoblasts.* Biol Reprod, 2002. **67**(1): p. 178-83.

146.   Bevilacqua, E., et al., *Trophoblast phagocytic program: roles in different placental systems.* Int J Dev Biol. **54**(2-3): p. 495-505.

147.   Moors, M.A., et al., *Expression of listeriolysin O and ActA by intracellular and extracellular Listeria monocytogenes.* Infect Immun, 1999. **67**(1): p. 131-9.

148.   Myatt, L., et al., *Immunohistochemical localization of nitric oxide synthase in the human placenta.* Placenta, 1993. **14**(5): p. 487-95.

149. Martin, D. and K.P. Conrad, *Expression of endothelial nitric oxide synthase by extravillous trophoblast cells in the human placenta.* Placenta, 2000. **21**(1): p. 23-31.

150. Webster, R.P., V.H. Roberts, and L. Myatt, *Protein nitration in placenta - functional significance.* Placenta, 2008. **29**(12): p. 985-94.

151. Myatt, L. and X. Cui, *Oxidative stress in the placenta.* Histochem Cell Biol, 2004. **122**(4): p. 369-82.

152. Bogdan, C., M. Rollinghoff, and A. Diefenbach, *The role of nitric oxide in innate immunity.* Immunol Rev, 2000. **173**: p. 17-26.

153. Fang, F.C., *Antimicrobial reactive oxygen and nitrogen species: concepts and controversies.* Nat Rev Microbiol, 2004. **2**(10): p. 820-32.

154. Beckerman, K.P., et al., *Release of nitric oxide during the T cell-independent pathway of macrophage activation. Its role in resistance to Listeria monocytogenes.* J Immunol, 1993. **150**(3): p. 888-95.

155. Muller, M., et al., *Reduced antilisterial activity of TNF-deficient bone marrow-derived macrophages is due to impaired superoxide production.* Eur J Immunol, 1999. **29**(10): p. 3089-97.

156. Ouadrhiri, Y., et al., *Mechanism of the intracellular killing and modulation of antibiotic susceptibility of Listeria monocytogenes in THP-1 macrophages activated by gamma interferon.* Antimicrob Agents Chemother, 1999. **43**(5): p. 1242-51.

157.   Ohya, S., et al., *Killing mechanism of Listeria monocytogenes in activated macrophages as determined by an improved assay system.* J Med Microbiol, 1998. **47**(3): p. 211-5.

158.   Ohya, S., et al., *The contributions of reactive oxygen intermediates and reactive nitrogen intermediates to listericidal mechanisms differ in macrophages activated pre- and postinfection.* Infect Immun, 1998. **66**(9): p. 4043-9.

159.   Ouadrhiri, Y., Y. Sibille, and P.M. Tulkens, *Modulation of intracellular growth of Listeria monocytogenes in human enterocyte Caco-2 cells by interferon-gamma and interleukin-6: role of nitric oxide and cooperation with antibiotics.* J Infect Dis, 1999. **180**(4): p. 1195-204.

160.   Jin, Y., et al., *Interferon-gamma mediates neuronal killing of intracellular bacteria.* Scand J Immunol, 2004. **60**(5): p. 437-48.

161.   Myers, J.T., A.W. Tsang, and J.A. Swanson, *Localized reactive oxygen and nitrogen intermediates inhibit escape of Listeria monocytogenes from vacuoles in activated macrophages.* J Immunol, 2003. **171**(10): p. 5447-53.

162.   Callewaert, L. and C.W. Michiels, *Lysozymes in the animal kingdom.* J Biosci. **35**(1): p. 127-60.

163.   Liu, N., et al., *Vitamin D induces innate antibacterial responses in human trophoblasts via an intracrine pathway.* Biol Reprod, 2009. **80**(3): p. 398-406.

164. King, A.E., et al., *Expression of natural antimicrobials by human placenta and fetal membranes.* Placenta, 2007. **28**(2-3): p. 161-9.

165. King, A.E., et al., *Innate immune defences in the human uterus during pregnancy.* Placenta, 2007. **28**(11-12): p. 1099-106.

166. Boneca, I.G., et al., *A critical role for peptidoglycan N-deacetylation in Listeria evasion from the host innate immune system.* Proc Natl Acad Sci U S A, 2007. **104**(3): p. 997-1002.

167. Vollmer, W. and A. Tomasz, *The pgdA gene encodes for a peptidoglycan N-acetylglucosamine deacetylase in Streptococcus pneumoniae.* J Biol Chem, 2000. **275**(27): p. 20496-501.

168. Bera, A., et al., *Why are pathogenic staphylococci so lysozyme resistant? The peptidoglycan O-acetyltransferase OatA is the major determinant for lysozyme resistance of Staphylococcus aureus.* Mol Microbiol, 2005. **55**(3): p. 778-87.

169. Thedieck, K., et al., *The MprF protein is required for lysinylation of phospholipids in listerial membranes and confers resistance to cationic antimicrobial peptides (CAMPs) on Listeria monocytogenes.* Mol Microbiol, 2006. **62**(5): p. 1325-39.

170. Rae, C.S., et al., *Mutations of the Listeria monocytogenes peptidoglycan N-deacetylase and O-acetylase result in enhanced lysozyme sensitivity, bacteriolysis, and hyperinduction of innate immune pathways.* Infect Immun. **79**(9): p. 3596-606.

171. Golberg, A., C.S. Rae, and B. Rubinsky, *Listeria monocytogenes cell wall constituents' charge effect on electroporation threshold.* Biochim Biophys Acta.

172. Meyer-Morse, N., et al., *Listeriolysin O is necessary and sufficient to induce autophagy during Listeria monocytogenes infection.* PLoS One. **5**(1): p. e8610.

173. Ogawa, M., et al., *Autophagy targeting of Listeria monocytogenes and the bacterial countermeasure.* Autophagy. **7**(3): p. 310-4.

174. Huang, J. and J.H. Brumell, *Autophagy in immunity against intracellular bacteria.* Curr Top Microbiol Immunol, 2009. **335**: p. 189-215.

175. Bowman, E.J., A. Siebers, and K. Altendorf, *Bafilomycins: a class of inhibitors of membrane ATPases from microorganisms, animal cells, and plant cells.* Proc Natl Acad Sci U S A, 1988. **85**(21): p. 7972-6.

176. Oda, K., et al., *Bafilomycin A1 inhibits the targeting of lysosomal acid hydrolases in cultured hepatocytes.* Biochem Biophys Res Commun, 1991. **178**(1): p. 369-77.

177. Brundage, R.A., et al., *Expression and phosphorylation of the Listeria monocytogenes ActA protein in mammalian cells.* Proc Natl Acad Sci U S A, 1993. **90**(24): p. 11890-4.

178. McCaffrey, R.L., et al., *A specific gene expression program triggered by Gram-positive bacteria in the cytosol.* Proc Natl Acad Sci U S A, 2004. **101**(31): p. 11386-91.

179. O'Riordan, M., et al., *Innate recognition of bacteria by a macrophage cytosolic surveillance pathway.* Proc Natl Acad Sci U S A, 2002. **99**(21): p. 13861-6.

180. Stockinger, S., et al., *IFN regulatory factor 3-dependent induction of type I IFNs by intracellular bacteria is mediated by a TLR- and Nod2-independent mechanism.* J Immunol, 2004. **173**(12): p. 7416-25.

181. Kobayashi, K.S., et al., *Nod2-dependent regulation of innate and adaptive immunity in the intestinal tract.* Science, 2005. **307**(5710): p. 731-4.

182. Mariathasan, S., et al., *Cryopyrin activates the inflammasome in response to toxins and ATP.* Nature, 2006. **440**(7081): p. 228-32.

183. Leber, J.H., et al., *Distinct TLR- and NLR-mediated transcriptional responses to an intracellular pathogen.* PLoS Pathog, 2008. **4**(1): p. e6.

184. Woodward, J.J., A.T. Iavarone, and D.A. Portnoy, *c-di-AMP secreted by intracellular Listeria monocytogenes activates a host type I interferon response.* Science. **328**(5986): p. 1703-5.

185. Auerbuch, V., et al., *Mice lacking the type I interferon receptor are resistant to Listeria monocytogenes.* J Exp Med, 2004. **200**(4): p. 527-33.

186. Zenewicz, L.A. and H. Shen, *Innate and adaptive immune responses to Listeria monocytogenes: a short overview.* Microbes Infect, 2007. **9**(10): p. 1208-15.

187. Nomura, T., et al., *Essential role of interleukin-12 (IL-12) and IL-18 for gamma interferon production induced by listeriolysin O in mouse spleen cells.* Infect Immun, 2002. **70**(3): p. 1049-55.

188. Baldwin, D.N., et al., *A gene-expression program reflecting the innate immune response of cultured intestinal epithelial cells to infection by Listeria monocytogenes.* Genome Biol, 2003. **4**(1): p. R2.

189. Carrero, J.A., B. Calderon, and E.R. Unanue, *Listeriolysin O from Listeria monocytogenes is a lymphocyte apoptogenic molecule.* J Immunol, 2004. **172**(8): p. 4866-74.

190. Herskovits, A.A., V. Auerbuch, and D.A. Portnoy, *Bacterial ligands generated in a phagosome are targets of the cytosolic innate immune system.* PLoS Pathog, 2007. **3**(3): p. e51.

191. Rose, F., et al., *Human endothelial cell activation and mediator release in response to Listeria monocytogenes virulence factors.* Infect Immun, 2001. **69**(2): p. 897-905.

192. Kayal, S., et al., *Listeriolysin O-dependent activation of endothelial cells during infection with Listeria monocytogenes: activation of NF-kappa B and upregulation of adhesion molecules and chemokines.* Mol Microbiol, 1999. **31**(6): p. 1709-22.

193. Trundley, A. and A. Moffett, *Human uterine leukocytes and pregnancy.* Tissue Antigens, 2004. **63**(1): p. 1-12.

194. Abrahams, V.M., et al., *Macrophages and apoptotic cell clearance during pregnancy.* Am J Reprod Immunol, 2004. **51**(4): p. 275-82.

195. Fest, S., et al., *Trophoblast-macrophage interactions: a regulatory network for the protection of pregnancy.* Am J Reprod Immunol, 2007. **57**(1): p. 55-66.

196. Mor, G., et al., *Is the trophoblast an immune regulator? The role of Toll-like receptors during pregnancy.* Crit Rev Immunol, 2005. **25**(5): p. 375-88.

197. Abrahams, V.M. and G. Mor, *Toll-like receptors and their role in the trophoblast.* Placenta, 2005. **26**(7): p. 540-7.

198. Dominguez, F., A. Pellicer, and C. Simon, *The chemokine connection: hormonal and embryonic regulation at the human maternal-embryonic interface--a review.* Placenta, 2003. **24 Suppl B**: p. S48-55.

199. Hess, A.P., et al., *Decidual stromal cell response to paracrine signals from the trophoblast: amplification of immune and angiogenic modulators.* Biol Reprod, 2007. **76**(1): p. 102-17.

200. Fisher, S.J. and C.H. Damsky, *Human cytotrophoblast invasion.* Semin Cell Biol, 1993. **4**(3): p. 183-8.

201. Graham, C.H. and P.K. Lala, *Mechanism of control of trophoblast invasion in situ.* J Cell Physiol, 1991. **148**(2): p. 228-34.

202. Angeloni, M.B., et al., *Apoptosis and S phase of the cell cycle in BeWo trophoblastic and HeLa cells are differentially modulated by Toxoplasma gondii strain types.* Placenta, 2009. **30**(9): p. 785-91.

203. Aldo, P.B., et al., *Viral ssRNA induces first trimester trophoblast apoptosis through an inflammatory mechanism.* Am J Reprod Immunol. **64**(1): p. 27-37.

204. Kakinuma, C., et al., *Trophoblastic apoptosis in mice with preterm delivery and its suppression by urinary trypsin inhibitor.* Obstet Gynecol, 1997. **90**(1): p. 117-24.

205. Rose, J.A., et al., *Peptidoglycan induces necrosis and regulates cytokine production in murine trophoblast stem cells.* Am J Reprod Immunol. **66**(3): p. 209-22.

206. Pereira, L. and E. Maidji, *Cytomegalovirus infection in the human placenta: maternal immunity and developmentally regulated receptors on trophoblasts converge.* Curr Top Microbiol Immunol, 2008. **325**: p. 383-95.

207. Zarember, K.A. and P.J. Godowski, *Tissue expression of human Toll-like receptors and differential regulation of Toll-like receptor mRNAs in leukocytes in response to microbes, their products, and cytokines.* J Immunol, 2002. **168**(2): p. 554-61.

208. Abrahams, V.M., et al., *Divergent trophoblast responses to bacterial products mediated by TLRs.* J Immunol, 2004. **173**(7): p. 4286-96.

209. Rindsjo, E., et al., *Toll-like receptor-2 expression in normal and pathologic human placenta.* Hum Pathol, 2007. **38**(3): p. 468-73.

210. Holmlund, U., et al., *Expression and regulation of the pattern recognition receptors Toll-like receptor-2 and Toll-like receptor-4 in the human placenta.* Immunology, 2002. **107**(1): p. 145-51.

211. Kumazaki, K., et al., *Immunohistochemical distribution of Toll-like receptor 4 in term and preterm human placentas from normal and complicated pregnancy including chorioamnionitis.* Hum Pathol, 2004. **35**(1): p. 47-54.

212. Ma, Y., et al., *Cell type-specific expression and function of toll-like receptors 2 and 4 in human placenta: implications in fetal infection.* Placenta, 2007. **28**(10): p. 1024-31.

213. Cardenas, I., et al., *Nod1 activation by bacterial iE-DAP induces maternal-fetal inflammation and preterm labor.* J Immunol. **187**(2): p. 980-6.

214. Abrahams, V.M., et al., *TLR6 modulates first trimester trophoblast responses to peptidoglycan.* J Immunol, 2008. **180**(9): p. 6035-43.

215. de la Torre, E., et al., *Chlamydia trachomatis infection modulates trophoblast cytokine/chemokine production.* J Immunol, 2009. **182**(6): p. 3735-45.

216. Komine-Aizawa, S., et al., *Stimuli through Toll-like receptor (TLR) 3 and 9 affect human chorionic gonadotropin (hCG) production in a choriocarcinoma cell line.* J Obstet Gynaecol Res, 2008. **34**(2): p. 144-51.

217. Azenabor, A.A., P. Kennedy, and S. Balistreri, *Chlamydia trachomatis infection of human trophoblast alters estrogen and progesterone*

biosynthesis: an insight into role of infection in pregnancy sequelae. Int J Med Sci, 2007. **4**(4): p. 223-31.

218. Wan, H., et al., *Chorionic gonadotropin can enhance innate immunity by stimulating macrophage function.* J Leukoc Biol, 2007. **82**(4): p. 926-33.

219. Radtke, A.L., et al., *TBK1 protects vacuolar integrity during intracellular bacterial infection.* PLoS Pathog, 2007. **3**(3): p. e29.

220. Flannagan, R.S., G. Cosio, and S. Grinstein, *Antimicrobial mechanisms of phagocytes and bacterial evasion strategies.* Nat Rev Microbiol, 2009. **7**(5): p. 355-66.

221. Forbes, K., et al., *Methods for siRNA-mediated reduction of mRNA and protein expression in human placental explants, isolated primary cells and cell lines.* Placenta, 2009. **30**(2): p. 124-9.

222. Leiser, R. and P. Kaufmann, *Placental structure: in a comparative aspect.* Exp Clin Endocrinol, 1994. **102**(3): p. 122-34.

223. Bradbury, F.M. and C.D. Ockleford, *A confocal and conventional epifluorescence microscope study of the intermediate filaments in chorionic villi.* J Anat, 1990. **169**: p. 173-87.

224. Strauss, J.F., 3rd, et al., *The cAMP signalling system and human trophoblast function.* Placenta, 1992. **13**(5): p. 389-403.

225. Wice, B., et al., *Modulators of cyclic AMP metabolism induce syncytiotrophoblast formation in vitro.* Exp Cell Res, 1990. **186**(2): p. 306-16.

226. Orendi, K., et al., *The choriocarcinoma cell line BeWo: syncytial fusion and expression of syncytium-specific proteins.* Reproduction. **140**(5): p. 759-66.

227. Morrish, D.W., J. Dakour, and H. Li, *Functional regulation of human trophoblast differentiation.* J Reprod Immunol, 1998. **39**(1-2): p. 179-95.

228. Tanaka, S., et al., *Promotion of trophoblast stem cell proliferation by FGF4.* Science, 1998. **282**(5396): p. 2072-5.

229. Maltepe, E., A.I. Bakardjiev, and S.J. Fisher, *The placenta: transcriptional, epigenetic, and physiological integration during development.* J Clin Invest. **120**(4): p. 1016-25.

230. Rossant, J. and J.C. Cross, *Placental development: lessons from mouse mutants.* Nat Rev Genet, 2001. **2**(7): p. 538-48.

231. Maltepe, E., et al., *Hypoxia-inducible factor-dependent histone deacetylase activity determines stem cell fate in the placenta.* Development, 2005. **132**(15): p. 3393-403.

232. Okazaki, K. and E. Maltepe, *Oxygen, epigenetics and stem cell fate.* Regen Med, 2006. **1**(1): p. 71-83.

233. Cameron, L.A., et al., *Biophysical parameters influence actin-based movement, trajectory, and initiation in a cell-free system.* Mol Biol Cell, 2004. **15**(5): p. 2312-23.

234. Fisher, S.J., *The placental problem: linking abnormal cytotrophoblast differentiation to the maternal symptoms of preeclampsia.* Reprod Biol Endocrinol, 2004. **2**: p. 53.

235. Cardenas, I., et al., *Placental viral infection sensitizes to endotoxin-induced pre-term labor: a double hit hypothesis.* Am J Reprod Immunol. **65**(2): p. 110-7.

236. Pereira, L., et al., *Human cytomegalovirus transmission from the uterus to the placenta correlates with the presence of pathogenic bacteria and maternal immunity.* J Virol, 2003. **77**(24): p. 13301-14.

237. Keelan, J.A., et al., *Innate inflammatory responses of human decidual cells to periodontopathic bacteria.* Am J Obstet Gynecol. **202**(5): p. 471 e1-11.

238. Rours, G.I., et al., *Chlamydia trachomatis and placental inflammation in early preterm delivery.* Eur J Epidemiol. **26**(5): p. 421-8.

Publishing Agreement

It is the policy of the University to encourage the distribution of all theses, dissertations, and manuscripts. Copies of all UCSF theses, dissertations, and manuscripts will be routed to the library via the Graduate Division. The library will make all theses, dissertations, and manuscripts accessible to the public and will preserve these to the best of their abilities, in perpetuity.

Please sign the following statement:

I hereby grant permission to the Graduate Division of the University of California, San Francisco to release copies of my thesis, dissertation, or manuscript to the Campus Library to provide access and preservation, in whole or in part, in perpetuity.

_____
Author Signature

12/16/11
_____
Date